University of Alberta

Kinetics and Phase Behavior in Asphaltene Cracking

by

©

Samina Rahmani

A thesis submitted to the Faculty of Graduate Studies and Research in partial fulfillment

of the requirements for the degree of Doctor of Philosophy in Chemical Engineering

Department of Chemical and Materials Engineering

Edmonton, Alberta

Fall, 2002

The author has granted a non-exclusive licence allowing the National Library of Canada to reproduce, loan, distribute or sell copies of this thesis in microform, paper or electronic formats.

The author retains ownership of the copyright in this thesis. Neither the thesis nor substantial extracts from it may be printed or otherwise reproduced without the author's permission.

L'auteur a accordé une licence non exclusive permettant à la Bibliothèque nationale du Canada de reproduire, prêter, distribuer ou vendre des copies de cette thèse sous la forme de microfiche/film, de reproduction sur papier ou sur format électronique.

L'auteur conserve la propriété du droit d'auteur qui protège cette thèse. Ni la thèse ni des extraits substantiels de celle-ci ne doivent être imprimés ou autrement reproduits sans son autorisation.

0-612-81255-3

Canada

University of Alberta

Library Release Form

Name of Author: *Samina Rahmani*

Title of Thesis: *Kinetics and Phase Behavior in Asphaltene Cracking*

Degree: *Doctor of Philosophy*

Year this Degree Granted: *2002*

Permission is hereby granted to the University of Alberta Library to reproduce single copies of this thesis and to lend or sell such copies for private, scholarly or scientific research purposes only.

The author reserves all other publication and other rights in association with the copyright in the thesis, and except as herein before provided, neither the thesis nor any substantial portion thereof may be printed or otherwise reproduced in any material form whatever without the author's prior written permission.

Rahmani
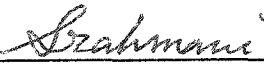
521-O Michener Park
Edmonton, AB
Canada, T6H 4M5

Dated: 6th Aug, 02

University of Alberta

Faculty of Graduate Studies and Research

The undersigned certify that they have read, and recommend to the Faculty of Graduate Studies and research for acceptance, a thesis entitled *Kinetics and Phase Behavior in Asphaltene Cracking* by Samina Rahmani in partial fulfillment of the requirements for the degree of Doctor of Philosophy in Chemical Engineering.
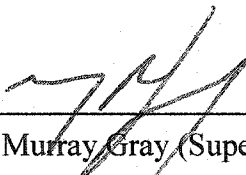
Dr. Murray Gray (Supervisor)
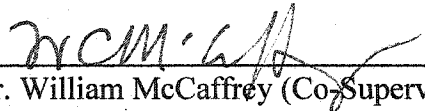
Dr. William McCaffrey (Co-Supervisor)
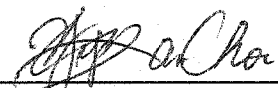
Dr. Philip (Yip-Kam) Choi
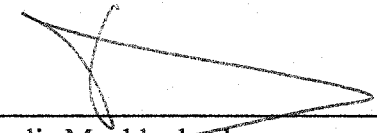
Dr. Karlis Muehlenbachs

Dr. Philip Savage

Date: August 1st, 2002

ABSTRACT

The formation of coke from reacting asphaltenes is significantly affected by both reactions with the liquid components and the solvent properties of the liquid medium. Both the kinetics and phase behavior in the cracking of asphaltenes were studied in this thesis. The kinetics of solvent interactions with asphaltenes were studied by reacting Athabasca asphaltenes in a closed batch reactor at 430 °C. Reactions of asphaltene in maltene at different concentrations and reactions in a series of aromatic solvents (1-methyl naphthalene, naphthalene and tetralin) were used to investigate the role of solvent properties and hydrogen donation reactions. The most important characteristics of the liquid phase were hydrogen donating ability and the ability to initiate cracking reactions. The latter mechanism was confirmed by adding n-dodecyl sulfide as an initiator compound. A modified kinetic model for coke formation, incorporating phase separation and hydrogen transfer to the asphaltenes, was consistent with the experimental results over a range of asphaltene concentrations and solvent conditions.

Coking kinetics as a function of asphaltenes structure were also examined by reacting several different asphaltenes from around the world in 1-methyl naphthalene and tetralin. The selected asphaltenes were Athabasca asphaltenes from Canada, Arabian Light and Arabian Heavy from Saudi Arabia, Maya from Mexico and Gudao from China. The data from the cracking reactions could be fitted to the modified phase separation model. The two fitting parameters for the thermolysis in 1-methyl naphthalene were found to correlate with two structural properties of the asphaltenes. Consequently, the model can be used for the prediction of coke formation in 1-methyl naphthalene from the structural properties of asphaltenes.

Phase behavior during coke formation was investigated by examining the coke produced from selected reactions under scanning electron microscopy (SEM). Asphaltenic material from Athabasca bitumen, with and without fine solids, was reacted in liquid phase mixed with either 1-methyl naphthalene or maltene fractions from Athabasca. Both fine solids and solvents were found to help the dispersion of coke spheres. Phase inversion was observed in some sections of coke produced from pure asphaltene. The thermodynamic feasibility of phase inversion was confirmed by calculating the entropy difference for a set of representative conditions.

Acknowledgments

I would like to thank my supervisor Dr. Murray Gray and co-supervisor Dr. William McCaffrey for being excellent supervisors and for their support and guidance throughout my doctoral program. I would also like to thank Dr. Janett Elliott for her insightful suggestions and help in the thermodynamic section of the thesis. I like to thank Dr. Heather Dettman for her help in NMR analysis. I would like to thank Idemitsu Kosan Co. Ltd. and the New Energy and Industrial Technology Development Organization (Japan) for letting use some experimental results that were done in a collaborative research and development project.

I would like to thank my friends in Heavy Oil Upgrading group, Yingzian, Sanyi, Liming, Srini, Shakir, Suresh, Tuyet, Richard, Jeff, Moruf, Lisa and Pedro, for making this an enjoyable experience.

I like to thank my parents, Shamsul Huda and Monju akhter Huda, and my brothers, Dr. Quamrul Huda and Sydul Huda, for the emotional support and encouragement. Finally, I like to thank my husband, Nazmul Rahmani, for his patience, constant support and encouragement and helping me get through the ups and downs of the past years.

TABLE OF CONTENTS

List of Tables

List of Figures

1. INTRODUCTION

1.1. Background

As the reserves of conventional crude oil are depleted, processing heavy oil and bitumen is becoming more and more important in filling the gap of the world's growing demand for fuels and petrochemicals. One of the largest supplies of heavy oil exists in Alberta, Canada, in the form of oil sands. There is a total bitumen resource of 2.9 trillion barrels. Of that, Alberta has about 1.6 trillion-barrels, of which over 300 billion are recoverable by current technology. The total amount is greater than the known reserves of Saudi Arabia. However, as much as 50 wt% of the bitumen consists of residuum, which has a boiling point higher than 524 °C. These heavier fractions of the bitumen require upgrading before they can find a market.

The goal of upgrading bitumen and residues is to convert high boiling residue components into lower boiling distillates, improve the H/C ratio and remove the heteroatoms, such as sulfur, nitrogen etc., down to environmentally acceptable levels. Achieving these process goals requires that the residue molecules undergo a number of thermal and catalytic reactions. Primary upgrading is the first step of residue conversion into distillate products, which requires a significant breakage of C-C bonds. In the secondary upgrading, the distillates or residues are selectively hydrogenated to reduce the heteroatom content to the levels of the light crude. The primary upgrading of bitumen and petroleum residue to distillate products is achieved by either coking or catalytic hydroconversion. Coking is a purely thermal process where the feed is thermally cracked to produce light ends (gases), distillable liquid and solid coke (Gray, 1994). Since thermal

1

processes do not require the addition of catalyst, coking is one of the oldest technologies available for residue conversion. Coking processes are very efficient in rejecting mineral solids and metals along with some rejection of organic nitrogen and sulfur in the coke. However, the rejection of sulfur into coke is low.

Coke is a carbon rich solid, which tends to form at high temperature during the upgrading process. Coke can cause potential operating problems. For example, in hydroconversion processes where catalyst is used, coke deposition on the catalyst will deactivate the catalyst. Coke produced in the coking processes is much less valuable than the distillable liquid. Thus, in coking processes, the objective is to maximize the yield of cracked products, while also producing a coke material of the desired quality. On the other hand, in hydroconversion processes, the objective is to avoid the formation of coke deposits. In all of these processes, formation of coke limits the possible conversion to distillable liquid products. To improve operability and efficiency of these units, it is important to control or manage coking and maximize the production of distillable oil. These goals are only achievable through a better understanding of the mechanism of the processes involved.

Petroleum asphaltenes, which are operationally defined as the pentane- or heptane-insoluble and toluene-soluble organic fraction of bitumen or vacuum residue, are largely responsible for coke formation. Many researchers have concluded that asphaltenes are mixtures of polydispersed condensed polyaromatic units, containing heteroatoms and aliphatic side chains. Heavy oil and residues can contain a significant amount of asphaltenes, e.g. 10–30 wt%. Therefore, it is necessary to have a complete understanding of asphaltene reaction pathways in order to understand the mechanism of

2

coke formation better. A number of researchers have studied the kinetics of isolated asphaltenes. Isolated asphaltene reaction pathways are complex due to the complicated nature of asphaltene molecules. These reaction paths are further complicated by the presence of the heptane soluble fraction of the vacuum residue, maltenes, which are smaller in molecular weight but have similar complex nature to asphaltenes. In industrial processes, asphaltenes are reacted as a component of the vacuum residue or bitumen. Therefore, it is extremely important to understand the effect of reaction environment on the asphaltene conversion.

In general, coker feedstocks include atmospheric and vacuum bottoms of the bitumen and their blends. Extent of distillation and the ratio of the blending streams will both have an effect on the feed composition. In addition, other upstream processes like extraction can also change the feed composition. Extraction processes will determine the solids or water content in the feed, which can have significant impact on the coking kinetics. Any change in the feed composition will have an impact on the rate and extent of coke formation, and also on the product composition and yield. In spite of the importance of feed composition, very few studies were done on the effect of feed composition on the coking kinetics (Liu et al., 1999).

1.2. Research Objectives

The main objective of this work was to study the kinetics and phase behavior in the cracking of asphaltenes during coking. Asphaltene reaction pathways are complex and affected by not only the processing parameters of temperature and pressure, but also solvents and the composition of the feed asphaltenes. The major research objectives are listed below:

3

1. To study the role of liquid medium. The liquid medium could play a very important role in providing a solvent environment for the asphaltenes and taking part in the radical reactions for coke formation. Asphaltenic phase separation, as suggested by many authors (Magaril et al., 1971; Wiehe, 1993), would be determined by the solvent strength of the liquid medium. Hydrogen donors would reduce coke formation by reacting with the olefinic compounds. The objective of this part was to study the kinetics of solvent interactions with asphaltenes during coke formation.

2. To study coking kinetics as a function of asphaltene structure. Several different feedstocks from around the world were chosen to examine their behavior under coking conditions. The final objective was to predict the coke formation as a function of feed properties.

3. To study the phase behavior during coke formation. Bitumen or vacuum residue extracted from oil sands may contain some fine solids. These fine solids were found to have significant influence on the initial stages of coking kinetics (Tanabe and Gray, 1997). This influence was suggested to be due to the change in dispersion arising from these fine solids. The influence of fine solids on the morphology of the coke phase was studied.

1.3. References

Gray,M.R., Upgrading Petroleum Residues and Heavy Oils, Marcel Dekker Inc., New York (1994)

Liu, C., Zhu, C., Jin, L., Shen, R., and Liang, W., "Step by Step Modeling for Thermal Reactivities and Chemical Compositions of Vacuum Tesidues and their SFEF Asphalts", *Fuel Proc. Technol.*, 1999, 59, 51-67

Magaril, R. Z. and Aksenova, E. I., "Study of the Mechanism of Coke Formation in The Cracking of Petroleum Resins", *Inter. Chem. Eng.*, **1968**, 8(4), 727-729

Tanabe, K., and Gray, M. R., " Role of Fine Solids in the Coking of Vacuum Residues", *Energy & Fuels*, **1997**, 11(5), 1040-1043

Wiehe, I. A., "A Phase Separation Kinetic Model for Coke Formation", *Ind. Eng. Chem. Res.*, **1993**, 44, 2447-2457

2. LITERATURE REVIEW

2.1. Bitumen and Vacuum Residue

Any petroleum or petroleum-like liquids or semisolids with a gas-free viscosity greater than 10,000 mPas at original reservoir temperature, or an API gravity of less than 10 at 15.6 °C, are considered to be bitumen. Vacuum residue is the 524 °C+ fraction, which can be obtained by vacuum distillation of petroleum crudes (Sanford, 1991). The first step in understanding the chemistry of vacuum residue processing is to understand the composition of the residuum itself. Bitumen and vacuum residue, however, are complex mixtures of thousands or millions of different molecules, without a repeating molecular unit. This complex behavior of the bitumen and residue makes component by component analysis extremely difficult. One way to address this issue is to use solvents to separate petroleum resids and their reaction products into pseudocomponents and then track the pathway of conversion of each pseudocomponent into others (Wiehe, 1992).

SARA (saturates-aromatic-resin-asphaltene) is a widely used separation scheme based on combined solubility and adsorption characteristics of bitumen or residue. By SARA method petroleum is separated into four fractions: saturates, aromatic, resin and asphaltenes. Asphaltenes are the class of compounds that are soluble in an aromatic solvent such as toluene or benzene and are insoluble in n-alkanes such as n-heptane or n-pentane. The yield and quality of this fraction depends on how it was separated, the ratio of the solvent to oil, the time before filtration, the pore size and material of the filter etc. However, by keeping these variables constant, a reproducible yield and quality can be obtained. n-alkane soluble fraction is defined as maltenes. Maltenes can further be separated into saturates, aromatics and resins by adsorption column chromatography.

6

Usually silica or alumina is used as the adsorbent, and the separation is carried out by elution with different solvents. Maltenes can thus be separated into three fractions: 1) resins eluted with benzene/ methanol, 2) aromatics eluted with benzene, and 3) saturates eluted with n-heptane (Speight, 1994). In addition to these four fractions, a toluene-insoluble fraction is often produced from the reacted residues. This toluene insoluble fraction is commonly defined as coke. Sometimes, toluene insoluble fractions may be present in the unreacted feed as well. These are mostly inorganic mineral solids, and classified as bitumen solids or fine solids.

Role of the resin fraction has often been described as an asphaltene stabilizer at coking conditions, following the model developed by Pfeiffer and Saal (1940). According to their microemulsion model, asphaltenes at ambient temperatures are dispersed by the surfactant-like property of resins, which in turn are held in solution by aromatics. The saturates are poor solvents for asphaltenes. Empirical observations indicate that without the resin fraction, asphaltenes are generally non-dispersible in the remaining oil (Koots and Speight, 1975). However, the role of resins as asphaltene stabilizers has so far been proved only at lower temperature. Storm et al. (1996) suggested that the asphaltene phase flocculate due to disruption of the dispersing resins well below the temperature at which chemical reactions occur. Consequently, role of the resin as asphaltene stabilizer is not important at the temperatures typical of coking.

Many studies have been carried out using SARA fractions to determine the interconversion of these classes of compounds and kinetic models had been developed for coking and hydrocracking for example, Trauth et al., 1992; Mazza and Cormack, 1988. However, several authors (Bunger and Cogswell, 1981; Sanford, 1994) raised concerns

7

about this approach because there is no discernible chemical difference between, for instance, resins and asphaltenes (Strausz, 1989) and because pseudocomponents can undergo chemical changes without being completely converted to other pseudocomponents. Wiehe (1992) developed a solvent-residue phase diagram where he plotted the number average molecular weight versus hydrogen content for fractions of eight different residues and their thermal reaction products. Each of the pseudocomponents occupied areas of the graph without overlapping with points representing other pseudocomponents (Figure 2.1).
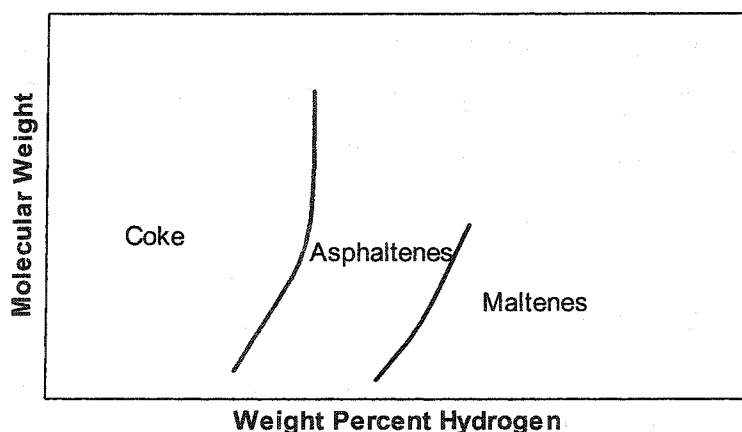
Figure 2.1 Schematic presentation of solvent-residue phase diagram (Wiehe, 1992)

The fact that the psedocomponents occupied areas instead of points suggested that they represented large distributions of molecules, and that chemical changes could occur within each pseudocomponent. However, each fraction had a common range of molecular weights and hydrogen contents and could be distinguished from the others. In balance, solubility fractionation that divides the residue into asphaltenes and maltenes is a logical

experimental approach for tracking residue conversion as long as the limitations are well understood.

2.2. Asphaltenes Structure and Molecular weight

Asphaltenes occupy a central, often hindering role in the utilization of hydrocarbon resources. Petroleum asphaltenes are operationally defined as n- heptane or n-pentane insoluble and toluene soluble organic material of bitumen or vacuum residue, and they contain the highest molecular weight, most aromatic and most polar components of the bitumen. They are not only the most reactive fraction of the bitumen (Wiehe, 1993), but also the least stable physically. The increase in viscosity in crude oil, which is associated with increased asphaltene content, together with the tendency of asphaltenes to phase separate, creates significant difficulties in the production and transportation of crude oil. From the upgrading point of view, asphaltenes are mostly responsible for sludge formation due to flocculation, which reduces the flow and plugs downstream separators, exchangers and towers. The coking tendencies of asphaltenes along with their heavy metal content interfere with the catalytic processing of crude oils. Most importantly, they are believed to be mostly responsible in the production of coke (Speight, 1970, 1987). The substantial importance of asphaltenes necessitates detailed understanding of these materials. Although an enormous amount of effort has been spent on the structural elucidation of asphaltenes for several decades, their precise and unambiguous molecular description is not yet possible due to the complexity of the molecules.

9

2.2.1. Molecular Structure

The molecular nature of the asphaltene fraction has been the subject of numerous investigations, but determining the actual structures of the constituents of the asphaltene fraction proved to be difficult due to the self-organization of the heavier parts and the almost continuous distribution of the molecular properties (Murgich et al., 1999). Much of the information available on the carbon skeleton of asphaltenes has been derived from spectroscopic studies such as nuclear magnetic resonance (NMR) studies of asphaltenes isolated from various petroleum and natural asphalts. The data from these studies support the hypothesis that structurally asphaltenes are condensed polynuclear aromatic ring systems bearing alkyl sidechains (Yen, 1972). For many years a large number of benzene rings, from six to twenty, were assumed to form the aromatic system of asphaltenes (Yen, 1972). Asphaltene pyrolysis (350 – 800 °C) produces substantial amounts of alkanes in the distillate, with individual molecules having up to forty carbon atoms. These products reflect the presence of such chains in the original asphaltenes (Speight, 1994). This observation provides an inconsistency in the structural types proposed in earlier studies, where alkyl side chains were deduced to contain approximately four carbon atoms (Speight, 1970). The application of thermal techniques to study the nature of the volatile thermal fragments from petroleum asphaltenes has produced strong evidence of the presence of small polynuclear aromatic systems containing 1-4 rings (Speight, 1987). Recent studies with HPLC-UV (high performance liquid chromatography with ultraviolet spectroscopy) of asphaltenes also do not show any evidence for polynuclear aromatic ring systems containing more than six rings. In all cases the evidence favored the

10

predominance of the smaller one to four ring systems (Speight, 1986; Strausz et al., 1992; Murgich et al. 1999).

Asphaltenes contain appreciable amounts of organic nonhydrocarbon constituents, mainly sulfur, nitrogen and oxygen and, in smaller amounts, organometallic compounds (Speight, 1991). Sulfur compounds are present mainly in two forms, in aromatic rings, which are very stable, and in thioethers or organic sulfides, which have weaker bonds and are more easily thermally cracked. Nitrogen is found in mainly two forms, basic and nonbasic. The basic nitrogen compounds are composed mainly of pyridine homologs. The nonbasic nitrogen compounds are usually of pyrrole, indole and carbazole types. Both types of nitrogen are highly resistant to removal. Oxygen may be present in aromatic rings, bonded directly to carbon ethers, and as other polar functional groups such as hydroxyls and acids. Trace amounts of metals, mostly nickel or vanadium, are found in two organic forms in asphaltenes: porphyrin metals, which are chelated in porphyrin structures and nonporphyrin metals which are thought to be associated with the polar groups of asphaltenes (Gray, 1994).

Strausz et al. (1992) presented a hypothetical asphaltene structure from chemical and thermal decomposition studies performed in acetone-extracted asphaltene from Athabasca bitumen. Instead of a highly condensed aromatic system with a large number of rings, a set of much smaller aromatic groups linked by polymethylene bridges, many containing S atoms, was obtained for the asphaltene fractions studied. Figure 2.2 shows a slightly modified structure presented by Murgich et al. (1999). This type of open, linked structure is consistent with results of pyrolysis studies.

11
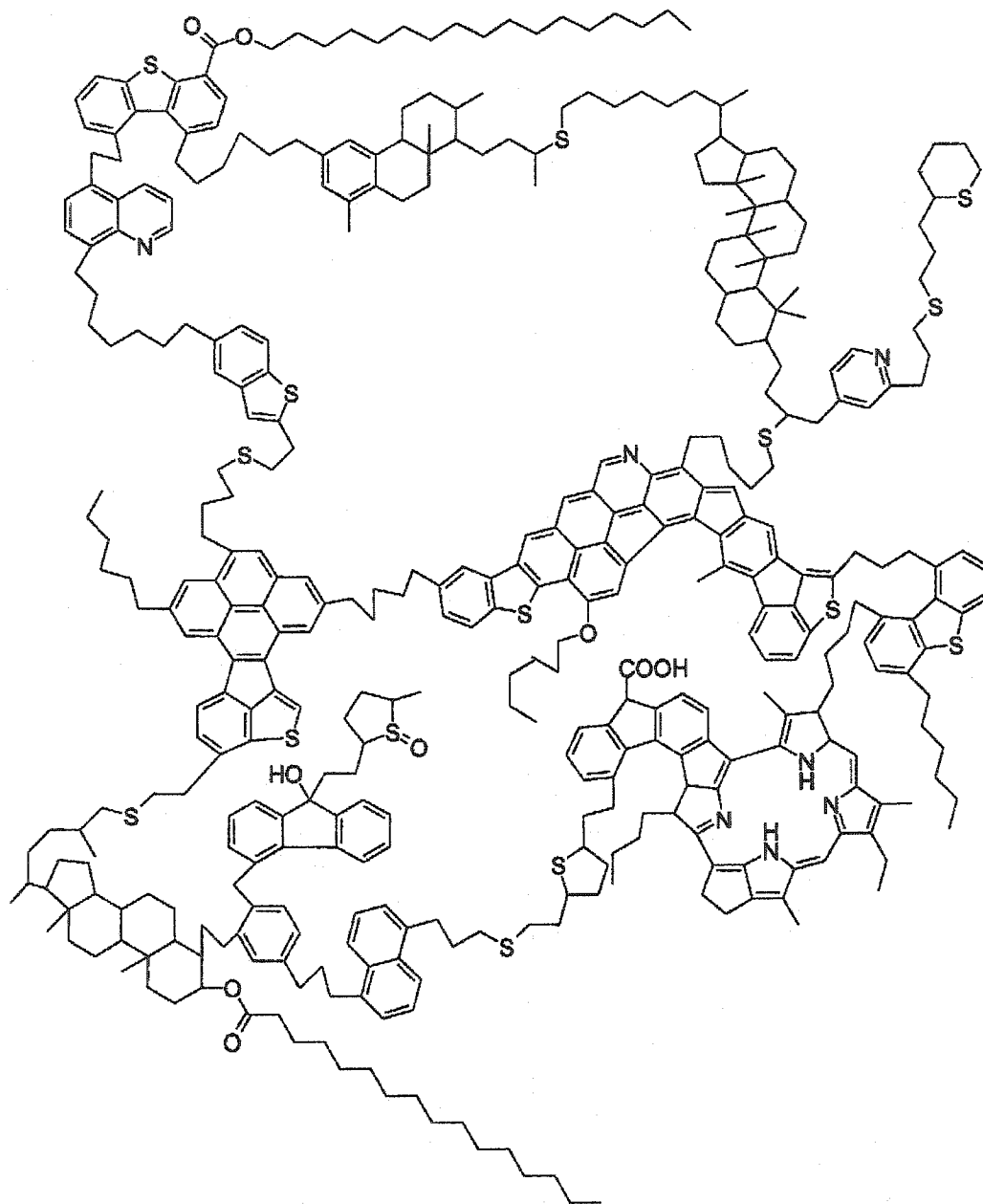
Figure 2.2 A hypothetical asphaltene molecule from Athabasca bitumen (Murgich et al., 1999)

12

2.2.2. Molecular Weight

Molecular weight may be determined by a number of methods including vapor pressure osmometry (VPO); size exclusion chromatography (SEC) which is often referred to gel permeation chromatography (GPC); and nonfragmenting mass spectroscopy, also called parent ion MS (Altgelt et al., 1994). The accuracy of molecular weight determinations of asphaltenes is a debatable issue because the data from same asphaltenes vary considerably depending upon the technique employed for the measurement. Various measurements have yielded values that differ by as much as a factor of 10 or more. For example, field ionization mass spectroscopy results have indicated a molecular weight in the range of 700 amu; while vapor pressure osmometry indicated much larger molecular weights for the same asphaltenes sample, e.g. 4000 amu (Mieczyslaw and Boduszynski, 1981).

VPO and GPC have been extensively used for determining asphaltene molecular weight. Vapor pressure osmometry is one of a group of techniques that measure colligative properties. The method itself is relatively simple and cheap but suffers from a tendency to overestimate the molecular weight, due to asphaltene aggregation. The measured asphaltene molecular weight depends not only on the nature of the solvent and the temperature but also on the solute concentration. Use of elevated temperature and excellent solvents for asphaltenes yields smaller values of molecular weight, indicating that aggregation is an important issue in this technique (Boduszynski, 1984). Table 2-1 gives an example of how the estimated MW from VPO varies with solvent and temperature.

13

Table 2-1 Effect of solvent and Temperature on the MW of hexane insoluble Asphaltenes from Iraqi crude oil measured by VPO (Al-Jarrah et al., 1989)

Solvent	Temperature, °C	M_n, g/mol
Benzene	37	16,840
	45	16,440
	60	14,920
Chlorobenzene	37	6,375
	45	2,750
	60	2,080
	90	2,025
THF	37	13,900
	45	7,550
Nitrobenzene	90	1,400
	120	935

Wiehe (1992) obtained the most consistent results for molecular weights of petroleum fractions using o-dichlorobenzene at a temperature of 130 °C using VPO method. It was found that at 130 °C there was a little change in the apparent molecular weight with concentration whereas the molecular weight increased linearly at 70°C with concentration. Wiehe obtained number average molecular weight of 2980 for unreacted asphaltenes from Cold Lake. Peramanu et al. (1999) reported the number average

14

molecular weight of Athabasca and Cold Lake asphaltenes to be 2005 and 1599, respectively, following the same conditions as Wiehe (1992).

GPC is another attractive technique that sorts molecules according to molecular size and shape (Altgelt et al., 1994). In a recent study Peramanu et al. (1999) found that asphaltene fractions from Athabasca and Cold Lake bitumen contain compounds of molecular weights ranging from 100 to more than 100,000, although their molar average molecular weights were 1801 and 1504, respectively. In GPC, calibration curves are used to convert elution volumes into molecular weight. Compared to polymers, however, the components in petroleum have wide range of polarities and types. Each type would interact with gel surface to a different degree depending on their polarity. Also, petroleum components have a variety of different configurations ranging from largely paraffinic molecules to compact polynuclear ring systems. Different groups of equal molecular weight would have different elution time depending on the molecular structure. Hence, the choice of standards becomes very difficult. In principle, GPC is a very powerful method and can describe the heterogeneity of asphaltenes nicely; however, it suffers from the lack of realistic standards of known number average molecular weight distributions and of chemical nature similar to that of asphaltenes.

Mass spectrometry yields molecular weight values of approximately 700 amu (Boduszynski, 1984), but suffers from possible fragmentation and volatilization issues. Since asphaltene has a broad distribution of molecular weight and fragmentation may occur in a structure like Figure 2.2, the molecular weight measured by the above process may not be the representative molecular weight of the asphaltenes. In a recent study, Groenzin and Mullins (2000) used fluorescence depolarization measurements to

15

determine the size of asphaltene molecules, and used model compounds for comparison. They found mean molecular weights to be in rough agreement with the mass spectroscopy work. A mean molecular weight of roughly 750 amu with a range of 500 to 1000 amu was found for petroleum asphaltenes. The difficulty in this use, as with GPC, is the lack of proper standards for calibration. The best compromise for studying changes in molecular weight appears to be VPO in o-dichlorobenzene at 130°C, to minimize effects due to aggregation.

2.3. Chemical Reactions During Thermal Processing

2.3.1. Cracking Reactions

The various upgrading processes for residue conversion share common reaction chemistry and thermodynamics. The commercial processes for production of distillate products from residue operate at 410-555 °C where thermal cracking reactions are significant. At the temperatures typical of commercial operating conditions, a fraction of the feed will vaporize depending on the severity of the reaction temperature. Even at the maximum temperatures of commercial processes, a significant portion of the feed will be in the liquid phase. The largest thermochemical and kinetic data base exists for the gas phase; however, pyrolysis reactions also occur in liquid or even solid phases. A common approximation is that gas phase equilibrium constants and rate constants for reactions involving carbon-centered radicals are transferable to reactions in relatively nonpolar liquid media (Stein, 1981). It is likely a poorer assumption for radicals centered on heteroatoms.

16

Free radical pathways dominate mechanisms for thermal cracking reactions of organic materials (Poutsma, 2000). Free radical species are highly energetic, short lived and present at very low concentrations. Radical reactions consist of three elementary steps: initiation, propagation and termination. Hydrocarbon thermal cracking reaction mechanisms usually involve a set of reversible reactions that are drawn from a relatively small number of reaction families. Figure 2.3 shows these reaction families, taken from a recent review by Savage (2000). Homolytic dissociation is usually the initiation step, which can require high activation energy. β-scisson and hydrogen abstraction often occurs together in a chain propagation sequence. Energetically these two reactions are preferred reactions, as they require much lower activation energies.

17
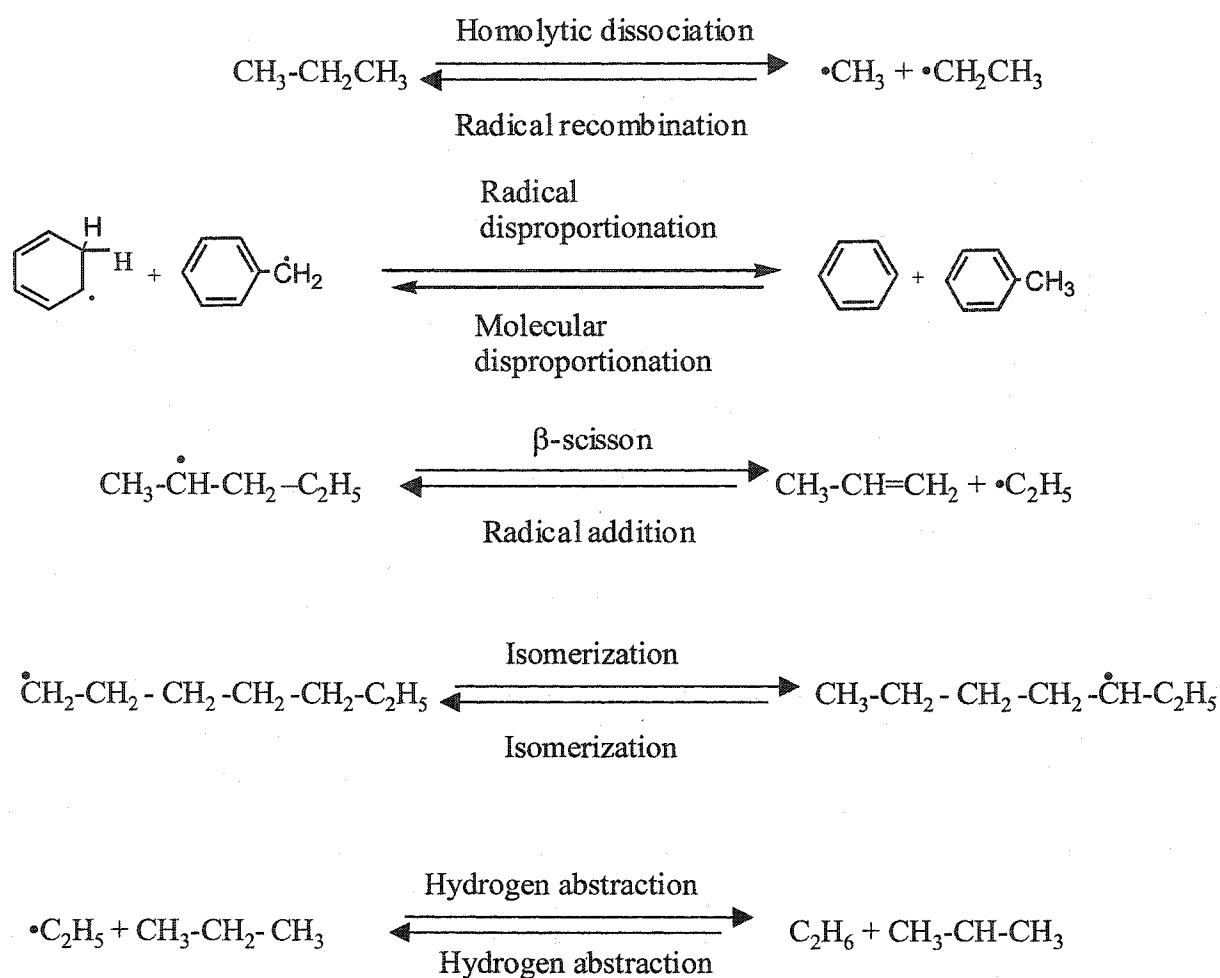
Figure 2.3 Main reaction families for hydrocarbon pyrolysis (Savage, 2000)

For homolytic dissociation, the path that involves cleavage of the weakest chemical bond is expected to be the fastest. The main bonds of interest during primary upgrading are C-C, C-S and C-H bonds. Bond energies give an indication of the difficulty of breakage of the bonds. The C-C bonds in aromatic hydrocarbons are much stronger because of the resonance stabilization, which renders them unbreakable at normal process temperatures (<600 °C) until the aromatic character is destroyed by hydrogenation (Gray, 1994).

18

Table 2-2 Bond dissociation energies (McMillen and Golden, 1982 and Savage, 2000)

Chemical Bond	Representative bond	Energy, KJ/mol
C-C (aliphatic)	C_2H_5-nC_3H_7	365 ± 4
C-H (primary)	C_2H_5-H	420 ± 2.5
C-H (secondary)	iC_3H_7-H	411 ± 2.2
C-H (aromatic)	C_6H_5-H	464 ± 8
C-S	CH_3S-C_2H_5	307 ± 8
C-N	C_2H_5-NH_2	342 ± 8
C-O	C_2H_5O-C_2H_5	344 ± 4

In the initial mechanistic formulation of coal reactivity, homolytic bond scission was postulated to generate free radicals (Curran et al., 1967). The overall reaction mechanism suggested by them was that these free radicals then abstracted hydrogen from the donor solvent, H_2, or coal itself and became "capped". Given the breaking of enough bonds, stable fragments of volatile and soluble products would be formed. However, in the absence of a reactive hydrogen source, these radicals would undergo "condensation" with themselves or other parts of the coal to form stable compounds. In the radical capping mechanism, the rate-determining step is the rupture of covalent bonds that are highly energy intensive (Table 2-2). Observed activation energies for cracking reactions

19

are considerably lower than the bond dissociation energy required for homolytic scission, both for pure compounds and for residues (Olmstead and Freund, 1998) suggesting that homolytic scission is not the rate determining step. The radical capping mechanism does not have proper propagation steps as normally defined, since the hydrogen radicals can only give termination product and would suppress the cracking reactions by shutting down the chain reaction. If every bond-dissociation requires homolytic breakage, without a chain reaction, then the reactions would be too slow to be of any commercial interest.

In recent years several authors have suggested that alkylaromatic materials such as heavy oil undergo cracking via free radical chain reactions (Blanchard and Gray, 1997; Strausz, 1989). In chain reactions, a radical can participate in number of reactions, each with a much lower energy requirement than homolytic bond-cleavage. This type of reaction was first described by Rice and Hertzfield (1934) for n-alkanes. The general mechanism arising from the work by Rice and Hertzfield is depicted below.

Initiation: $\qquad M \xrightarrow{k_1} 2R^{\bullet}$

Propagation:

    Hydrogen abstraction: $R^{\bullet} + M \xrightarrow{k_2} RH + M^{\bullet}$

    β- scission: $\qquad M^{\bullet} \xrightarrow{k_3} R^{\bullet} + \text{Olefin}$

Termination: $\qquad \text{Radical} + \text{Radical} \rightarrow \text{Products}$

Here, M and $M^{\bullet}$ represent the parent alkane and parent radical, respectively; $R^{\bullet}$ and RH are lower alkyl radicals and the corresponding alkanes, respectively. This study was performed for gas phase. LaMarca et al. (1993) suggested a mechanism incorporating chain reactions for liquid-phase cracking reactions of a complex feed. They emphasized

20

the importance of extending the chain reaction as much as possible to maximize conversion of the coal material. Blanchard and Gray (1997) tested the importance of free radical chain reaction in cracking of vacuum residue by adding 1-methyl naphthalene as an alternate radical carrier to the residue. The abstraction of hydrogen from 1-methyl naphthalene would produce relatively stable benzylic radicals. This shift in chain carrier showed two measurable effects: 1) a decrease in the cracking of residue relative to control experiments without diluent and 2) a 3.64 fold increase in the 1-methyl naphthalene derived termination product. Their result was consistent with the general predictions of the mechanism proposed by LaMarca et al. (1993) and indicated a free radical chain mechanism for residue conversion.

2.3.2. Hydrogen Transfer

Hydrogen Transfer is one of the few basic free radical reactions where a hydrogen atom is transferred directly from a donor to an acceptor. Four categories of hydrogen transfer are possible. In *Hydrogen abstraction* a radical abstracts a hydrogen atom from a molecular donor. *Radical disproportion* reactions involve radicals as both donor and acceptor. In *Radical hydrogen transfer* a radical donates a β- hydrogen to an unsaturated acceptor. Finally, in the *Molecular disproportionation* reaction, both the donor and acceptor are spin-paired molecules. This process is often called reverse radical disproportionation (RRD) (Poutsma, 1990). Hydrogen transfers are typically fast reactions and often influence the overall rates of free radical chain processes such as hydrocarbon pyrolysis. These reactions also strongly influence the selectivity to the final products as discussed below.

21

2.3.2.1 Well Defined Mixtures

Hydrogen donors are extremely important in hydrogen transfer reactions. Tetralin had long been recognized as an effective hydrogen donor that is representative of a series of hydroaromatic hydrocarbons used in coal liquefaction. Hooper and co-workers (1979) studied the thermal dissociation of tetralin between 300 and 450 °C. They observed in the temperature range of 400 to 450 °C that the reaction to produce 1-methyl indane was dominant. The reaction was shown not to occur to any measurable degree until some dehydrogenation of tetralin to naphthalene had occurred. From this result they suggested that hydrogen is required for the initiation of the reaction. They observed a sharp increase in the formation of naphthalene at 450 °C for reaction period longer than 2 h. In conjunction with the increased rate of naphthalene formation significant quantities of ethyl benzene, propyl benzene, toluene and indane were formed. From this observation they suggested the following three main processes that were occurring during tetralin dissociation:

22
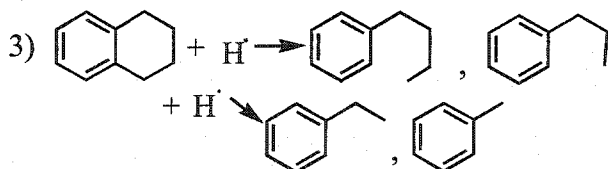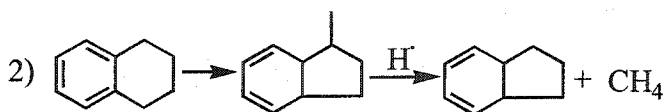
Khorasheh and Gray (1993) studied thermal cracking of n-hexadecane in tetralin at 400-460 °C and 13.9 MPa nitrogen pressure. The rate of cracking of n-C_{16} in tetralin was decreased significantly from the rate observed for the pure compound. The selectivity of α-olefins was decreased with increasing n-C_{16} conversion. They suggested that alkyl radicals from the decomposition of hexadecyl radicals preferentially abstracted hydrogens from tetralin rather than n-C_{16}, which inhibited the chain mechanism for the conversion of n-C_{16}. Hydrogen abstraction from tetralin involved hydrogen in both α- and β- positions of the saturated rings, leading to the formation of 1- and 2-tetralyl radical, which in turn participated in addition reactions with α-olefins leading to the formation of alkyltetralin as major products. Contrary to the radical capping hypothesis, the n-alkyl radicals were not quenched; rather they were transferred to tetralin as an alternate chain carrier.

Product distributions from decomposition of tetralin depend on reaction conditions. In a recent review Poutsma (1990) summarized the following major classes of products from thermal cracking of tetralin: 1) ring contraction to form 1-methylindane and indene, 2) dehydrogenation to form 1,2-dihydronaphthalene and/or naphthalene, 3) ring-opening hydrogenolysis to form n-butylbenzene, and 4) loss of two carbons to give benzocyclobutene, styrene and ethylbenzene. For gaseous tetralin at 400-750 °C, dehydrogenation was the main decomposition path. Whereas, under low pressure, dense phase conditions, isomerization to 1-methylindan, and ring opening to various alkylbenzenes, became significant (Hooper et al, 1979). Khorasheh and Gray (1993) found that the selectivities for naphthalene slightly increase while selectivities for 1-methylindane and indan decreased in the presence of n-C_{16} compared to the thermal

23

cracking of pure tetralin. Also the rate constants for overall conversion of n-C_{16} were decreased in the presence of tetralin. Above discussion suggests that the selectivity and kinetics of donor solvent can be significantly different in the presence of actual residue sample. Many studies were done on the hydrogen transfer of donor solvent to actual oil, some of which are discussed in the following section.

2.3.2.2   Hydrogen Transfer to Actual Oil

Much of the study of hydrogen transfer reaction was done in connection with coal liquefaction. The product selectivity and the kinetic rate of a donor solvent change significantly in the presence of coal. For example, when tetralin was thermolyzed alone in the absence of any resid component, 1- methyl indane was found to be the major product. When Curran et al. (1967) performed experiments with a mixture of tetralin and coal in the temperature range 320 to 440 °C, the principal product resulting from the transfer of hydrogen to the coal was naphthalene, with appreciable quantities of indane and C_4 benzenes. Clearly, coal has an important influence on the behavior of tetralin. Bockrath and Schroeder (1981) showed that the yields of 1- methyl indane and naphthalene were enhanced by the addition of coal at 450 °C. At higher coal to tetralin ratios, naphthalene yield was higher than 1- methyl indane yield.

Similar observations were found by Collin et al. (1985). They studied ring contraction and dehydrogenation in polycyclic hydroaromatics at temperature range 400 to   500   °C.   1,2,3,4,5,6,7,8-Octahydroanthracene   and   1,2,3,4,5,6,7,8,9,10,11,12-dodecahydrotriphenylene were reacted in the presence or absence of bituminous coal. In the absence of coal, they found that the ratio of ring-contracted product to dehydrogenated product increased with increasing reaction temperature, whereas the

24

amount of ring dehydrogenated product was increased considerably by the presence of coal. At 425 °C for a reaction time of 1h, dehydrogenation was favored over ring contraction by a factor of 8 when coal was present, but only by a factor of 2 when coal was absent.

The transfer of hydrogen from hydroaromatic species such as tetralin and 9,10-dihydroanthracene is extremely important in helping to control coking in petroleum residues (Sanford and Chung, 1991; Del Bianco, 1993a). Much of the discussion of the mechanism of hydrogen transfer from donor solvents to various coal and petroleum residue structures is based on the presumption that the principle mechanism involves thermal scission of covalent bonds, following by capping of the resulting free radicals by hydrogen atom abstraction from donor solvents (Curran et al., 1967). However, a number of researchers have pointed out that alternative possibilities such as radical chain processes, and hydrogen atom and radical addition-elimination processes could play important roles in the degradation of coal structures (Franz and Camaioni, 1980; Khorasheh and Gray, 1993). McMillen et al. (1989) suggested a radical hydrogen transfer (RHT) mechanism for the cleavage of strongly bonded coal structures in donor-solvent system. Khorasheh and Gray (1993) suggested a similar mechanism, which consists of reactions in which a radical donates a β-hydrogen to an unsaturated acceptor. Removal of olefins eliminates the pathway for polymerization and coke formation, consequently coke formation is suppressed in the presence of a donor solvent (Gray and McCaffrey, 2002).

2.4. Mechanism of Coke Formation

Coke is defined operationally in petroleum refining as a carbonaceous material that is insoluble in an aromatic solvent such as benzene or toluene. A number of

25

researchers have studied coke formation, and suggested that asphaltenes are mostly responsible for coke formation.

An induction period was observed by a number of investigators during which no coke was formed (Magaril et al., 1968, Savage et al., 1985, 1988; Wiehe, 1993; Srinivasan and McKnight, 1994). From that observation, it was previously suggested that coke was not formed directly from the feed hydrocarbon, but from its cracking products. Following the work of Levinter (1967), many investigators postulated that coke formed as a result of successive reactions of cracking and polymerization steps from the lightest to the heaviest fractions. A general scheme for the coke formation was suggested as:

$$\text{Hydrocarbons} \rightarrow \text{Resins} \rightarrow \text{Asphaltenes} \rightarrow \text{Coke}$$
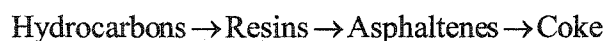
However, the kinetic models including such sequences failed to predict the induction period before the coke formation started.

At present, evidence suggests that coke formation is preceded by phase separation in the liquid phase. Magaril et al. (1968) were the first to theoretically develop the concept of a second liquid phase that they suggested as the precursor of coke, emerging in the early stage of coke formation. Later, many researchers had suggested that the cracking and polymerization could cause incompatibility in the liquid phase, leading to the formation of a separate, dense aromatic liquid phase (Mochida et al., 1988; Wiehe, 1993). Subsequent reactions and phase separation lead to the formation of lamellar mesophase that appears bright under cross-polarized light, indicating ordering of the structures. Based on the studies of oils and its solubility fractions (Magaril et al., 1968; Savage, 1988), Wiehe (1993) proposed a comprehensive model of the coke formation mechanism involving kinetics and phase separation. Thermal cracking reactions leave

26

behind aromatic compounds, which were defined as aromatic cores. These aromatic cores, still soluble in toluene, differ from the original asphaltene in that they have lower H/C and S/C ratios and a higher N/C ratio and of lower molecular weights. When they reach a critical concentration, they separate from the main liquid phase and coke formation follows quickly.

Storm et al. (1996) suggested an alternate mechanistic view of the coke formation. They observed that there was a dispersed phase of particles in vacuum residue associated with the heptane insoluble asphaltenes. Based on the rheological and small angle X-ray scattering data for the vacuum residue of Arabian Medium crude oil, they suggested that the dispersed asphaltenic phase would flocculate at elevated temperatures. This asphaltenic phase, formed by flocculation at temperatures well below the temperature at which chemical reactions occur, was suggested to be the coke precursor phase in the reacting residue as discussed by Wiehe (1993).

In summary, coke formation involves formation of a new phase, either by phase separation or flocculation of asphaltenes. Phase behavior during coking is discussed in greater detail in the following section.

2.5. Phase Behavior during Coke Formation

Many of the ideas of asphaltene phase behavior are guided by the observations at room conditions. At coking conditions, however, asphaltene phase behavior is significantly different from that observed at ambient conditions. Coke materials exhibit fluid properties at elevated temperatures such as coalescence and deformation by shear (Brooks and Taylor, 1965; Mochida et al., 1988). Brooks and Taylor (1965) were the first to observe the thermal transformation of graphitizing carbon to mesophase and coke. In

27

the early stage of graphitization they observed the melting of the original material and the formation of an isotropic pitch like mass. After further heating, anisotropic, micron sized spherical bodies were observed which coalesced with time. This observation is an indication of the separation of a heavy liquid phase.

There have been a number of studies on mesophase formation and their development. Mesophase forms initially as small spheres in a liquid medium of isotropic pitch that can then grow and coalesce, thus producing a two- phase emulsion of spheres. As the heat treatment progresses, the spherules grow and coalesce to form large bulk anisotropic regions. The bulk mesophase regions then spread throughout the carbon to surround the sphere containing isotropic regions (Mochida et al., 1988). Thus the two-phase emulsion goes through a phase inversion. Additional heat treatment leads to the formation of a very high softening point semicoke (Grienke, 1994). The final stage is the formation of large, optically anisotropic domains, known as isochromatic areas, having a mosaic texture (Rahimi et al., 1999).

While both the coke and mesophase are insoluble in toluene, mesophase is distinguished by its insolubility in strong solvents such as quinoline. However, in many of the literature studies, mesophase appearance is often used as an indication of coke formation. Previous study has shown that a significant portion of the toluene insoluble solids can be soluble in quinoline. Wang et al. (1998) showed that under some conditions, all of the toluene insoluble coke was soluble in quinoline, suggesting that the coke observed in that study was not mesophase.

Particulate matter present in the pitch, commonly referred to as quinoline-insoluble fraction (QI), profoundly affects both the thermal behavior of the pitch and

28

optical texture of the final product. Many types of QI have been identified, and their effects on mesophase formation during pitch processing were examined by many researchers (Marsh et al., 1985, Obara et al., 1985). The size of the optical texture of the coke was found to be reduced by the presence of primary QI materials that are usually <1μm diameter and resembles carbon black (Forrest and Marsh, 1983; Marsh and Latham, 1986). The QI material within the pitch adsorbed on the surface of the growth unit of mesophase and thereby prevented the coalescence of these domains. In a recent study, Rahimi et al. (1999) investigated the mesophase size and appearance time of a fraction of mineral-free Athabasca vacuum bottom using hot-stage microscopy. They showed that kaolinite clay had an influence on mesophase formation, growth, and coalescence similar to that of QI observed by others. Kaolinite is the dominant clay mineral in Athabasca bitumen that is produced by oil sand extraction in Alberta (Rahimi et al., 1999).

Tanabe and Gray (1997) suggested that the role of the fine solids in the oil and coke mixture would be equivalent to the observations wherein fine solids inhibited the coalescence of mesophase in a mixture of isotropic pitch and mesophase. They found that the presence of naturally occurring fine mineral solids in the residue fraction of Athabasca bitumen suppressed the rate of coke formation relative to solids-free feed. A highly dispersed coke phase would have more contact with hydrogen donor compounds in the oil phase, that would in turn inhibit the rate of dehydrogenation and polymerization and thus reduce coke formation. Wang et al. (1998) studied the interaction of coke fraction with fine solids by reacting coker gas oil from Athabasca bitumen under

29

hydrogen pressure. Their result suggested that the liquid coke fraction wetted and spread on non-polar surfaces or surfaces with very high surface area.

From the above discussion it can be concluded that apparent phase behavior of coke is affected by: 1) thermodynamics of multiple phases, 2) kinetics of reactions and coalescence and 3) interactions with fine solids. A liquid-liquid phase separation is often suggested to precede coke formation. The phase separation would be affected by the thermodynamic properties of the reactive mixtures and reaction kinetics. The separated phase initially forms as isotropic pitch. After further reactions and coalescence, anisotropic mesophase forms that appear bright under cross-polarized light. Fine solids present in the reaction mixture, greatly affect the phase behavior of coke, likely by providing nucleation sites and helping to disperse the coke material.

2.6. Kinetic Models

The chemistry of coke formation is very complex due to the complexity of the individual reactions. In addition to the complex chemistry, coke formation is believed to involve thermodynamic solubility behavior. In a mixture as complex as petroleum, the reaction processes can only be generalized because of the difficulties in analyzing the product and feedstock. Experimental studies on each possible reactant and intermediate molecules would be tedious, if at all possible. One approach is to do chemical modeling of residue reactions based on structural distribution functions derived from analytical information. The reaction pathways and kinetics of these molecules are determined through model compound experiment. Finally, with an explicit residue structure, a Monte Carlo simulation of its reaction can provide quantitative assessment of the reaction that can be compared with the experimental data. Several authors have modeled the pyrolysis

30

reactions of asphaltenes following this approach (Neurock et al., 1990; Savage and Klein, 1989).

A more empirical approach is to divide the feed and product into pseudo-components and model the reactions between them. One of the most comprehensive studies was done by Banerjee et al. (1986), where they investigated the kinetics of coke formation from five fractions of four different types of bitumen over reaction temperatures ranging from 395 to 510 °C. The five fractions were classified as asphaltenes, soft resin, hard resin, aromatics, and saturates. They found that the coke formation was higher for the feed with higher degree of aromaticity and the order of rate constants for coke formation was as follows:

Asphaltene> Resins> Aromatics > Saturates

They suggested a tentative reaction scheme (Figure 2.4) where the coke was formed in a fast reaction from large aromatic molecules, which in turn were produced by the condensation of small aromatic molecules, or through the formation of resins or of asphaltenes.

31
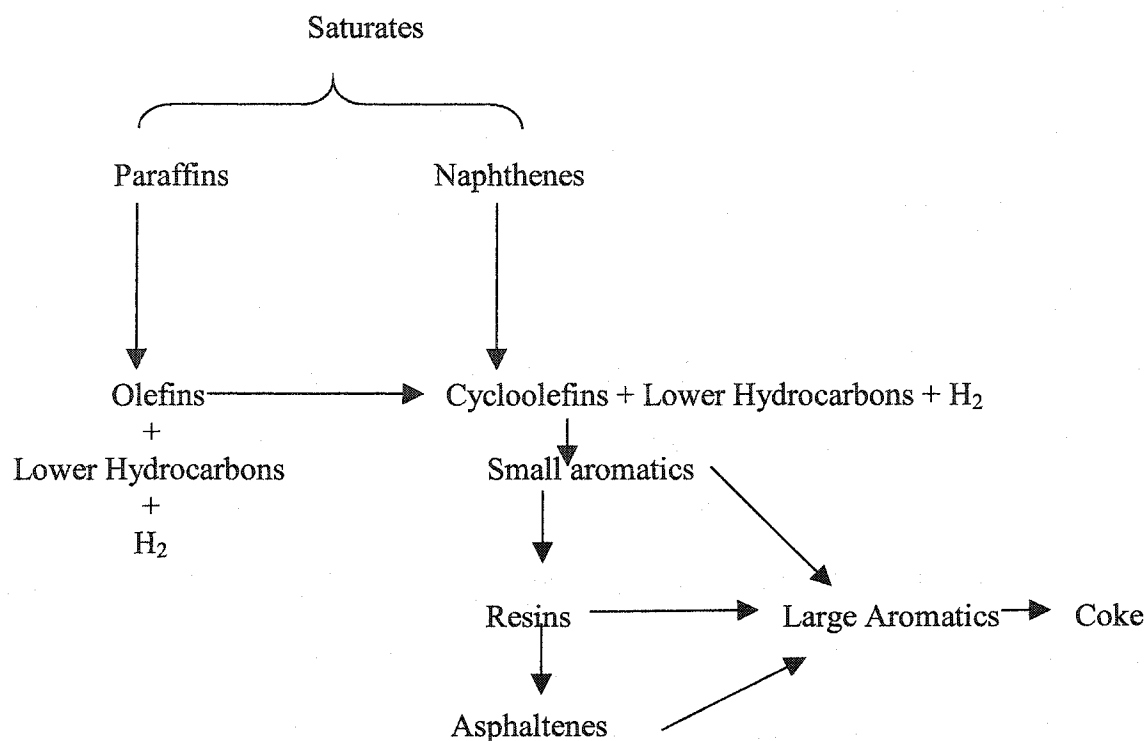
Figure 2.4 Tentative reaction scheme for coke formation (Banerjee et al., 1986)

While many kinetic studies have examine isolated asphaltenes, few researchers had studied the effect of reaction environment (Savage et al., 1988; Trauth et al., 1992). Savage et al. (1988) studied asphaltene pyrolysis and hydropyrolysis, both neat and in solvent, in the temperature range of 350 to 450 °C. They found that the reaction environment altered both the kinetics of asphaltene disappearance and the selectivity to the gas, maltenes, and coke fractions. They interpreted the coke fraction to be a primary product of asphaltene thermolysis, representing the asphaltenic core stripped of its hydrogen rich peripheral substituents and perhaps aromatized. The difference between

32

the coke and asphaltene would be that coke is more hydrogen deficient and insoluble in toluene. Figure 2.5 shows their suggested reaction pathways. Original asphaltenes (A) first lost their peripheral moieties to produce maltenes (M) and gases (G) along with reacted asphaltenes (A*). In the absence of hydrogen or a catalyst, the reacted asphaltenes could only undergo further thermal degradation and ultimately produced coke (C), along with some lighter product (G). For reactions in a hydrogen donor, an additional pathway was available for A* by which they could produce lower molecular weight, heptane-soluble products. In the reaction scheme x, y and z represented the stoichiometric coefficients.

$$
\begin{array}{c}
\quad\quad G \\
\quad zC + (1-z)M \\
A \longrightarrow xA^* + yM + (1-x-y)G \\
\quad\quad M \longrightarrow G
\end{array}
$$
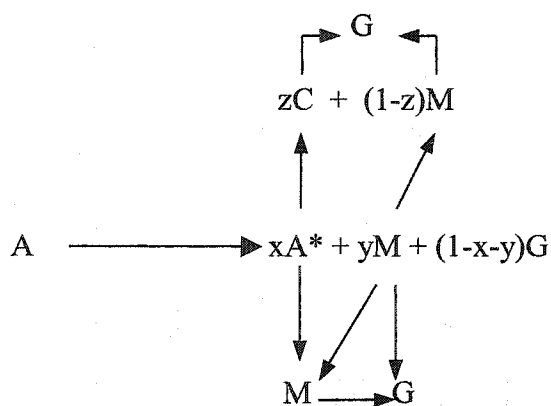
Figure 2.5 Asphaltene thermal and catalytic reaction pathways (Savage et al., 1988)

Trauth et al. (1992) studied the reactivity of isolated asphaltenes and asphaltenes in residue using Hondo and Maya residue as feedstock. Their results were summarized in terms of a lumped reaction network (Figure 2.6).

33
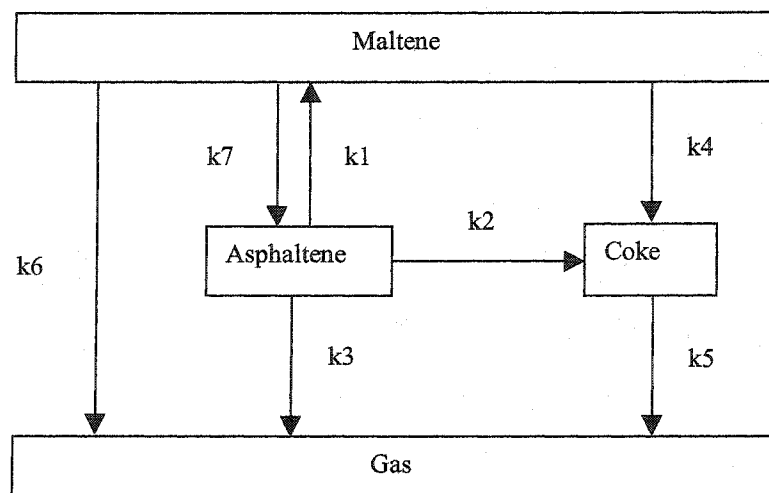
Figure 2.6 Asphaltene pyrolysis pathways model (Trauth et al., 1992)

Del Bianco et al. (1993) developed a simple kinetic scheme from their study of thermal cracking of vacuum residue of Belayam crude at 410 to 470 °C. Three pseudo-components (vacuum residue, distillate and coke) were used to develop the kinetic model. In order to account for the induction period, they introduced a reaction intermediate, I, in their model (Figure 2.7). VR' is the fraction of vacuum residue not converted at time t. They used the relationship VR= VR' + I in order to estimate the concentration of I, where, VR was used as the experimental datum. D and C are the distillate and coke fractions, respectively.

34
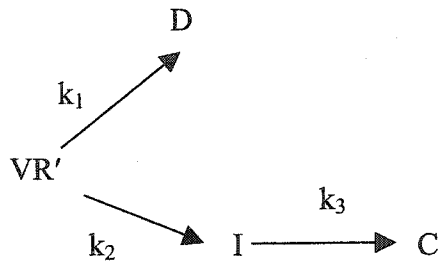
Figure 2.7 A kinetic model of thermal cracking of vacuum residue (Del Bianco, 1993)

Wiehe (1993) developed a kinetic model for coke formation using the concept of Magaril et al. (1968, 1971), that coke formation is triggered by phase separation. According to this model, aromatic asphaltene cores (A*) are formed from unreacted asphaltenes (A$^+$) and heptane solubles (H$^+$) along with volatile liquids (V). When these cores reaches a critical value, defined by solubility limit (S$_L$) in the model, they separate from the hydrogen rich main liquid phase and coke formation follows rapidly. The model was described as follows:

$$H^+ \xrightarrow{k_H} aA^* + (1-a)V$$

$$A^+ \xrightarrow{k_A} mA^* + nH^* + (1-m-n)V$$

Solubility limit: $A^*_{max} = S_L(H^+ + H^*)$

$$A^*_{ex} = A^* - A^*_{max}$$

$$A^*_{ex} \xrightarrow{\alpha} (1-y)TI + yH^*$$
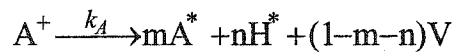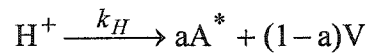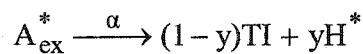
Although many aspects of coke formation were studied before, Wiehe's model was the first where both the kinetics and phase behavior were considered in a single model. The model described the four common features of residue conversion i.e. an induction period prior to coke formation, a maximum concentration of asphaltenes in the reacting liquid, a decrease in the asphaltene concentration that parallels the decrease in

35

heptane soluble material, and the high reactivity of the unconverted asphaltenes. The model was able to correlate data from pyrolysis of maltenes and whole residue with a single set of stoichiometric parameters. Thus the model has considerable potential in describing coking kinetics.

2.7. References

Al-Jarrah, M. M., and Al-Dujaili, A. H., "Characterization of Some Iraqi Asphalts. II. New Findings on the Physical Nature of Asphalts", *Fuel Sci. Tech. Int.,* **1989**, 7(1), 69-88

Altgelt, K. H. and Boduszynski, M. M., "Composition and Analysis of Heavy Petroleum Fractions", Marcel Dekker, Inc., New York, **1994**, Chapter 4

Banarjee, D. K., Laidler, K. J., Nandi, B. N. and Patmore, D.J., "Kinetic Studies of Coke Formation in Hydrocatbon Fractions of Heavy Crudes", *Fuel,* **1986**, 65, 480-484

Blanchard, C. A. and Gray M. R., "Free Radical Chain Reactions in Thermal Hydrocracking of Residues", *Abstr Pap Am Chem Soc.,* **1997**, 42, 137-141

Bockrath, B. C., and Schroeder, K. T., "Coal Mineral Matter Catalysis in Liquefaction, New Approaches in Coal Chemistry", *ACS Symposium Ser. No. 196, chap. 11, American Chemical Society*, Washington D.C., **1981**

Bunger, J. W., and Cogswell, D. E., "Characteristics of Tar Sand Bitumen Asphaltenes as Studied by Conversion of Bitumen by Hydro-pyrolysis", In *Chemistry of Asphaltenes*, Bunger, J. W., Li, N. C., Eds., American Chemical Society, Washington, D. C., **1981**, 219-236

Boduszynski, M. M., "Chemistry of Asphaltenes", Bunger, J. w., Li, N. C., Eds., American Chemical Society, Washington, D. C., **1984**, Chapter 2

Brooks, J. D. and Taylor, G. H., " Formation of Graphitizing Carbons from the Liquid Phase", *Nature*, **1965**, 206, 697-699

Collin, P. J., Gilbert, T. D., Rottendorf H. and Wilson, M. A., "Ring Contraction and Dehydrogenation in Polycyclic Hydroaromatics at Coal Liquefaction Temperatures", *Fuel*, **1985**, 64, 1280-1285

Curran, G. P., Struck, R. T., and Gor, E., "Mechanism of the Hydrogen-Transfer Process to Coal and Coal Extract", *Ind. Eng. Chem. Proc. Des. Dev.* **1967**, 6(2), 166-173

Del Bianco, A., Panariti, N., Anelli, M., Beltrame, P. L. and Carniti, P., "Thermal Cracking of Petroleum Residues 1. Kinetic Analysis of the Reaction", *Fuel*, **1993**, 72, 75-80

Del Bianco, A., Panariti, N., Anelli, M., Beltrame, P. L. and Carniti, P., "Thermal Cracking of Petroleum Residues 1. Hydrogen-Donor Solvent addition", *Fuel*, **1993a**, 72, 81-85

Forrest, M. and Marsh, H., "Growth and Coalescence of Mesophase in Pitches with Carbon- Black Additives and in Coal", *Fuel*, **1983**, 62(5), 612-615

Franz, J. A. and Camaioni, D. M., "Radical Pathways of Coal Dissolution in Hydrogen Donor Media. 2. β Scission and 1, 2 Aryl Migration Reactions of Radicals Derived from Methylindans and Tetralin at 327-627 °C", *J. Org. Chem.*, **1980**, 45, 5247-5255

Freund, H. and Olmstead, W., "Thermal Conversion Kinetics of Petroleum Residua", AIChE Spring Meeting, New Orleans, LA, **1998**, paper 34b

37

Gray, M. R. and McCaffrey, W. C., "Role of Chain Reactions and Olefin Formation in Cracking, Hydroconversion, and Coking of Petroleum and Bitumen Fractions", *Energy & Fuels*, **2002**, 16, 756-766

Greinke, R. A., " Early Stages of Petroleum Pitch Carbonization-Kinetics and Mechanisms", *Chemistry and Physics of Carbon*, Thrower P. A., Ed, **1994**, 24, 1-43

Groenzin, H., and Mullins, O. C., "Molecular Size and Structure of Asphaltenes from Various Sources", *Energy & Fuels*, **2000**, 14, 677-684

Hooper, R. J., Hendrik, A. J., and David G. E., " Thermal Dissociation of Tetralin between 300 and 450 °C", *Fuel*, **1979**, 58, 132-138

Khorasheh, F. and Gray, M. R., "High-Pressure Thermal Cracking of n-Hexadecane in Tetralin", *Energy & Fuels*, **1993**, 7, 960-967

Koots, J.A. and Speight, J.G., "Relation of Petroleum Resins to Asphaltenes", *Fuel*, **1975**, 54, 179-184

LaMarca, C., Libanti, C., Klein, M. T. and Cronauer, D. C., "Enhancing Chain Transfer During Coal-Liquefaction- A Model System Analysis", *Energy & Fuels*, **1993**, 7, 473-478

Levinter, M. E., Medvedeva, M. I., Panchenkov, G. M., Agapov, G. I., Galikbarov, M., Galikeev, R. K., "The Mutual Effect of Group Components During Coking", *Khim. Tekhnol. Topl. Masel.*, **1967**, No 4, 20-22

Magaril, R. Z. and Aksenova, E. I., "Study of the Mechanism of Coke Formation in the Cracking of Petroleum Resins", *Inter. Chem. Eng.*, **1968**, 8(4), 727-729

Magaril, R. Z., Ramazaeva, L. F. and Aksenova, E. I., "Kinetics of the Formation of Coke in Thermal Processing of Crude Oil", *Inter. Chem. Eng.*, **1971**, 11(2), 250-251

Marsh, H., Latham, C. S. and Gray, M. E., "The Structure and Behavior of QI Material in Pitch", *Carbon*, **1985**, 23, 555- 570

Marsh, H. and Latham, C. S., "The Chemistry of Mesophase Formation", *Petroleum Derived Carbon*, Bacha, J. D., Newman, J. W. and White, J. L., Eds., Am. Chem. Soc., Washington, D. C., **1986**, 1-28

Mazza, A. G. and Cormack, D. E., "Thermal Cracking of the Major Chemical Fractions of Athabasca Bitumen", *AOSTRA J. Res.*, **1988**, 4, 193-208

McMillen, D. F. and Golden, D.M., " Hydrocarbon Bond-Dissociation Energy", *Annu. Rev. Phys. Chem.*, **1982**, 33, 493-532

McMillen, D. F., Malhotra, R. and Nigenda, S. E., "Mechanism of Hydrogen Transfer and Bond Scisson of Strongly Bonded Coal Structures in Donor-Solvent Systems", Fuel, **1987**, 66, 1611-1620

Mieczyslaw, M. and Boduszynski, M. M., "Asphaltenes in Petroleum Asphalts", In *Chemistry of Asphaltenes*, Bunger, J. W., Li, N. C., Eds., Am. Chem. Soc., Washington, D. C., **1981**, 119-135

Mochida, I., Oyama, T., Korai, Y., and Fei, Y. Q., " Study of Carbonization using a Tube Bomb: Evaluation of Lump Needle Coke, Carbonization Mechanism and Optimization", *Fuel*, **1988**, 67, 1171-1181

Murgich J., Abanero, J. A. and Strausz, O. P., "Molecular Recognition in Aggregates Formed by Asphaltene and Resin Molecules From Athabasca Oil Sand", *Energy & Fuels*, **1999**, 13, 278-28

Neurock, M., Libanti, C., Nigam, A. and Klein, M. T., "Monte-Carlo Simulation of Complex Reaction Systems- Molecular Structure and Reactivity in Modeling Heavy Oils", *Chem. Eng. Sci.*, **1990**, 45, 2083-2088

Obara, T., Yokono, T., Sanada, Y. and Marsh, H., "Carbonization Behavior of Pitch in the Presence of Inert Material", *Fuel*, **1985**, 64, 995-998

Peramanu, S., Pruden, B. B., and Rahimi, P., "Molecular Weight and Specific Gravity Distributions for Athabasca and Cold Lake Bitumens and Their Saturate, Aromatic, Resin and Asphaltene Fractions", *Ind. Eng. Chem. Res.*, **1999**, 38, 3121-3130

Pfeiffer I. and Saal R.N., "Asphaltic Bitumens as a Colloidal System", *J. Phys. Chem.*, **1940**, 44, 139-149

Poutsma, M. L., " Free Radical Thermolysis and Hydrogenolysis of Model Hydrocarbons Relevent to Processing of Coal", *Energy & Fuels*, **1990**, 4(2), 113-131

Poutsma, M. L, "Fundamental Reactions of Free Radicals Relevant to Pyrolysis Reactions", *J. Anal. Appl. Pyrolysis.*, **2000**, 54, 5-35

Rahimi, P., Gentzis, T. and Faribridge, C., "Interaction of Clay Additives with Mesophase Formed during Thermal Treatment of Solid-Free Athabasca Bitumen Fraction", *Energy & Fuels*, **1999**, 13, 817-825

Sanford, E. C., "The Nomenclature and Jargon of Residuum Upgrading: A Critical Review", *AOSTRA J. Res.*, **1991**, 7, 201-208

Sanford, E. C and Chung, K. H., "The Mechanism of Pitch cConversion During Coking, Hydrocracking and Catalytic Hydrocracking of Athabasca Bitumen", *AOSTRA J. Res.*, **1991**, 7, 37-45

Savage, P. E., Klein, M. T., Kukes, S. G., "Asphaltene Reaction Pathways. 1. Thermolysis", *Ind. Eng. Chem. Proc. Des. Dev.*, **1985**, 24, 1169-1174

Savage, P. E., Klein, M. T., Kukes, S. G., "Asphaltene Reaction Pathways. 3. Effect of Reaction Environment", *Energy & Fuels*, **1988**, 2, 619-628

Savage, P. E. and Klein, M. T., "Asphaltene Reaction Pathways. V. Chemical and Mathematical Modeling", *Chem. Eng. Sci.*, **1989**, 44(2), 393-404

Savage, P. E., "Mechanisms and Kinetics models for Hydrocarbon Pyrolysis", *J. Anal. Appl. Pyrolysis.*, **2000**, 54, 109-126

Speight, J. G., "Thermal Cracking of Athabasca Bitumen, Athabasca Asphaltenes, and Athabasca Deasphalted Heavy Oil", *Fuel*, **1970**, 49, 134-145

Speight, J. G., "Polynuclear Aromatic Systems in Petroleum", *Preprints. Div. Petrol. Chem. Am. Chem. Soc.*, **1986**, 31(4), 818-825

Speight, J. G., "Initial Reactions in the Coking of Residua", *Preprints. Div. Petrol. Chem. Am. Chem. Soc.*, **1987**, 32(2), 413-418

Speight, J. G., "The Chemistry and Technology of Petroleum", 2nd edition, Marcel Dekker, Inc., New York, **1991**, Chapter 11

Speight, J. G., "Asphaltenes and Asphalts,1", Yen, T. F., and Chilingarian, G. V., Eds., Elsevier Science, New York, **1994**, Chapter 2

Srinivasan, N. S. and McKnight, C. A., "Mechanism of Coke Formation from Hydrocracked Athabasca Residuum", *Fuel*, **1994**, 73, 1511-1517

41

Stein, S. E, *J. Am. Chem. Soc.*, "Comparison of Equilibrium Constants in Gas and Liquid Phases", **1981**, 103, 5685

Strausz, O. P., "Structural Studies on Resids: Correlation Between Structure and Reactivity", *AIChE Symp. Ser.*, **1989**, 85 (273), 1-6

Strausz, O. P., Mojelsky, T. W., Lown, E. M., "The Molecular Structure of Asphaltene-An Unfolding Story", *Fuel*, **1992**, 71, 1355-1362

Storm, D. A., Barresi, R.J. and Sheu, E.Y., " Flocculation of Asphaltenes in Heavy Oil at Elevated Temperatures", *Fuel Sci and Technol Int'l.,* **1996**, 14 (1&2) , 243-260

Tanabe, K., and Gray, M. R., " Role of Fine Solids in the Coking of Vacuum Residues", *Energy & Fuels*, **1997**, 11(5), 1040-1043

Trauth, D. M., Yasar, M., Neurock, M., Nigam, A., Klein, M. T. and Kukes, S. G., "Asphaltene and Resid Pyrolysis: Effect of Reaction Environment", *Sci. and Technol. Int'l.,* **1992**, 10(7), 1161-1179

Wang, S., Chung, K., Masliyah, J. H. and Gray, M. R., " Toluene-Insoluble Fraction from Thermal Cracking of Athabasca Gas Oil: Formation of a Liquid-In Oil Emulsion that Wets Hydrophobic Dispersed Solids", *Fuel*, **1998**, 77(14), 1647-1653

Wiehe, I. A., "A Solvent Resid Phase Diagram for Tracking Resid Conversion", *Ind. Eng. Chem. Res.,* **1992**, 31, 530-536

Wiehe, I. A., "A Phase Separation Kinetic Model for Coke Formation", *Ind. Eng. Chem. Res.,* **1993**, 44, 2447-2457

Yen, T. F., "Present Status of the Structure of Petroleum Heavy Ends and its Significance to Various Technical Applications", *Am. Chem. Soc. Div. Pet. Chem. Prepr.,* **1972**, 17, 102-104

3. MATERIALS AND METHODS

3.1. Materials

3.1.1. Solvent Interactions with Asphaltene during Coke Formation

In order to study the kinetics of solvent interactions, asphaltenes (A) were separated from Athabasca vacuum residue (VR). First, the mineral solids were removed by digesting VR in 40 parts of toluene for overnight and then filtering it on 0.22 µm filter paper. Toluene was removed by a rotary evaporator and 40 parts of heptane was mixed overnight. Heptane-insoluble asphaltenes were separated by filtration through a 0.22 µm Millipore™ filter. Table 3-1 gives the properties of Athabasca VR and asphaltenes.

For the kinetic experiments, Athabasca asphaltenes (A) and vacuum residue (VR) in different proportions were dissolved in heptane and then sonicated for half an hour. The heptane was then evaporated at 70°C under vacuum until the weight of the mixture became constant. This procedure gave mixtures with different ratios of asphaltenes to maltenes, which was then used as the feed for a series of experiments.

In the experiments with solvents, Athabasca asphaltene was mixed with each of the three diluents: 1-methyl naphthalene (1-MN), tetralin (TN) and naphthalene (NP). The 1-MN and TN of 95% purity were obtained from Aldrich (Mississauga, Ontario). Laboratory grade NP was obtained from Fisher Scientific (Toronto, Ontario). n-Dodecyl sulfide (DDS) was used as initiator. DDS of 93% purity was obtained from Acros Organics (Fairlawn NJ).

43

Table 3-1 Properties of Athabasca Vacuum Residue and Asphaltenes

Property	Vacuum Residue[a]	Asphaltenes
Density, g/cm^3 at 20 °C	1.0868	nd[b]
Carbon, wt%	81.6	80.84
Hydrogen, wt%	9.1	7.99
H/C Ratio	1.34	1.19
Sulfur, wt%	5.72	7.47
Nitrogen, wt%	0.72	1.27
Molecular weight (VPO)	1190	4253
Aromatic carbon, %	39	53
Microcarbon residue, wt%	27.8	nd[b]

a) Properties of Athabasca Vacuum residue are taken from McCaffrey *et al.* (1998)

b) nd=not done

3.1.2. Coking Kinetics as a function of Asphaltene Structure

Asphaltenes from five different sources were used to study the effect of asphaltene structure on reaction kinetics. Athabasca, Gudao, Arab Heavy and Arab Light asphaltenes were separated from the vacuum residue and Maya asphaltenes from bitumen. Asphaltenes were separated following the same procedure as mentioned in section 3.1.1. Only Athabasca vacuum residue had significant amount of fine solids in it (1.8 wt%). All other feeds did not have a measurable amount of toluene insoluble fine

44

soids. Therefore, toluene filtration was omitted for the separation of the other four asphaltenes.

3.1.3. Phase Behavior

Materials from only Athabasca were used to study the phase behavior during coking. Athabasca asphaltene mixed with maltene or 1-methyl naphthalene was used to study the influence of diluent on the phase behavior. Two supercritical fluid extraction (SFE) fractions (the lightest fraction, fraction-1 and the heaviest, or end cut) were used as feed materials to study the role of fine solids. Supercritical fluid extraction using pentane is capable of cutting deep into bitumen at a temperature much lower than the cracking temperature of the feedstock. Fraction-1 and end cut constitute approximately 10 and 40 wt% of the vacuum residue. Syncrude Research Center in Edmonton, Canada, provided the fractionated samples. The properties of the two fractions used in this study are listed in Table 3-2.

Table 3-2 Composition of SFE fractions of Athabasca residue (524 $^{\circ}$C +) fraction

Fraction #	1	end cut
Molecular weight	506	4185
S, wt%	4.1	6.51
MCR, wt%	5.64	48.94
Asphaltene, wt%	0	88.03

3.2. *Experimental Methods*

3.2.1. Thermolysis Experiments

Experiments were carried out batchwise in a 15 ml micro reactor made from Swagelock™ fittings and tubing. The reactor was loaded with 3 g of reactant and then pressure tested with nitrogen at 4 MPa. The gas was then vented, and the reactor was pressurized twice more with nitrogen and vented to purge residual oxygen. The reactor was heated in a fluidized sand bath and agitated at ca. 1 Hz for the duration of the reaction interval, then quenched by plunging the reactor in cold water. The contents of the reactor reached the final temperature within 5 minutes. All of the reactions were carried out at 430 °C under nitrogen environment. The initial cold pressure of nitrogen was atmospheric for maltene system and 3-4 MPa for the aromatic solvents. Higher pressure was used for the aromatic solvents to keep them in the liquid phase at the reactor condition. Approximately 85% of each solvent was estimated to be in the liquid phase at 430°C, using the Peng-Robinson equation of state (ASPEN Plus software, Aspen Technology, Cambridge, MA).

3.2.2. Separation

Liquid product and coke were washed out of the reactor with 40 parts of toluene, then kept overnight at 70 °C to ensure the extraction of liquid products from the solid coke. Coke was then removed from the toluene solution by filtration on a 0.22 μm Millipore™ filter. Coke yield was determined by weighing the filter after drying in vacuum at 70 °C for 12 hours. Toluene was removed from the filtrate by rotary

46

evaporation, the oil was then blended with 40 parts of n-heptane to precipitate asphaltenes. Solid asphaltenes were recovered by filtration and vacuum dried at 70 °C for 12 hours to give the asphaltene yield. Heptane was removed from the heptane soluble fraction by rotary evaporation and then by vacuum drying at 70 °C.

3.2.3. GC Analysis

The heptane-soluble fractions of the product were analyzed by a Hewlett Packard 5890 GC using a HP-1 crosslinked methyl silicone gum column (25m, 0.32 mm ID, 0.17μm) equipped with a flame ionization detector (FID) and a computer for storing the chromatograms. The temperature program for the GC was as follows: initial oven temperature of 50 °C, then heating to 300 °C at a rate of 5 °C/minute and then held at constant temperature for 15 minutes.

To evaluate hydrogen donor ability of the solvents, anthracene (ANT) was used as a hydrogen acceptor compound. Solvents were reacted in excess ANT for 40 min. Heptane soluble fractions of the reaction product from the solvent and ANT were analyzed by capillary gas chromatography. The GC analysis of the reacted ANT alone showed no detectable amount of decomposition products under the reaction conditions. When solvents were added with ANT, two major hydrogenated products, 9,10-dihydroanthracene (DHA) and 1,2,3,4-tetrahydroanthracene (THA) were found. DHA was identified by comparing the retention time with the actual component. The presence of both DHA and THA were also confirmed by GC-MS analysis. Hydrogen donor ability was determined by measuring the amount of DHA and THA, and the amount was calculated using the following equation:

47

$$\text{Amount H Donated} = \frac{\text{mole DHA} * 2 + \text{mole THA} * 4}{\text{g initial solvent}}$$

Hydrogen donation was quantified by analyzing the liquid product from A+TN reaction. Tetralin would be dehydrogenated to produce 1,2-dihydro naphthalene and/or naphthalene. Only naphthalene could be detected in the samples. The quantity of hydrogen transferred from tetralin was estimated from the amount of naphthalene, considering that for every mole of naphthalene produced, 4 atoms of hydrogen were transferred from tetralin.

3.2.4. Scanning Electron Microscopy (SEM)

Coke samples were prepared for SEM by drying and then dispersing by sonication in ethanol for approximately 15 minutes. A drop of this mixture was taken on a plate and was dried in air. The sample holder was then coated with gold. This sample was then observed under a Hitachi S-2700 SEM with a Princeton Gamma- Tech EDX.

3.2.5. Nuclear Magnetic Resonance Spectroscopy

The ^{1}H NMR samples was prepared by mixing approximately 20 mg of the sample with 700μL deuterochloroform ($CDCl_3$). For the ^{13}C NMR samples, approximately 100mg of material were used in 600 μL $CDCl_3$ for the distillate fraction and 700 μL $CDCl_3$ for residue samples. The NMR experiments were performed at room temperature (20 ± 1 °C) on a Varian XL-300 NMR spectrometer, operating at 299.943 MHz for proton and 75.429 MHz for carbon.

48

The proton spectra were collected with an acquisition time of 2.1 s, a sweepwidth of 7000 Hz, a pulse flip angle of 30.8° (8.2 μs), and a 1-s recycle delay. These pulse recycle conditions permit the collection of quantitative spectra for all protonated molecular species in the petroleum samples where the maximum spin lattice relaxation time (T_1) is expected to be less than 20 s. The spectra, resulting from 128 scans and using 0.3-Hz line broadening, were referenced to the residual chloroform resonance at 7.24 ppm.

The quantitative carbon spectra were acquired using an acquisition time of 0.9 s and a sweepwidth of 16,500 Hz. For distillate, a flip angle of 26.2° (4.6μs) and recycle delay of 10 s were used, and for the residue samples, a flip angle of 31.9° (5.7μs) and a 4-s delay were used. These parameters are quantitative for carbons with spin lattice relaxation times (T_1) of the order of 100 s in distillate and 30 s in the residue. Reverse-gated waltz proton decoupling was used to avoid nuclear Overhauser effect enhancements of the carbon signals. The spectra were the result of 5000 scans for the distillate and 15,000 scans for the residue. Line broadening was used to improve the signal-to-noise ratio of the spectra. Distillate spectra used 5-Hz line broadening while residue spectra used 10 Hz. All spectra were referenced to the $CDCl_3$ resonance at 77.0 ppm.

The chemical shift assignments for the ^{1}H and ^{13}C NMR are shown in Table 3-3 and Table 3-4 respectively. These assignments were based on model compound assignments (Snape et al., 1979; Thiel and Gray, 1988), 2-D NMR spectroscopic techniques like HETCOR (heteronuclear chemical shift correlation) and COSY (homonulear correlation spectroscopy) (Sarpal et al., 1996) as well as 1-dimensional

49

techniques such as DEPT (distortionless enhanced polarization transfer) (Netzel, 1987; Kotlyar et al., 1987).

Table 3-3   Chemical shifts of proton spectral regions

Region	Chemical Shifts (ppm)	Structural type
HA1	10.7 to 7.4	Polyaromatic
HA2	7.4 to 6.2	Monoaromatic
HO1	6.2 to 5.1	Olefinic CH
HO2	5.1 to 4.8	Olefinic CH_2
HO3	4.8 to 4.3	Olefinic CH_2
HP1	4.3 to 2.4	α to Aromatic
HP2	2.4 to 2.0	α to Aromatic
HP3	2.0 to 1.09	Paraffinic CH_2
HP4	1.09 to -0.5	Paraffinic CH_3

The final calculations performed to obtain the different carbon functionalities are shown in Table 3-5 (Japanwala et al., 2002). The aromatic CH's, terminal methyls and the methyls of aromatic ethyls were determined directly from the carbon spectra. These groups are based on minimal assumptions and may be considered to be very accurate.

50

Table 3-4   Chemical shifts of carbon spectral regions

Region	Chemical Shifts (ppm)	Structural Type
CA1	190 to 170	Oxygenated
CA2	170 to 129	Quaternary aromatic
CA3	129 to 115.5	Aromatic CH
CA4	115.5 to 113.5	Olefinic CH_2
CA5	113.5 to 100	Olefinic CH_2
CP1	70 to 45	Paraffinic CH
CP2	45 to 32.7	Paraffinic CH & CH_2
CP3	32.7 to 30.8	Chain γ -CH_2 β to aromatic CH_2
CP4	30.8 to 28.5	Chain δ -CH_2 α to aromatic naphthenes, Aromatic-attached ethyl CH_2
CP5	28.5 to 25	Cycloparaffin CH_2
CP6	25 to 21.9	Chain β -$CH_{2,}\alpha$ to aromatic or isobutyl CH_3
CP7	21.9 to 17.6	α to Ring CH_3
CP8	17.6 to 14.7	Aromatic-attached ethyl CH_3
CP9	14.7 to 12.3	Chain α -CH_3
CP10	12.3 to 0	Branched-chain CH_3

51

The other groups listed below were calculated using data from both proton and carbon spectra or had to be estimated due to spectral overlap and are therefore subject to larger margins of error. The substituted quaternary carbon (Qar-S) was determined from the proton spectra by converting the α to aromatic CH_2 and CH_3 protons to their respective amounts of carbon. The remaining amount of quaternary carbon was considered to be bridgehead carbon (Qar-P). The methyl carbons attached to aromatic (Ar-CH3) were determined by evaluating the respective proton spectral region HP2. The remaining α to ring CH_3's were assumed to be attached to cycloparaffinic rings (Cy-CH_3). The olefinic carbon was also obtained from the proton spectra. Half of region CP2 was estimated to be paraffinic CH's and the total CH's were calculated as the sum of region CP1 and one-half of region CP2. The CHAIN carbon were calculated from region CP4 after the contributions of CH_2 carbon from aromatic attached ethyls and β to aromatic cycloparaffinic CH_2 was removed. The β to aromatic cycloparaffinic CH_2 were estimated as half of the cycloparaffinic region CP5. Finally, NAPH fraction was evaluated from region CP5 only as an indicator of cycloparaffinic content.

52

Table 3-5   Group classifications of chemical species

Chemical Species	Spectral Region
Oxygenated carbon (C=O)	CA1
Aromatic CH (CHar)	CA3
Methyl of an aromatic ethyl (E-CH$_3$)	CP8
Terminal methyl of a paraffinic chain	CP9
Paraffin-substituted Qar (Qar-S)	HP1 + HP2 converted to C wt.%
Polyaromatic quaternary (Qar-P)	CA2 – S-Qar
α -to Aromatic ring methyl (Ar-CH$_3$)	HP2 converted to C wt.%
α -to Cycloparaffin ring methyl	(CP7 + CP6/2) - Ar-CH$_3$
Olefin CH	HO1 converted to C wt.%
Olefin CH2	HO2 converted to C wt.%
Paraffinic CH (CH)	CP1 + CP2/2
> C5 chains (CHAIN)	CP4 – CP8 – CP5/2
Cycloparaffin CH$_2$ (NAPH)	CP5

3.2.6. Sulfide Analysis

Aliphatic sulfides were measured by selectively oxidizing them to sulfoxide followed by infrared spectroscopy (IR) determination. Aliphatic sulfides in the asphaltenes were mildly oxidized using the method of Green et al. (1993). About 0.2 g of

53

sample was dissolved in 25 ml of toluene plus 5 ml of methanol and then about 0.2 g of tetrabutylammonium periodate was added as oxidant. Tetrabutylammonium periodate was obtained from Aldrich Chemical Company, Inc. The resulting mixture was stirred and refluxed for 30 min in a 100 ml round bottom flask connected with a short condenser and a magnetic stirrer. This mild oxidation converted the aliphatic sulfides to sulfoxide without appreciably affecting aromatic sulfur. The oxidized mixture was then cooled and extracted in a separatory funnel three times, with about 100 ml of high purity water per extraction. The organic phase was then dried in rotary evaporator, followed by an additional 2 hr drying in vacuum oven at about 70°C. A measured quantity of the dried product, at about 0.2 g, was dissolved in dicloromethane to make a solution of 4 ml, and its sulfoxide content was measured by IR absorbance. All IR measurements were performed with a FTS 6000 infrared spectrometer with a removable cell containing KBr windows and a 0.015 mm teflon spacer. Background was subtracted from the spectrum of the sample solution. Sulfoxides were measured via their maximum absorbance near 1025 cm^{-1}. The molar absorptivity of 245 L mol^{-1} cm^{-1} was used to calculate sulfoxide in all the asphaltenes (Green et al., 1993). The absorptivity was measured from a calibration based on a petroleum fraction, and therefore, should be more reliable than the absorptivity from a pure compound that may not be totally representative of petroleum derived species. The weight percent of sulfur in the sulfoxide form was calculated from the Equation 1:

$$\text{Wt \% S (SO type)} = \frac{32A}{abc} \times 100 \qquad (1)$$

A = absorbance

a = molar absorptivity, 245×10^3 ml mol^{-1} cm^{-1}

54

b= cell path length, cm

c= sample concentration, g/ml

32= atomic weight of S

3.3. Reference

Green J.B., Yu S.K.T., Pearson, C. D., Reynolds J. W.," Analysis of Sulfur Compound Types in Asphalt", *Energy & Fuels*, **1993**, 7, 119-126

Japanwala, S., Chung, K. H., Dettman, H. D. and Gray, M. R, "Quality of Distillates from Repeated Recycle of Residue", *Energy & Fuels*, **2002**, 16, 477-484

Kotlyar, L.S., Morat, C. and Ripmeester, J.A., "Structural Analysis of Athabasca Maltenes Fractions Using Distortionless Enhancement By Polarization Transfer (DEPT) Related C-13 NMR Sequences", *Fuel*, **1991**, 70, 90-94

McCaffrey, W. C., Cameron, R. A. and Gray, M. R., "Physical Behavior of Bitumen Under Rapid Heating", *Prepr. ACS Div. Petrol. Chem.*, **1998**, *43*, 616-618

Netzel, D. A., "Quantitation of Carbon Types Using DEPT Quat NMR Pulse Sequences-Application to Fossil Fuel Derived Oils", *Anal. Chem.*, **1987**, 59(14), 1775-1779

Sarpal, A.S., Kapur, G.S. and Chopra, A., "Hydrocarbon Characterization of Hydrocracked Base Stocks by One- and Two-Dimensional NMR Spectroscopy", Fuel, **1996**, 75, 483-490

Snape, C. E. and Ladner, W. R., "Survey of Carbon-13 Chemical Shifts in Aromatic Hydrocarbons and Its Application to Coal-Derived Materials", *Anal. Chem.*, **1979**, 51(13), 2189-2198

Thiel, J. and Gray, M. R., "NMR Spectroscopic Characteristics of Alberta Bitumens", *AOSTRA J.*, **1988**, 4, 63-73

4. PHASE BEHAVIOR

4.1. Introduction

Phase behavior plays an important role in coke formation. Reactions such as cracking and polymerization can lead to the incompatibility in the liquid phase, resulting in phase separation (Magaril, 1968; Wiehe, 1993). Coking follows the formation of a new phase either via liquid phase separation (Magaril, 1968; Wiehe, 1993) or by flocculation of asphaltene micelles (Storm et al., 1996). Subsequent reactions and phase separation within the coke material lead to the formation of anisotropic mesophase that appears bright under the cross polarized light (Brooks and Taylor, 1965). Storm et al. (1996) suggested an alternative mechanistic view of coke formation. Based on data for the size of dispersed asphaltenes and rheological measurements, they suggested that asphaltenic phase form by flocculation at around 200°C, well below the temperatures at which chemical reactions occur. This flocculated phase is the precursor to the coke-producing phase in the reacting residue. An alternate explanation for the rheological changes observed by Storm et al. (1996) is the formation of dispersed droplets of liquid phase. For example, Rand (1986) found that the viscosity tends to increase as the volume fraction of the mesophase increases.

If fine solids are present during coking, the developing coke components in the new phase may interact with fine solids via mechanism such as nucleation of the coke phase, dispersion of the coke, or flocculation with coke solids. Fine solids are originally present in Athabasca bitumen and are characterized as mainly mineral clays coated with strongly bound toluene insoluble organic materials (Kotlyar et al., 1998). Several studies have indicated the importance of interaction of fine solids with the mesophase formation.

56

The addition of fine solids was found to interfere with the coalescence of mesophase in coal tar (Bradford et al., 1971; Dubois et al., 1970). Tanabe and Gray (1997) have suggested that the fine solids may prevent coalescence of coke particles as observed in mesophase formation, thereby altering the coking kinetics. They showed that fine solids inhibited coke formation in Athabasca vacuum residue when reacted in a batch reactor at 430 °C. The reduction of coke yield was as much as 7-9 wt% after 20-30 min when compared to the coke yield from residue without fine solids. Fine solids are potentially important in affecting the coalescence of the coke phase, which in turn affects the total coke formation kinetics.

Normally, when two immiscible components form a dispersion, the major component forms the continuous phase. The average particle size increases with the volume fraction of the dispersed phase. A dual phase continuity of the two phases is commonly observed during the mixing of polymer blends at approximately 50/50 composition (Hietaoja et al., 1994). At higher concentrations, phase inversion generally takes place, i.e. the dispersed particles form the continuous phase after they disintegrate. Dispersed particles will disintegrate when the total force acting on the particle is greater than the surface tension. The phase inversion point generally depends on the concentration and viscosity ratio of the components under the conditions of blending (Hietaoja et al., 1994). Analogous to polymer blends, a situation may arise during coke formation when the coke particles will form the continuous phase i.e. a phase inversion may take place.

The objective of this study was to investigate the phase behavior of coke during cracking of asphaltenic material. Two aspects of the phase behavior were studied: 1) the

57

influence of fine solids and diluent on the morphology of the coke phase and 2) the possibility of phase inversion during coking. Athabasca asphaltenes mixed with 1-methyl naphthalene or maltenes and a mixture of two supercritical fluid extraction (SFE) fractions of Athabasca vacuum residue were used as the feed materials. The end cut of the SFE fraction was used as a source of fine solids since it contained almost 4.9 wt% of solids. Scanning electron microscopy (SEM) was used as the main tool for examining the phase behavior. SEM is a very useful tool as it is very simple to operate; and gives three dimensional images that are easier to analyze than the two dimensional micrographs obtained by most optical and TEM techniques (Sawyer et al., 1987). However, SEM did not provide information on internal details of the coke particles.

4.2. Experimental Observation of Coke Morphology

4.2.1. Coke formation with solvent dilution

Coke samples from different reactions were observed under SEM to define the morphology of the coke phase. Coke samples from the thermal cracking of Athabasca asphaltenes mixed with different solvents at different dilution were chosen for this study. Asphaltenes were made solid free following the procedure mentioned earlier (Chapter 3). Selected solvents were heptane-soluble maltene, which is the naturally occuring solvent in the vacuum residue, and aromatic solvent 1-methyl naphthalene. Sample preparation for SEM is described in Chapter 3. Selected micrographs of coke particles are presented in Figure 4.1 to Figure 4.5. Figure 4.1 shows the SEM micrograph of toluene insoluble coke produced from the coking reaction of Athabasca asphaltenes in 1-methyl naphthalene. Spherical particles of coke were observed, mostly of the order of 1 µm.

58

Most of the spheres were lightly attached with each other, due to the lower rate of coalescence in this dilute system. Some coalescence of spheres was also observed (Figure 4.1). Coalescence of small spheres gave rise to larger spheres. Observation of coke spheres and agglomerated spheres suggest that this material was liquid or plastic at reactor conditions. To minimize the surface energy, a liquid coke phase dispersed in a continuous oil phase would be expected to assume the shape with the smallest area and exist as an emulsion of spheres, analogous to spheres of mesophase in pitch at similar temperatures (Mochida et al., 1988).

59
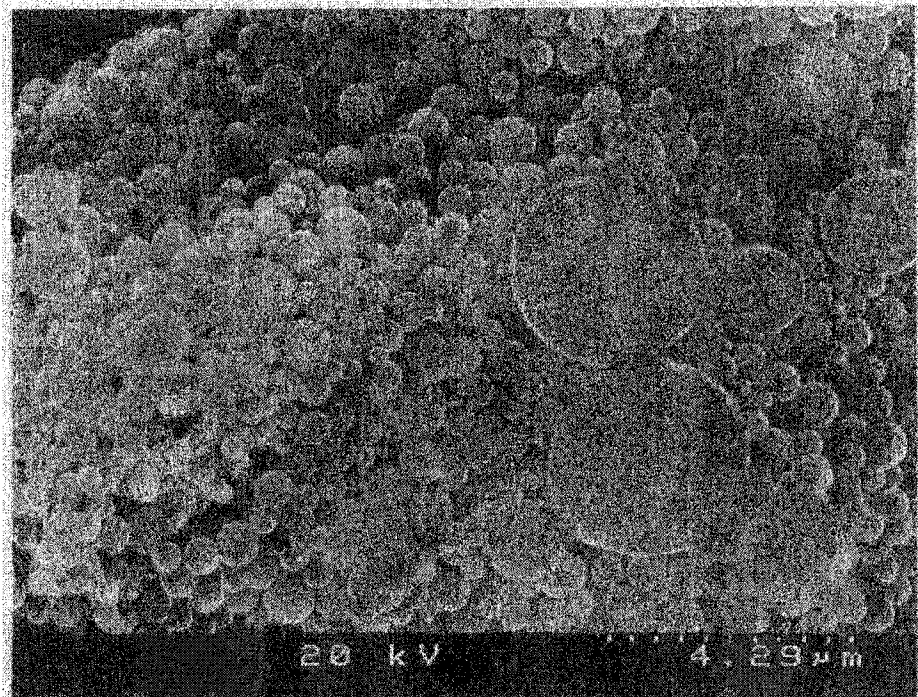
Figure 4.1 Micrograph of coke from 30 wt% asphaltene in 1-methyl naphthalene (MN) at

430°C and 40 min
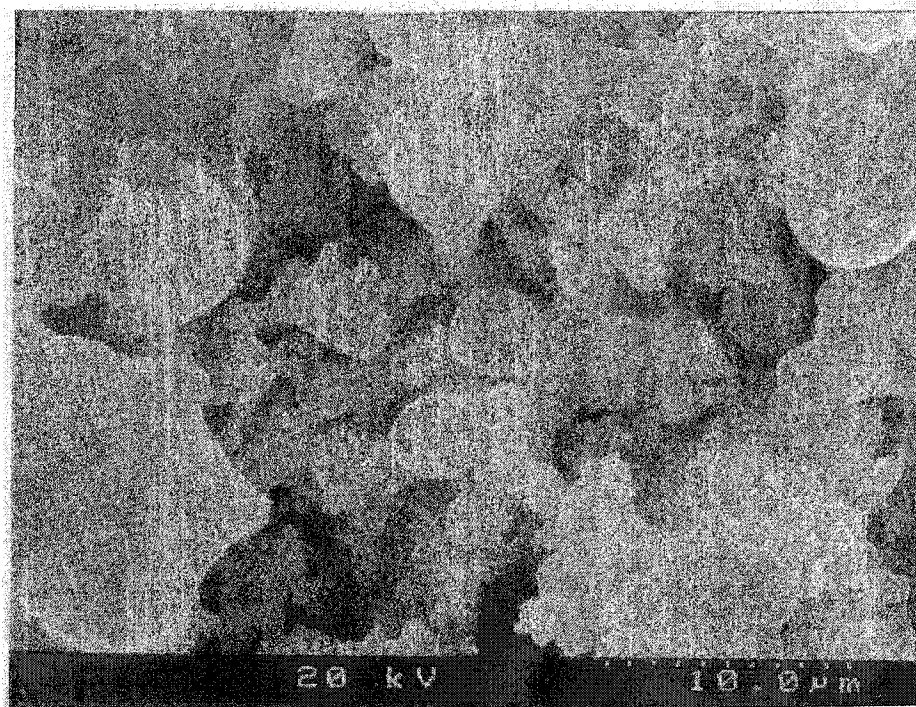
Figure 4.2 Micrograph of coke from Athabasca asphaltene at 430°C and 40 min

61
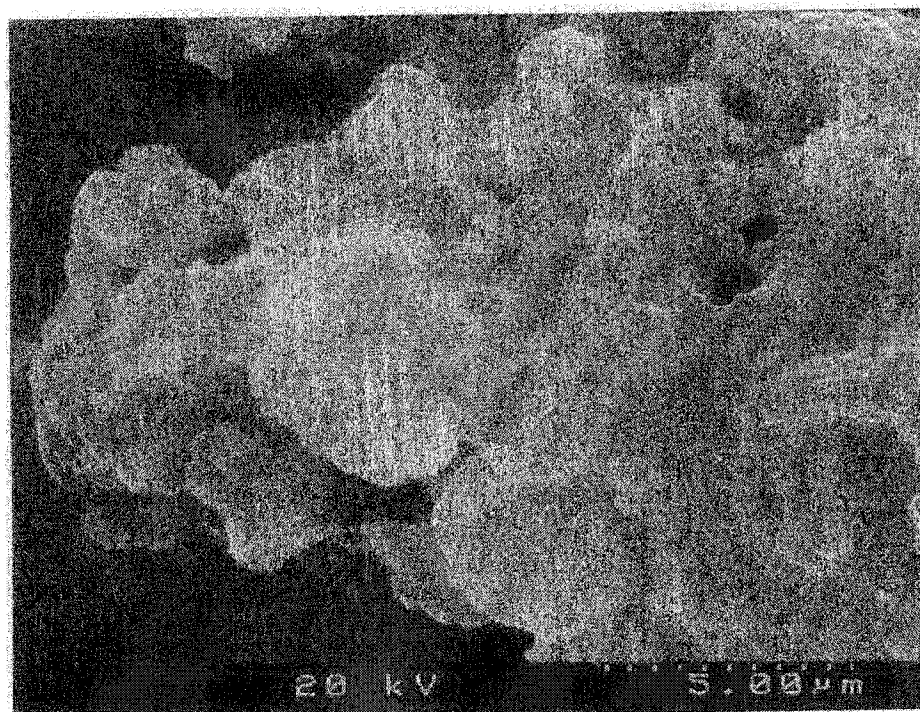
Figure 4.3 Micrograph of coke from 75.6 wt% Athabasca asphaltene in maltene at 430°C
and 40 min
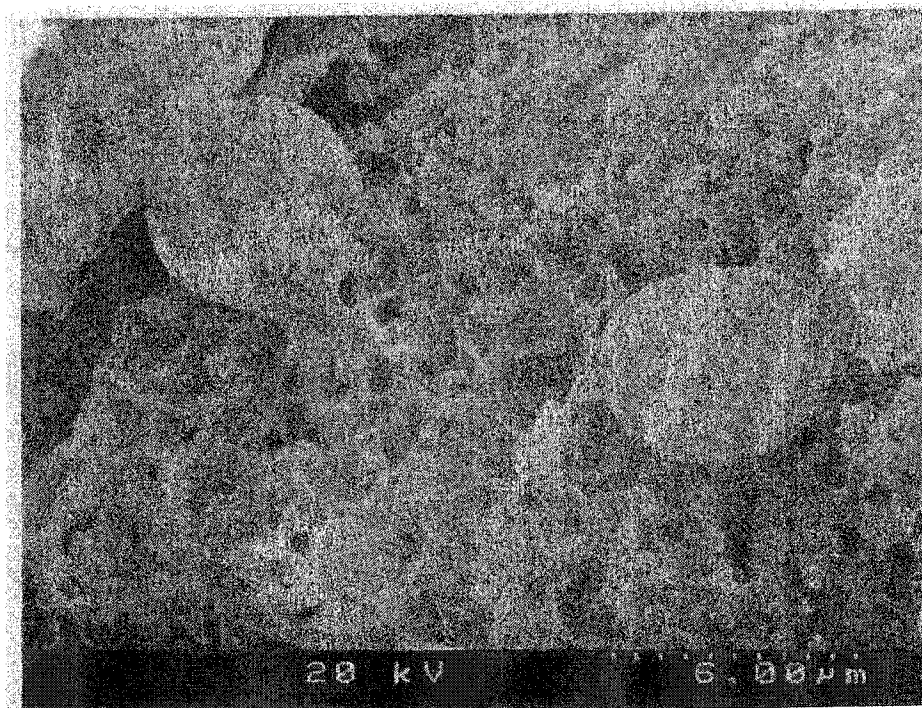
Figure 4.4 Micrograph of coke from Athabasca asphaltene at 430°C and 40 min

63
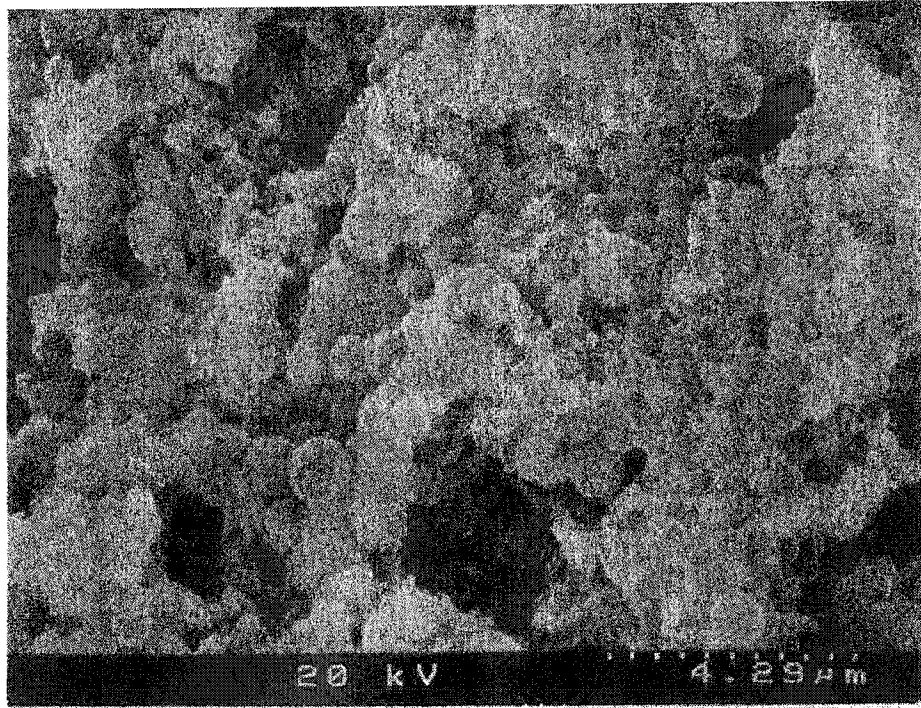
Figure 4.5 Micrograph of coke from the end cut of SFE fraction at 430°C and 40 min

64

During coalescence, attractive dispersion forces as well as Brownian and hydrodynamic forces act as the driving force for the droplets to merge whereas high viscosity of the polymeric phase existing between the droplets inhibits the growth (Yarranton, 1997). Due to two opposing forces, a relaxation time is required to merge the coalescing particles into a single sphere. It is well known that any two droplets of like phase separated by a second continuous phase have an attractive dispersion force (Van der Waals force), which is inversely proportional to the square of the separating distance between them. Thus, there should exist a stronger attractive force between the particles in concentrated mixture. Hence coalescence was more prominent for the coke produced from the thermal cracking of asphaltene without solvent (Figure 4.2). The average particle size was found to be larger for coke from pure asphaltenes compared to the coke from a dilute system, e.g. 30 wt% asphaltenes in 1-MN, likely due to the higher concentration of coalescing particles in pure asphaltenes.

Frequent coalescence, flowing features and larger particles were also observed for 75.6 wt% asphaltene in maltene (Figure 4.3). Figure 4.4 shows a SEM micrograph of coke from asphaltenes. This micrograph is quite different from the one presented in Figure 4.2, although both of them are from the same coke sample. Figure 4.1 and Figure 4.2 are examples of situation where coke separated out as spheres from the continuous oil phase. In contrast, Figure 4.4 shows a situation where coke was the continuous phase and oil was dispersed in it. The holes in the picture suggest the presence of spherical droplets of a dispersed oil phase in the continuous coke phase. During the filtration, the oil droplets were washed out, leaving these honeycomb like structures. Although, this type of phenomenon was observed from a sample from pure asphaltenes, it does not confirm

65

that other feeds would not have such a phenomenon. Depending on the concentration and viscosity of the materials, a phase inversion may take place, examples of which are abundant in polymer science (Hietaoja et al., 1994; Willis et al., 1991).

4.2.2. Role of fine solids in coke morphology

Coke samples from the thermal cracking of end cut of the SFE fraction of vacuum residue were compared with the ones mentioned in section 4.2.1 in order to study the role of fine solids in coke morphology. The end cut of the vacuum residue contained almost 88 wt% asphaltene and about 4.9% toluene insolubles. These toluene insolubles, commonly reffered to as bitumen solids, are predominantly nano-sized (<200 nm) aluminosilicate clay particles with an irregular surface coverage of polar and aromatic toluene insoluble organic matter (Bensebaa et al., 2000). Although end cut contained almost 88 wt% asphaltene, the observed morphology was quite different between the sample from 75.6% asphaltene in maltenes and end cut (Figure 4.3 and Figure 4.5). Less coalescence in the coke from end cut may be due to the presence of mineral solids. The presence of mineral solids in the residue fraction of Athabasca bitumen and in the end cut fraction were found to have an influence on the coke formation rate compared to the solid free feed (Tanabe and Gray, 1997). The above authors suggested that the fine solids might have helped the dispersion of the coke precursor phase at the reaction conditions by accumulating at the interface between the coke and the oil phase. The accumulation at the interface prevented the coalescence and thereby altered the rate of formation of solid coke. Later Wang et al. (1998) studied the formation of coke fraction and its interaction with fine solids by reacting coker gas oil from Athabasca bitumen in a stirred batch reactor at 300- 420°C and a total pressure of 13 MPa of hydrogen. The addition of 5

66

micron kaolin particles gave a small reduction in the mean size of the spheres. EDX analysis showed that some clay was trapped inside or adsorbed on the surface. However, the formation of coke spheres was completely suppressed by the presence of either non-polar particle surfaces or a very large particle surface area, although the coke yield remained unchanged. Their observation suggested that the liquid coke fraction wetted and spread on the clay surfaces. Similarly, solids present in end cut might initially act as highly dispersed nucleation sites and let coke deposit at those sites, providing a better dispersion for the coke particles. Enhanced mass transfer area would promote the hydrogen transfer reactions between the coke phase and the bulk oil phase, consequently forming a reduced amount of coke as observed by Tanabe and Gray (1997). Comparison of the Figure 4.3 and Figure 4.5 suggest that coke from end cut was better dispersed than the coke from 75.6% asphaltene, although the asphaltene content was similar in both cases. Due to better dispersion, the resultant particles were smaller and coalescence was less. The average particle diameter was 0.78 ± 0.06 μm for the coke resulting from end cut, whereas average particle diameter for the coke from asphaltenes was 2.19 ± 0.4 μm. Particle diameter was measured using image analysis software (Sigmascan Pro), and the sample size was minimum 60 or greater for each case.

Rahimi et al. (1999) found that clay particles affected the size of the mesophase that was formed from Athabasca bitumen vacuum bottoms during hot stage microscopy experiment. They found that kaolinite with a mediun size of 3μm had a significant effect in reducing the size and deformation of the mesophase, resulting in a nonflow type domain optical texture. The formation of the small sized mesophase was explained in terms of increasing apparent viscosity of the isotropic matrix. The presence of kaolinite

67

prevented the molecules in the pitch matrix from acting as lubricants and restricted the coalescence of the mesophase. The phenomenon observed during the mesophase formation can be compared with the behavior observed in this study. If the mineral solids are trapped inside the coke particles, the viscosity of the coke phase will increase and allow less coalescence. The extent of coalescence is a function of viscosity of the polymeric phase, and requires that the polymer remains sufficiently deformable to respond to the requirements of minimum surface energy and hence develops the new spherical shape (Marsh, 1974).

Based on the study of the morphology of the coke, it was found that the coke spheres stay better dispersed in dilute system and in the presence of mineral solids. A series of experiments were done where both the concentrations of fine solids and diluent were varied. Two supercritical fluid extraction (SFE) fractions: the lightest fraction, fraction-1 and end cut, were mixed at different weight ratios to give the feed materials. The properties of fraction-1 and end cut were listed in Chapter 3. End cut of SFE fraction served as the source of coke precursor phase, also as a source of mineral solids. Fraction-1, which had no asphaltene and mineral solid content and a very low MCR content, acted as the diluent. The feed materials were then thermally cracked at 430°C for 40 min and the coke materials were separated following the procedure mentioned earlier.

All the SEM micrographs of the coke samples showed similar morphology (Appendix A2). They were mostly small spheres with little coalescence between the particles. Table 4-1 shows the average size of the coke spheres for the different feeds. Although the feed composition varied from nearly 10 wt% end cut to 100 wt% end cut, the average size of the spheres did not show a statistically significant difference (based on

68

95% confidence limits). The reason for this similarity is likely that both solvent and mineral solids help the spheres to be better dispersed. Due to good dispersion in each case, the coke spheres are of similar sizes over a wide range of concentration of end cut.

Table 4-1 Average diameter of the spherical coke particles produced from reaction of mixtures SFE end cut and SFE fraction #1

Weight fraction of end cut	Coke yield, g/100 g Feed	Mean diameter, micron	Standard deviation
0.1055	2.3	0.81	0.11
0.2017	6.3	0.71	0.06
0.3986	15.8	0.82	0.27
0.497	23.6	1.08	0.21
0.695	33.4	0.61	0.05
1	43	0.78	0.12

4.3. Thermodynamics of Phase Inversion During Coking

4.3.1. Theory

Consider the case of configuration 1 in Figure 4.6 where coke is dispersed in the continuous oil phase similar to the situation shown in Figure 4.1. In configuration 2, the dispersed phase became the continuous phase as in Figure 4.4. In both cases the reservoir temperature is T_R. For convenience, the coke phase is represented by α and the oil phase is represented by β. The coke and oil phases constitue the system and the rest of the

69

reactor along with the fluidized sand bath constitutes the reservoir. If for a given volume

fraction and composition, the entropy of the system and reservoir in state 2 becomes

greater than the entropy of the system and reservoir in state 1, i.e. S_2-S_1>0, then from the

thermodynamic point of view, configuration 2 can spontaneously form from

configuration 1.

Configuration 1   Configuration 2
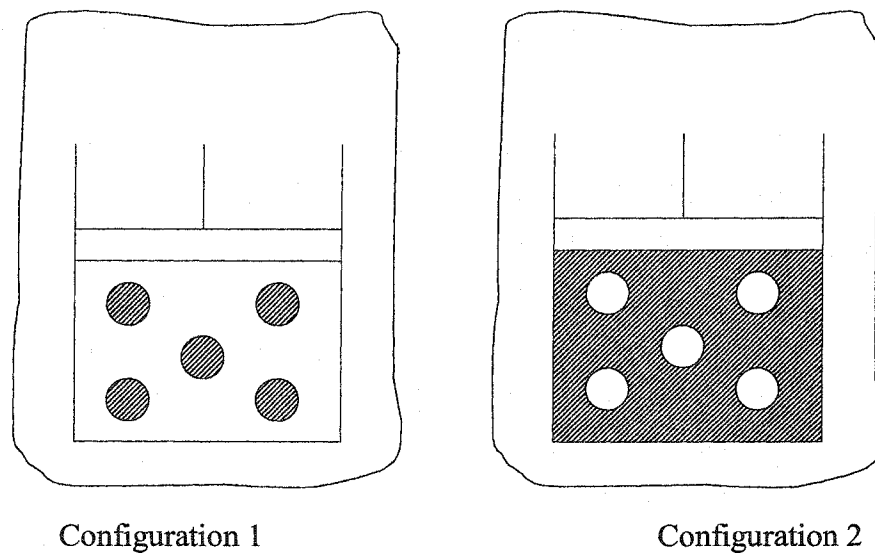
Figure 4.6 Schematic representation of phase inversion. Shaded area is the α phase and

unshaded area is the β phase

One can show from the Euler equation that the entropy for a bulk phase, assuming

one component, can be represented by the following equation:

$$S = \frac{U}{T} + \frac{PV}{T} - \frac{\mu N}{T}$$ (1)

70

where, U is the internal energy, T is the temperature, P is the pressure and V is the total volume of the phase, μ is the chemical potential and N is the number of moles.

The Euler equation for a surface would be as follows:

$$S^\sigma = \frac{U^\sigma}{T^\sigma} - \frac{\gamma A^\sigma}{T^\sigma} - \frac{\mu^\sigma N^\sigma}{T^\sigma} \tag{2}$$

where the superscript σ is used to denote the surface, A is the area of the surface, and γ is the interfacial tension. The total entropy for configuration 1 contains four contributions

$$S_1 = S_1^\alpha + S_1^\beta + S_1^\sigma + S_1^R \tag{3}$$

Superscript R denotes the reservoir. Introducing equations (1)-(2) in equation (3) one can get the entropy for configuration 1 as follows

$$S_1 = \frac{U_1^\alpha}{T_1^\alpha} + \frac{P_1^\alpha V_1^\alpha}{T_1^\alpha} - \frac{\mu_1^\alpha N_1^\alpha}{T_1^\alpha} + \frac{U_1^\beta}{T_1^\beta} + \frac{P_1^\beta V_1^\beta}{T_1^\beta} - \frac{\mu_1^\beta N_1^\beta}{T_1^\beta} + \frac{U_1^\sigma}{T_1^\sigma} - \frac{\gamma_1^\sigma A_1^\sigma}{T_1^\sigma} - \frac{\mu_1^\sigma N_1^\sigma}{T_1^\sigma}$$

$$+ \frac{U_1^R}{T_1^R} + \frac{P_1^R V_1^R}{T_1^R} - \frac{\mu_1^R N_1^R}{T_1^R} \tag{4}$$

A similar expression can be obtained for configuration 2

$$S_2 = \frac{U_2^\alpha}{T_2^\alpha} + \frac{P_2^\alpha V_2^\alpha}{T_2^\alpha} - \frac{\mu_2^\alpha N_2^\alpha}{T_2^\alpha} + \frac{U_2^\beta}{T_2^\beta} + \frac{P_2^\beta V_2^\beta}{T_2^\beta} - \frac{\mu_2^\beta N_2^\beta}{T_2^\beta} + \frac{U_2^\sigma}{T_2^\sigma} - \frac{\gamma_2^\sigma A_2^\sigma}{T_2^\sigma} - \frac{\mu_2^\sigma N_2^\sigma}{T_2^\sigma}$$

$$+ \frac{U_2^R}{T_2^R} + \frac{P_2^R V_2^R}{T_2^R} - \frac{\mu_2^R N_2^R}{T_2^R} \tag{5}$$

Certain constraints can be imposed in view of the reactor conditions and the feed properties. The reaction was carried out in a constant volume closed reactor at a constant temperature. Therefore, it has been assumed that

71

$$T_1^{\alpha} = T_1^{\beta} = T_1^{\sigma} = T_1^{R} = T_2^{\alpha} = T_2^{\beta} = T_2^{\sigma} = T_2^{R} = T \qquad (6)$$

By definition of the system

$$P_1^{R} = P_2^{R} = P^{R} \qquad (7)$$

It has also been assumed that

$$V_1^{R} = V_2^{R} = V^{R} \qquad (8)$$

since coke and the toluene soluble fraction can be considered as incompressible fluids. Conservation of mass

$$N_1^{\alpha} + N_1^{\beta} + N_1^{\sigma} = N_2^{\alpha} + N_2^{\beta} + N_2^{\sigma} = N \qquad (9)$$

The reaction is taking place inside the reactor; however, after the reaction is almost complete, it can be considered that at certain time the total number of molecules in the reservoir has a certain value that does not change when inversion takes place.

$$N_1^{R} = N_2^{R} = N^{R} \qquad (10)$$

Total internal energy should be equal in states 1 and 2, since the reservoir plus the reactor forms a closed system.

$$U_1^{\alpha} + U_1^{\beta} + U_1^{\sigma} + U_1^{R} = U_2^{\alpha} + U_2^{\beta} + U_2^{\sigma} + U_2^{R} \qquad (11)$$

At any time if phases α and β constitute the volume V, then

$$V_1^{\alpha} + V_1^{\beta} = V_2^{\alpha} + V_2^{\beta} = V \qquad (12)$$

Volume of the molecules at the interface was accounted for in the bulk phases, using Gibb's dividing surface approximation. For a certain volume fraction

$$V_1^{\alpha} = V_2^{\alpha} \quad \text{and} \quad V_1^{\beta} = V_2^{\beta} \qquad (13)$$

72

There may be slight changes in the volume during phase inversion due to volume of mixing, which was ignored here. When two liquid phases coexist at isothermal equilibrium, the chemical potential for each species is the same in both phases

$$\mu_1^\alpha = \mu_1^\beta = \mu_1^\sigma \tag{14}$$

$$\mu_2^\alpha = \mu_2^\beta = \mu_2^\sigma \tag{15}$$

For a spherical surface in equilibrium, pressure inside and outside a liquid sphere can be presented by the Laplace equation as follows

$$P^I - P^O = \frac{2\gamma}{R} \tag{16}$$

where, P^I is the pressure inside the sphere and P^O is the pressure outside the sphere, and R is the radius of the sphere. For state 1 and state 2 the Laplace equation becomes

$$P_1^\alpha - P_1^\beta = \frac{2\gamma}{R_1} \tag{17}$$

$$P_2^\beta - P_2^\alpha = \frac{2\gamma}{R_2} \tag{18}$$

The pressure in the continuous phase should remain essentially constant, i.e.

$$P_2^\alpha = P_1^\beta \tag{19}$$

Therefore, equation (18) becomes

$$P_2^\beta - P_1^\beta = \frac{2\gamma}{R_2} \tag{20}$$

For an incompressible fluid or a slightly compressible fluid, the chemical potential can be represented as

$$\mu\ (T,\ P) = \mu(T_o,\ P_o) + v\ (P - P_o) \tag{21}$$

73

where T_o and P_o are the reference temperature and pressure, and v is the molar volume. Therefore, the difference in chemical potential for β phase can be represented by the following equation

$$\mu_1^\beta - \mu_2^\beta = v^\beta (P_1^\beta - P_2^\beta) \tag{22}$$

Subtraction of equation (4) from equation (5) and use of equations (6) to (22) yields the entropy difference as

$$S_2 - S_1 = \frac{\gamma}{T}\left[\frac{2}{R_2}\left(V - Nv^\beta\right) - \left(A_2^\sigma - A_1^\sigma + \frac{2V^\alpha}{R_2} + \frac{2V^\alpha}{R_1}\right)\right] \tag{23}$$

4.3.2. Estimated Entropy Differences for Phase Inversion

In order to study the phase inversion during coke formation, coke from the reaction of only solids free feeds was considered, since solids were found to influence the coke morphology considerably. From the literature of polymer blends and mesophase formation, the phase inversion point depends mostly on the concentration and viscosity ratio. Therefore, it is more probable to find coke phase continuous for a higher volume fraction of coke.

In order to check the feasibility of phase inversion from a thermodynamic point of view, the entropy difference was calculated for a set of representative conditions. In calculating the entropy difference, the density of the oil phase and coke phase was assumed to be 0.96 (Gray, 1994) and 1.03 g/ml, respectively. The molecular weight of oil and coke was assumed to be 370 and 7000 g/mol, respectively, based on the work done by Zhao et al. (2001) and Wiehe (1993). Both molecular weights were measured

74

using VPO in o-dichlorobenzene at 130 °C. Wiehe measured the molecular weight of coke from the thermolysis of Cold Lake asphaltenes at the temperature of 400 °C for 70 min. Molecular weight of coke produced from longer reaction time could not be determined because of its insolubility in o-dichlorobenzene (Wiehe, 1992). The entropy difference was then calculated following equation (23) for different volume fractions (V^{α}/V) of coke. For each volume fraction a range of radii of the spheres were used based on the size range observed in the SEM micrographs. For each radius of spheres the average number of spherical particle was calculated and from the number of spheres, area of surface was calculated. Number of moles of coke and oil phase was calculated from the molecular weight and yields of the coke and oil. Total number of moles was then calculated from equation (9) assuming 1% of the total moles of coke and oil was in the interface. One sample entropy calculation is presented in Appendix A1.

The results are presented in Figure 4.7 to Figure 4.9. Phase inversion from continuous oil phase to continuous coke phase is thermodynamically possible when the entropy of the second phase is higher than the first one, i.e. ΔS presented in equation (23) is positive. A larger domain of positive entropy was obtained for higher volume fraction of coke. Consequently the chance of getting a configuration like Figure 4.4 is greater for higher volume fraction of coke. As the volume fraction of coke decreased the positive domain for phase inversion was reduced. There was no positive domain for the volume fraction of 0.1. Volume fraction of 0.51 and 0.1 roughly corresponds to the coke fraction produced from pure asphaltene and 25% asphaltene in methyl naphthalene, respectively.
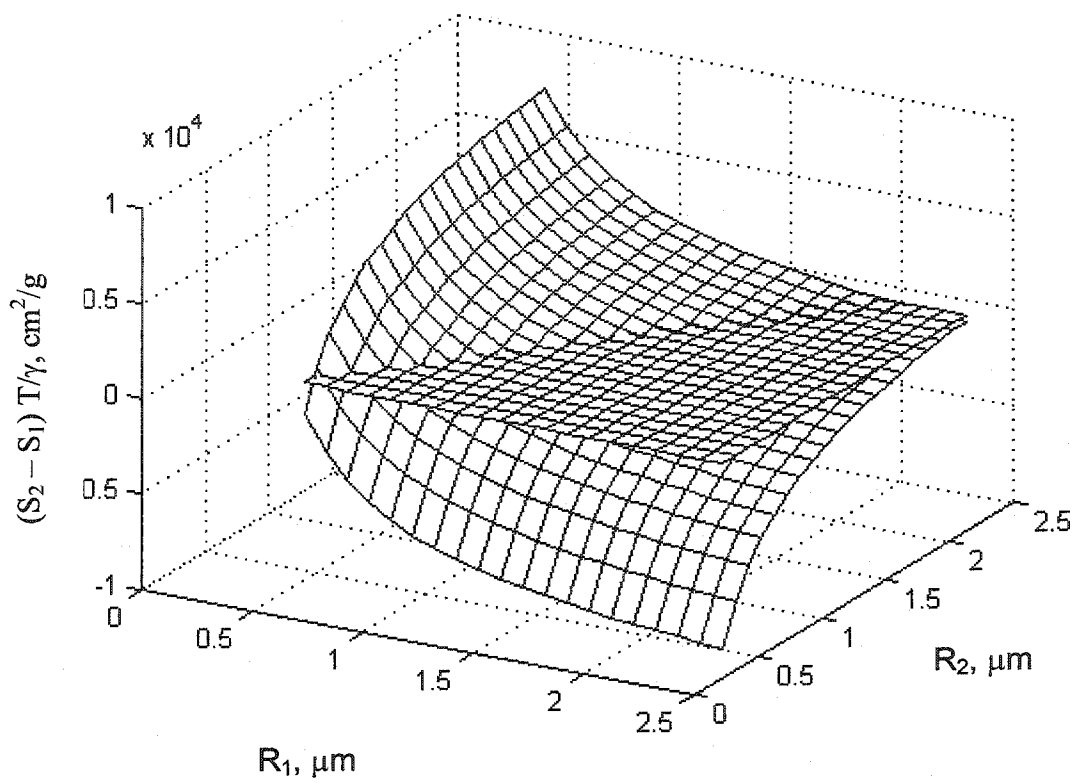
Figure 4.7 Estimated entropy difference, $(S_2 - S_1)$ T/γ, for coke volume fraction of 0.51

76

Figure 4.8 Estimated entropy difference, $(S_2 - S_1)$ T/γ, for coke volume fraction of 0.3

77

78

Figure 4.9 Estimated entropy difference, $(S_2 - S_1)T/\gamma$, for coke volume fraction of 0.096
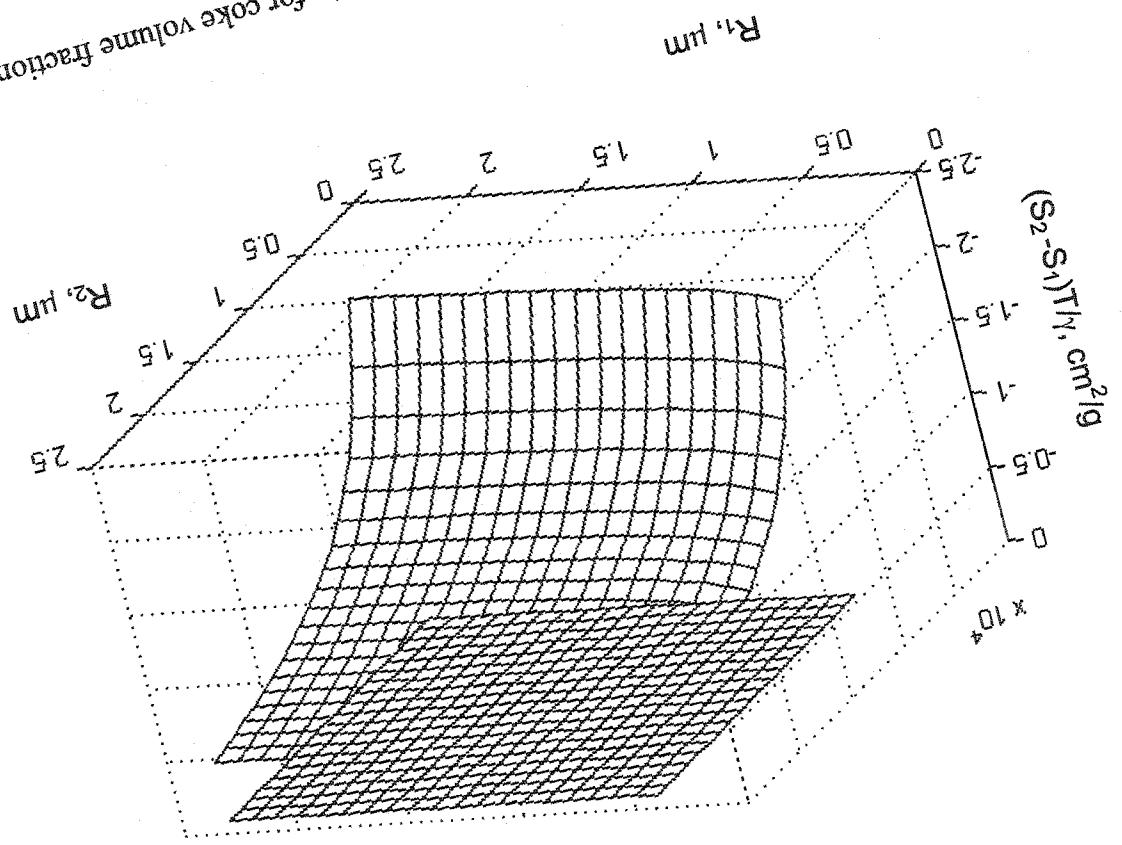
The pattern of the entropy difference with the radii of the spheres was not strongly influenced by changes in the density of the oil and coke phase within a reasonable range. One more assumption made during the calculation was the number of moles in the interface. The change of this number from 1% to 10% of the total moles of coke and oil did not have a strong influence on the entropy difference either (Table 4-2). Therefore, the entropy calculated in this work is qualitatively consistent. In order to get a more accurate quantitative result, more precise values of the parameters at reaction conditions are required. Qualitatively, as the volume fraction of the coke to oil increases there is more chance of having a phase inversion. This result agrees with the phenomena observed in polymer blends and mesophase formation where phase inversion occurs at high concentration depending on the viscosity ratio. The analysis done in this section suggests that the coke phase follows the behavior of polymer blends and provides a useful analogy for study of coke rheology and behavior.

Table 4-2 Sensitivity of entropy difference with parameters. Values shown in the table were calculated for coke volume fraction of 0.51 with $R_1=0.036$ μm and $R_2=2.36$μm

Parameters	Parameter Range	$\Delta S \times T/\gamma$ (cm^2/g) range
Coke density (g/ml)	1 ~1.2	$8.38 \times 10^3 \sim 7.6 \times 10^3$
Oil density (g/ml)	0.82 ~ 0.97	$8.95 \times 10^3 \sim 8.38 \times 10^3$
$N^\sigma/(N^\alpha + N^\beta)$	0.01~0.1	$8.54 \times 10^3 \sim 8.78 \times 10^3$
Coke MW	6000~12000	$8.50 \times 10^3 \sim 8.76 \times 10^3$

79

4.4. Conclusions

The observed behavior of coke spheres was consistent with the fact that coke under coking conditions was in a well-defined second liquid phase. The separation of the dense aromatic phase may precede actual coke formation as suggested by many authors (Magaril et al. 1968; Wiehe, 1993). Coke spheres were better dispersed in samples from dilute feed. The size of the coke droplets was larger in concentrated feed samples i.e. asphaltenes without any solvent or 75.6 wt% asphaltenes in maltenes. The larger sizes were likely due to more coalescence observed in these samples. In addition to the larger size, phase inversion was observed in some areas of coke produced from pure asphaltene. The addition of fine solids decreased the coalescence and droplet size significantly. The solids initially acted as highly dispersed nucleation sites and let coke deposit on it. Therefore, the dispersion was better in presence of solids that resulted in less coalescence and smaller size of spheres. Both solvent and fine solids were found to help the dispersion of coke spheres. Therefore, simultaneous increase in dilution and decrease in solid content did not change the size of the spheres significantly. The calculated entropy difference suggested that as the volume fraction of the coke to oil increased there was more chance of having a phase inversion.

4.5. References

Bensebaa, F., Kotlyar, L. S., Sparks, B. D. and Chung, K. H., "Organic Coated Solids in Athabasca Bitumen: Characterization and Process Implications", *Can. J. Chem. Eng.,* **2000,** 78, 610-616

80

Bradford, D. J., Greenhalgh, E., Kingshott, R., Senior, A., and Bailey, P. A., "Interaction of Carbon Black with Coal Tar Pitch", *Third Conference on Industrial Carbons and Graphite*, Society of Chemical Industry, London, **1971**, 520-527

Brooks, J. D. and Taylor, G. H., " Formation of Graphitizing Carbons from the Liquid Phase", *Nature*, **1965**, 206, 697-699

Dubois, J., Ahache, C. and White, J. L., "The Carbonaceous Mesophase Formed in the Pyrolysis of Graphitizable Organic Materials", *Metallography*, **1970**, 3, 337-368

Gray,M.R., Upgrading Petroleum Residues and Heavy Oils, Marcel Dekkar Inc., New York ,**1994**

Hietaoja, P. T., Holsti, M. R. M., Seppala, J. V. and Ikkala, O. T., " Effect of Viscosity Ratio on the Phase Inversion of Polyamaide 66/ Polypropylene Blends", *Journal of Applied Polymer Science*, **1994**, 54(11), 1613-1623

Kotlyar L. S., Sparks, B. D., Woods, J. R., Raymond, S., Le Page, Y., and Shelfantook, W., "Distribution and Types of Solids Associated with Bitumen", *Petroleum Science and Technology*, **1998**, 16(1 & 2), 1-19

Marsh, H., "A Review of the Growth and Coalescence of Mesophase (Nematic Liquid Crystals) to form Anisotropic Carbon and its relevence to Coking and Graphitization", *Proceedings of the Fourth International Conference on Industrial Carbon and Graphite, 1974; Society of Chemical Industry, London,* **1979**, 2-38

Mochida, I., Oyama, T., Korai, Y., and Fei, Y. Q., " Study of Carbonization using a Tube Bomb: Evaluation of Lump Needle Coke, Carbonization Mechanism and Optimization", *Fuel*, **1988**, 67, 1171-1181

81

Magaril, R. Z. and Aksenova, E. I., "Study of the Mechanism of Coke Formation in theCracking of Petroleum Resins", *Inter. Chem. Eng.*, 1968, 8(4), 727-729

Rahimi, P., Gentzis, T. and Fairbridge, C., "Interaction of Clay Additives with Mesophase Formed during Thermal Treatment of Solid-Free Athabasca Bitumen Fraction" Energy and Fuels, 1999, 13, 817-825

Rand B., "The Pitch-Mesophase-Coke Transformation as Studied by Thermal Analytical and Rheological Techniques", *Petroleum Derived Carbons*, Bacha, J. D., Newman, J. W., White, J. L., Eds, American Chemical Society, Washington, DC, 1986, 45- 61

Sawyer, L. C. and Grubb, D. T., *Polymer Microscopy*, Chapman and Hall, 1987, New York, Chap 6

Storm, D. A., Barresi, R.J. and Sheu, E.Y., " Flocculation of Asphaltenes in Heavy Oil at Elevated Temperatures", *Fuel science and technology Int'l.*, 1996, 14 (1&2) , 243-260

Tanabe, K., and Gray, M. R., " Role of Fine Solids in the Coking of Vacuum Residues", *Energy and Fuels*, 1997, 11(5), 1040-1043

Wang, S., Chung, K., Masliyah, J. H. and Gray, M. R., " Toluene- insoluble Fraction from Thermal Cracking of Athabasca Gas Oil: Formation of a Liquid-in oil Emulsion that Wets Hydrophobic Dispersed Solids", *Fuel*, 1998, 77(14), 1647-1653

Wiehe, I. A., "A Phase Separation Kinetic Model for Coke Formation", *Ind. Eng. Chem. Res.*, 1993, 44, 2447-2457

Willis, J. M., Caldas, V. and Favis, B. D., " Processing- morphology Relationships of Compatibilized Polyolefin/ Polyamide Blends", *Journal of Materials Science*, **1991**, 26, 4742- 4750

Yarranton, H. W., *"Asphaltene Solubility and Asphaltene Stabilized Water-in-Oil Emulsions."* Ph.D. Thesis, Department of Chemical and Materials Engineering, University of Alberta, **1997**, 8-11

Zhao, Y., Gray, M. R. and Chung K. H., "Molar Kinetics and Selectivity in Cracking of Athabasca Asphaltenes", *Energy & Fuels*, **2001**, 15(3), 751-755

5. KINETICS OF SOLVENT INTERACTIONS WITH ASPHALTENES DURING COKE FORMATION[1]

5.1. Introduction

The content of the highest molecular weight constituents of petroleum, which are found in the asphaltene fraction, correlates with the formation of coke in thermal and catalytic processes (Speight, 1981, 1984). The literature provides ample information about the reactions of isolated asphaltenes (Moschopedis, 1978; Shucker and Kewshan, 1980; Savage et al., 1985; Neurock et al., 1990). During the industrial processes of hydrotreating, hydrocracking, and coking, however, the asphaltenes react as a component of a more complex mixture. To understand the mechanism of coke formation, it is therefore extremely important to understand the influence of solvent on the asphaltene conversion. Solvents affect phase behavior and hydrogen transfer reactions of asphaltenes, which in turn affect the formation of coke. For example, reaction of asphaltenes dissolved in a hydrogen donor solvent gave significant suppression of coke formation (Savage et al., 1988). A number of factors are important during coking, including severity of reaction, thermolysis of labile bonds, asphaltene structure, metal and heteroatom content of the asphaltenes, hydrogen abstraction from solvent, radical accepting capability of the solvent and solvent power (Savage et al., 1988; Blanchard and Gray, 1997; Wiehe, 1993).

The objective of this study was to examine the kinetics of coke formation from Athabasca asphaltenes in different liquid environments in a closed reactor under a

---

[1] A version of this chapter was published in Energy & Fuels, 2002, 16, 148

84

nitrogen atmosphere at 430 °C. Several liquid systems were chosen to determine the role of the liquid components as solvents, versus their possible role in reaction. In the first set of experiments the maltene fraction, which is the naturally occurring solvent in vacuum residue, was chosen as the solvent. Next, three aromatic solvents of similar solubility parameter but of different chemical behavior were chosen, so that the change in solubility could be neglected. Naphthalene (solubility parameter, δ = 19.1 MPa$^{1/2}$ @ 25 °C) ((Barton, 1983) was not reactive at these reaction conditions, therefore, it served as a solvent control. The role of free radical chain reactions was tested by adding 1-methyl naphthalene (1-MN) as an alternate radical carrier to the asphaltenes undergoing thermal cracking. 1-MN (δ=20.3 MPa$^{1/2}$ @ 25 °C) (Barton, 1983) can act as a radical acceptor at the reactor conditions (Blanchard and Gray, 1997). Tetralin (δ=19.5 MPa$^{1/2}$ @ 25 °C) (Barton, 1983) is a known hydrogen donor diluent. Comparison of the three solvents allowed correlation of coke formation with radical acceptance and hydrogen donation. To study the influence of initiating compounds in the liquid phase, n-dodecylsulfide (DDS) was added as an initiator. DDS simulated weak carbon-sulfur bonds in the maltenes, which could act as initiator for free radical reactions. The study done on the phase behavior (Chapter 4) along with some literature studies support the fact that liquid-liquid phase separation may precede coke formation. Therefore, the phase separation model proposed by Wiehe (1993) was used as a kinetic framework to analyze the coke yields.

5.2. Theory

The mechanism involved in forming insoluble solids, and ultimately petroleum coke, has received considerable attention. Magaril et al.(1968) linked coke formation explicitly with asphaltene content by suggesting that coke formed via condensation and

polymerization reactions in a new solid phase that formed by precipitation of asphaltenes. Storm et al. (1996) suggested a similar process, wherein interactions between asphaltene molecules in the oil give molecular aggregates, which eventually react to give coke. Wiehe (1993) suggested a coke formation model based on phase separation rather than molecular aggregation. According to this model, coke forms from an asphaltenic phase that has separated from the rest of the oil. Cracking of side chains from the asphaltene molecules gives a progressively more aromatic and less soluble core, eventually giving phase separation from the solvent medium to form a new phase that is lean in abstractable hydrogen. In this new phase, asphaltene free-radical interactions become quite frequent, causing a rapid reaction to form solid coke and a heptane-soluble byproduct (1993).

Although Wiehe (1993) developed this model for open reactors, the chemistry of the model should be applicable to any reactor system. In an open reactor, only the heavy fraction of the heptane-solubles can stay in the reactor as a liquid. In batch reactors, all of the products remain so that the heptane-solubles and most of the cracked products will remain in the liquid phase. The model of Wiehe (1993) can be restated as follows for the case of a closed reactor:

$$H^+ \xrightarrow{k_H} bA^+ + (1-b)V \qquad (1)$$

$$A^+ \xrightarrow{k_A} cA^* + (1-c)(H^* + V \qquad (2)$$
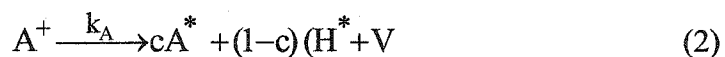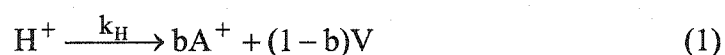
where A^+ = fraction of reactant asphaltene, A^* = fraction of reacted asphaltene cores, H^+ = fraction of reactant heptane solubles and H^* = fraction of product heptane solubles. In the case of a closed reactor, the cracked distillate products (V) are retained and remain mainly in the liquid phase. Parameters k_A and k_H are first order reaction rate constants for the thermolysis of reactant asphaltene and heptane solubles, respectively,

and b and c are stoichiometric coefficients. The solubility limit (S_L) in a closed reactor

defines how much of the reacted asphaltenes (A*) remain in solution in the liquid phase:

$$A_{max}^* = S_L \ (H^* + H^+ + V) \qquad (3)$$

The asphaltenes in excess of the solubility limit (A_{ex}^*) then react at an infinite rate

to form toluene-insolubles, or coke.

$$A_{ex}^* = A^* - A_{max}^* \qquad (4)$$

$$A_{ex}^* \xrightarrow{\ \infty\ } TI \qquad (5)$$

where TI= toluene-insoluble coke.

Wiehe (1993) evaluated the first order rate constants k_A and k_H from the

thermolysis of pure asphaltene and pure heptane soluble fractions. Product asphaltenes,

as measured experimentally, were the sum of reactant asphaltenes and asphaltene cores

that remained in the solution ($A^+ + A^*$). The ability of Wiehe's model to correlate data

from pyrolysis of maltenes and whole residue with a single set of stoichiometric

parameters suggest that this semi-empirical approach has significant merit. The model

was consistent with the common features of residuum conversion kinetics, including an

induction period for coke formation, a maximum in the concentration of asphaltenes at

the end of induction period and the high reactivity of asphaltenes.

5.3. *Cracking of Asphaltene in Maltene*

The data of Figure 5.1 show yields of coke and asphaltenes after 40 min at 430 °C

from different ratios of vacuum residue and maltene. Pure maltene produced 7.0% coke

and 13.9% residual asphaltenes. The total yield of coke for mixtures was a linear

combination of the contributions of the maltenes and asphaltenes. When the contribution

87

from the maltenes was subtracted from the total coke, the coke formation from asphaltenes was almost constant at 0.455 ± 0.035 g/g of initial asphaltene. This result was consistent with apparent first order kinetics for cracking of asphaltenes to form coke. If coke formation were higher order in asphaltenes concentration, then changing the initial concentration of asphaltenes would affect the yield of coke. The phase-separation kinetic model (equations 1-5) was fitted to the data. The infinite rate constant, used in equation 5, implied that the asphaltene cores phase separate to form coke instantly as in precipitation. Rather than using this approximate approach to account for the kinetics of asphaltene core conversion to coke, a finite rate constant, k_C, value was used in present study. Therefore, equation 5a was used instead of equation 5:

$$A_{ex}^{*} \xrightarrow{\ k_C\ } TI \hspace{2cm} (5a)$$

The first order rate constants, k_A and k_C, stoichiometric coefficient, c, and the solubility limit, S_L, were determined from experiments with pure asphaltenes (Figure 5.2) by minimizing the sum of squared residuals between the model value and the experimental value using equation (6).

$$SSR = \sum_{i=1}^{n} (YE_i - YM_i)^2 \hspace{2cm} (6)$$

where, YE_i is the i th experimental yield, YM_i is the i th yield calculated from the model and n is the number of data points. A quasi-Newton method with a mixed quadratic and cubic line search procedure was used to minimize the error between the experimental data and the solution of the differential equations developed from the model. The best fit values of k_A, k_C, c and S_L were determined to be 0.152 ± 0.05 min^{-1}, 0.17 ± 0.025 min^{-1},

0.543 $\pm$ 0.036 g/g and 0.15 $\pm$ 0.0195 g/g, respectively. The parameter errors were estimated by a 95% confidence limit. Each standard deviation parameter was calculated by using the principle diagonal terms in the variance-covariance matrix (Himmelblau, 1970). The rate constant, k_A, was within a factor of 2 of the value of 0.24-0.3 min^{-1} measured by Banerjee et al. (1986) for pyrolysis of Athabasca asphaltenes under nitrogen. Likewise, Wiehe (1993) obtained the value of the cracking rate constant, k_A, of 0.026 min^{-1} at 400 °C for Cold Lake asphaltene. If this value is extrapolated to 430 °C assuming a typical activation energy for cracking of residue components of 213 kJ/mol (Freund and Olmstead, 1998), then the estimated value of 0.132 min^{-1} is very similar to the value found in the present study. The value of S_L was lower than the value of 0.49 obtained by Wiehe (1993) for Cold Lake vacuum residue at 400 °C, likely due to the difference in the source of asphaltenes and the reaction temperature.
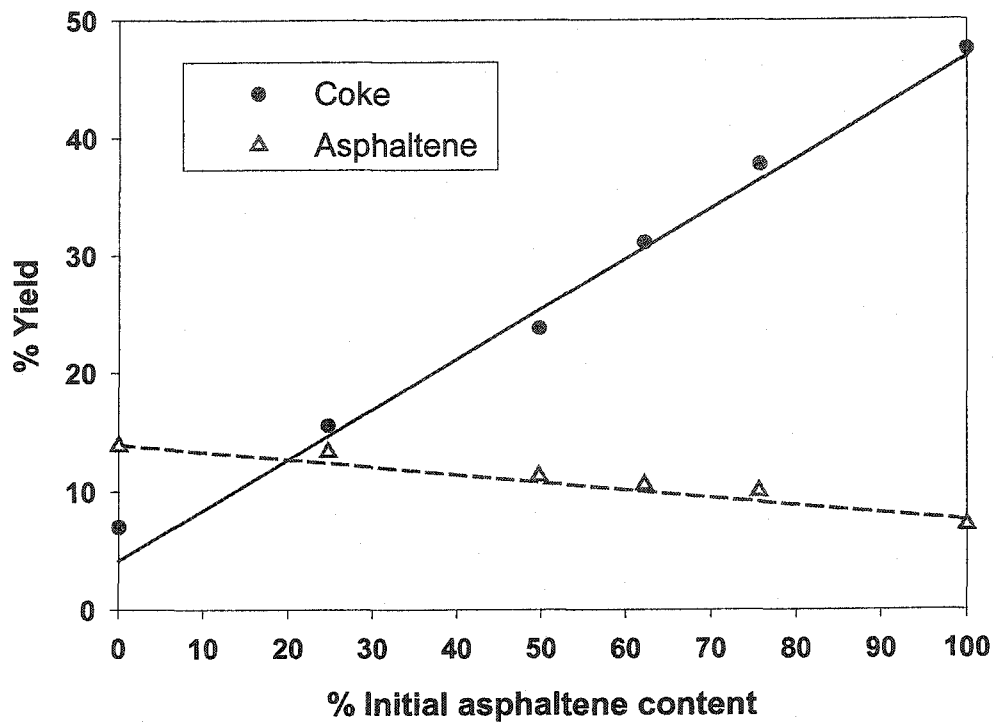
Figure 5.1. Variation of coke and asphaltene yield (●, coke; △, asphaltene) with initial

asphaltene content from the thermolysis of asphaltene in maltene. Yields are presented as

a percentage of total feed. Reaction time = 40 min. Curves are drawn from the model

90
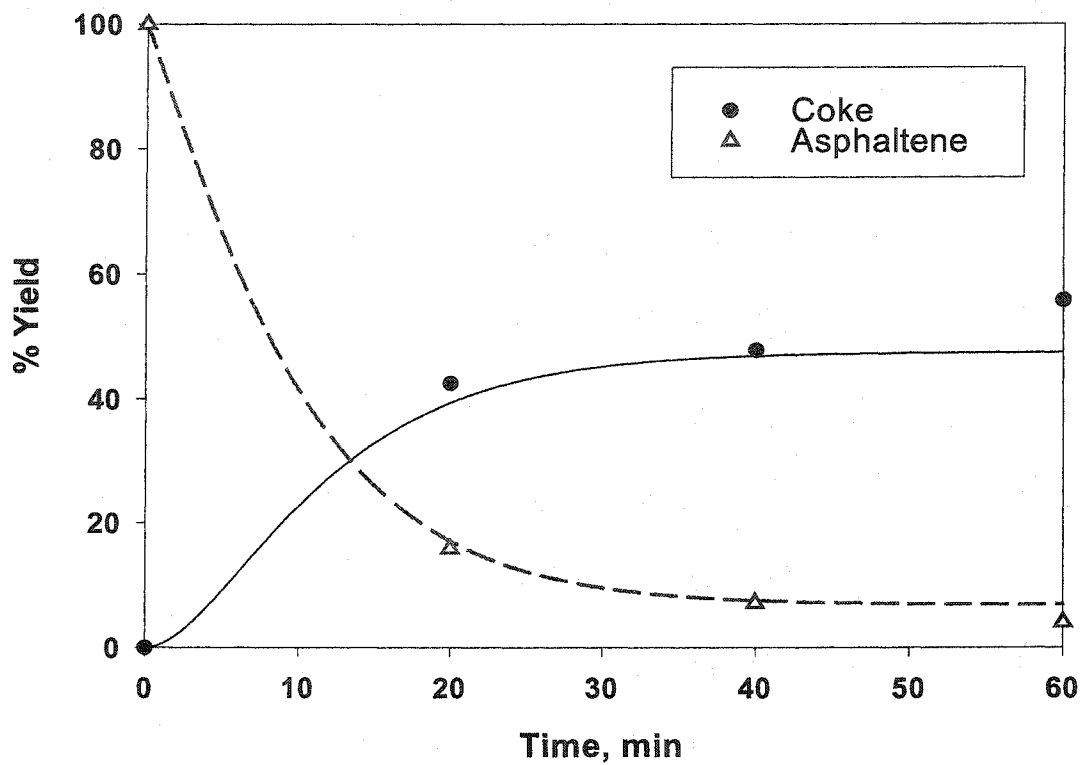
Figure 5.2 Temporal variation of coke and asphaltene yield (•, coke; Δ, asphaltene) from

the thermolysis of pure asphaltene. Curves are drawn from the model

91

These values of k_A and c were used for all subsequent modeling, since all experiments were performed at the same temperature and with the same asphaltenes. The batch system used in this study did not allow differentiation between the volatile and nonvolatile fractions of the heptane solubles; therefore, the model was fitted to the yields of coke and asphaltenes. The rate constants for the maltenes, k_H, and the stoichiometric coefficient, b, were determined by minimizing the error as described earlier. The model fit to the experimental values was satisfactory (Figure 5.1). The best-fit values of k_H and b were 0.11 ± 0.0006 min^{-1} and 0.33 ± 0.052 g/g, respectively. The original work of Wiehe (1993) demonstrated the utility of the phase-separation model for conversion of a fixed concentration of asphaltene in open reactors as a function of time. The results of Figure 5.1 demonstrate that the modified model is also useful for closed reactors with variable concentration of maltenes from 0 to 100 wt%, at a constant reaction time.

5.4. Asphaltene in aromatic solvents

The data in Figure 5.3 show yields of coke and asphaltenes from the thermal cracking of asphaltenes in different aromatic solvents and in maltenes. The value for coke from asphaltenes and maltenes was corrected for the contribution of coke from the maltenes. All the reactions were done for 40 min and 25 wt% initial asphaltene content. Tetralin gave a considerable decrease in coke formation compared to maltene solvent, i.e. whole vacuum residue, consistent with its ability to donate hydrogen. The residual asphaltenes content was higher with tetralin than when the other diluents were used. Coke formation was reduced when 1-MN was used as solvent instead of maltenes. Solvent strength of maltenes should be different than that of 1-MN which is more aromatic. The solubility parameters of asphaltene and maltenes were not determined in this study, but

92

values from the literature suggest that Athabasca asphaltenes and maltenes should have solubility parameters of approximately 19 $MPa^{1/2}$ and 15 $MPa^{1/2}$, respectively (Wiehe, 1992; Savastano and Salvatore, 1993). The difference in solvent strength could result in lower yield of coke in the presence of 1-MN; however, the reactivity of the maltene could also be significant.
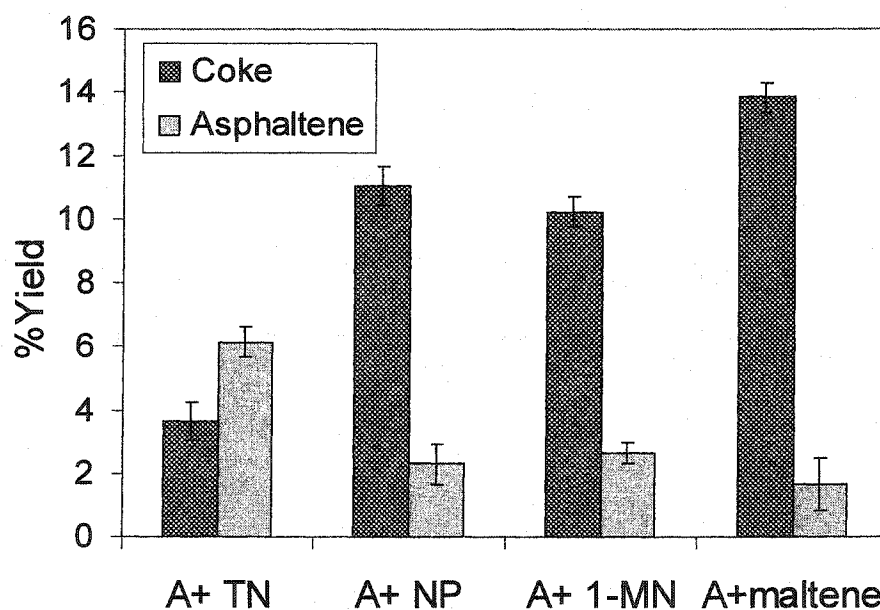
Figure 5.3 Comparison of coke and asphaltene yield from the thermolysis of asphaltene in different solvents- Tetralin (TN), Naphthalene (NP), 1-Methyl Naphthalene (1-MN) and maltene. Yields are presented as a percentage of total feed. Reaction time = 40 min.

From the data of Figure 5.3, it is evident that naphthalene gave the same amount of coke and product asphaltenes as 1-MN; therefore, the ability of 1-MN to readily form benzylic radicals did not affect the reactions leading to coke formation. Although products from naphthalene, such as dimers, were not detected by gas chromatography, the results of previous studies suggest that naphthalene could interact with asphaltenes and should not be regarded as completely inert (Savage, 1994; Khorasheh and Gray, 1993).

A series of reactions were done with asphaltenes in 1-MN for 60 min for a range of asphaltene concentrations (Figure 5.4). The yield of coke from the feed asphaltene was independent of solvent concentration, and had a value of 0.456 ± 0.025 g/g. In the 1-MN solvent, the initial concentration of heptane-soluble maltenes was zero. The pressure in these experiments was sufficient to ensure that most of the 1-MN was in the liquid phase, therefore, 1-MN along with the H^* and V produced from the thermal cracking of asphaltenes served as the liquid medium. Given the absence of initial heptane-solubles, equations 2-4 and 5a were used to fit the data. The solubility limit, S_L, was determined by minimizing the sum of squares of the error (equation 6) following the same procedure as before. Figure 5.4 shows the fit of the experimental data to the model. The optimal value of S_L was 0.0295 ± 0.0168 g/g. This value of S_L is much smaller than that found for maltene. Maltenes are more complex and reactive than 1-MN and can yield asphaltenes in thermal reactions. Therefore, direct comparison of S_L for solvent strength is not possible.

94
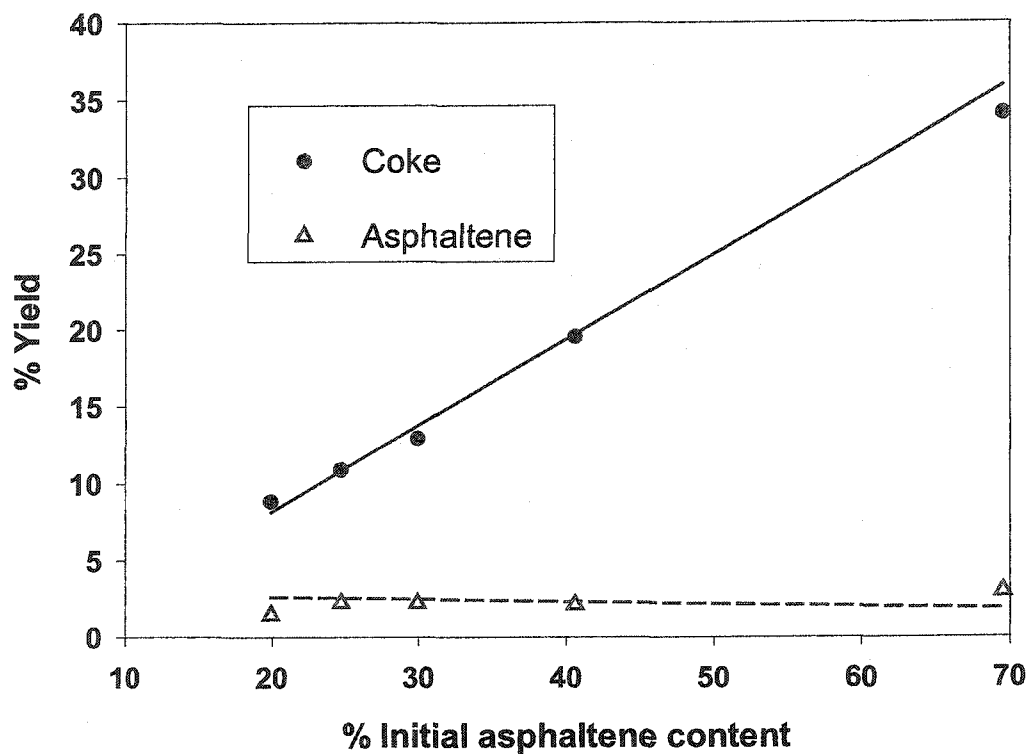
Figure 5.4 Variation of coke and asphaltene yield (●, coke; Δ, asphaltene) with initial asphaltene content from the thermolysis of asphaltene in 1-methyl naphthalene (1-MN). Yields are presented as a percentage of total feed. Reaction time = 60 min. Curves are drawn from the model (equations 1-5).

95

5.5. Initiation by Alkyl Sulfide

More than half the sulfur in heavy petroleum fractions is present in the form of thiophene derivatives. The remainder consists primarily of sulfides (cyclic thiolanes and acyclic thioethers) and a minor amount of sulfoxide (Altgelt and Boduszynski, 1994). The nature of sulfur compounds were found to be much the same in all the petroleum fractions; therefore, roughly 40-50 % of the sulfur of maltenes would be in the form of thermally reactive alkyl-sulfides. Consequently, maltenes can serve as initiators of free radical reactions. To study the role of initiator, n-dodecylsulfide (DDS) was added to a mixture of asphaltenes and 1-MN to match the approximate sulfide content of the maltenes.

The addition of DDS gave a significant increase in coke yield after 10 min of reaction, but it had no effect on coke after 40 min, compared to reaction of asphaltenes in 1-MN (Figure 5.5). Consequently, cracking of solvent to initiate reactions had a major impact on the kinetics of coke formation, but not on the ultimate yield. The model compound used in this study had some significant differences from the thiolane and thioethers in the maltenes. The sulfide components present in the maltenes are much higher molecular weight; therefore, reaction intermediates and cracked products are much more likely to stay in the liquid phase. DDS would also tend to form light products that are less likely to participate in the propagation reactions. Despite these differences, the data indicated that the overall effect of adding an initiator was an increase in the rate of reaction. DDS increased the rate of thermal cracking of asphaltenes, increasing the rate of coke formation but not its ultimate yield. This behavior was easily represented in the kinetic model by increasing the value of the rate constant in equation (2), k_A, to represent

96

faster cracking without any change in the final yield of coke. The behavior of the maltenes was consistent with the role of DDS as an initiator, because maltenes increased the rate of formation of coke from asphaltenes. After 40 min maltenes gave more coke from asphaltene than the aromatic solvents (Figure 5.3), the yields of coke per unit of asphaltenes cracked were equivalent to 0.455 ± 0.035 g /g in maltene versus 0.40 ± 0.025 g/g in 1-MN for 25 wt% initial asphaltenes. Maltenes are a more complex mixture of compounds than 1-MN and produce both asphaltenes and coke; therefore, identical behavior should not be expected from a simple mixture of DDS and 1-MN as from the maltenes.
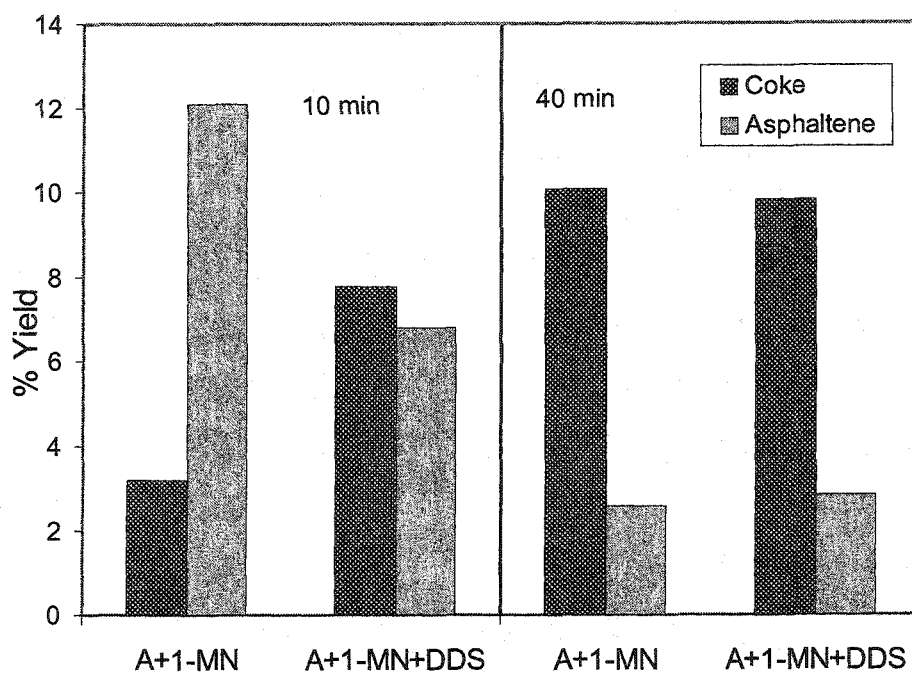
Figure 5.5 Thermolysis of asphaltene (A) in 1-methyl naphthalene (1-MN) with or without added *n*-dodecyl sulfide (DDS)

5.6. Hydrogen transfer

The data in Table 5-1 present the hydrogen donating ability of each of the solvents used in this study. Hydrogen donation was calculated as mg H donated per g of initial solvent. The data of Figure 5.6 show the temporal variation of coke and asphaltene from the thermolysis of asphaltenes in pure TN and in a mixture of TN and 1-MN in different ratios. Initial asphaltenes concentration of 25 wt% was used for both sets of reactions. A mixture of TN and 1-MN at 1:2 ratio should have approximately one third of the overall hydrogen donating ability of pure TN, but this reduction gave no significant change in yield of coke or asphaltenes relative to the pure solvent. This observation suggests that the hydrogen accepting capability of the asphaltenes also plays an important role, i.e. there is a limit up to which asphaltenes can accept hydrogen from the solvent.

To test this hypothesis, the amount of hydrogen transferred to asphaltenes was measured for a range of tetralin-1-methyl naphthalene mixtures (Table 5-2). The amount of hydrogen transfer was measured by measuring the concentration of naphthalene and dihydronapthalene produced from the tetralin and assuming that for each mole of naphthalene produced, 4 g of hydrogen was transferred to the asphaltenes. When anthracene was used as a hydrogen acceptor, the amount of hydrogen donated by the tetralin (based on naphthalene formation) was almost identical to the amount taken up by anthracene, validating this assumption. The data of Table 5-2 show the amount of hydrogen that was transferred to asphaltenes for the three sets of reactions, at a constant initial asphaltenes content of 25 wt%. The results showed that the amount of hydrogen transferred was the same with 75% and 25% tetralin in the reaction mixture, consistent with the equivalent yields of coke under these conditions. When the tetralin concentration

was reduced to 10wt%; however, hydrogen transferred to asphaltene was decreased for 40 and 60 min. reactions, compared to the other two series. As a consequence, the coke yields for this set of reactions (Figure 5.6) were higher than the other two experiments. The coke yield at this condition was also lower than the yield from reaction of asphaltenes in maltenes, despite the hydrogen donating capacity of the maltenes. This result emphasizes the multiple effects of initiation and hydrogen donation from maltenes.

Table 5-1 Comparison of the hydrogen donor ability of the solvents

Solvent	mg H donated/ g solvent
TN	10
Maltene	3.44
1-MN	0.16

Table 5-2 Hydrogen transferred to asphaltenes from tetralin during cracking

Reactant	mg H transfer/ g Asphaltenes		
	20 min	40 min	60 min
Asphaltene + 75 wt% TN	6	13.2	16.8
Asphaltene + 25 wt% TN + 50 wt% 1-MN	5	12	15.6
Asphaltene + 10 wt% TN + 65 wt% 1-MN	4.9	8	9.7

Data from the reactions with hydrogen donor solvent were then used in the modified phase separation kinetic model (equations 2-4 and 5a). The asphaltenes are highly reactive components, therefore, in this temperature range the thermal cracking of original asphaltenes should predominate over the influence of hydrogen donation to cracking. Consequently, the same values of k_A and c were used as before to fit the data. The solubility limit, S_L, for tetralin was taken to be the same as for 1-MN due to the equivalent solubility parameters for the two compounds. With these parameters, the model gave significantly higher coke yields and lower asphaltene yields than the experimental values. The model did not allow for any reactions between the solvent and asphaltenes; therefore, when a hydrogen donor solvent is present the model could not account for the difference in yields between tetralin, on the one hand, and naphthalene and 1-MN on the other (see data of Figure 5.3).

101
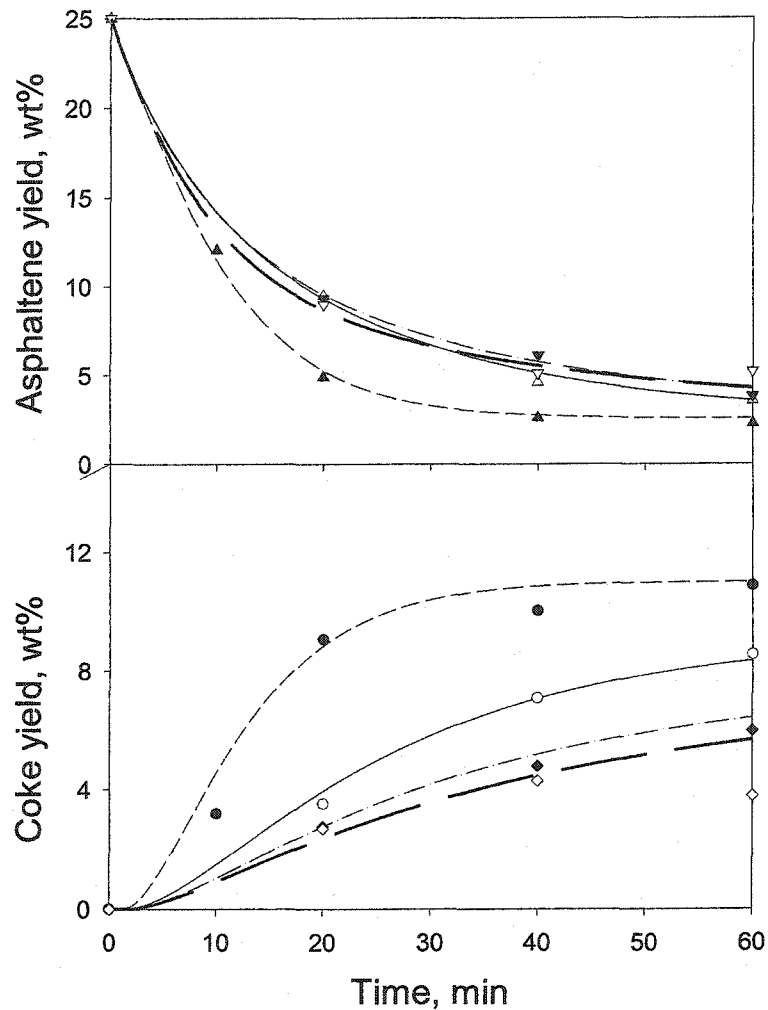
Figure 5.6 Temporal variation of coke and asphaltene yield from the thermolysis of 25 wt% asphaltene in a mixture of TN and 1-MN. Curves are drawn from the model. a) long dashed line - 75 wt% tetralin (◊, coke; ∇, asphaltene), b) dashed dot (__ . __) line – 25 wt% tetralin (●, coke; ▼, asphaltene), c) solid line- 10 wt % tetralin (o, coke; Δ, asphaltene) and dashed (— —) line- 0 wt% tetralin (◊, coke; ●, asphaltene). Yields are presented as percentage of total feed.

102

To account for the significant reduction in coke yield due to hydrogen donation, the phase-separation model was extended. The data of Table 5-2 suggest that hydrogen transfer to asphaltenes depends both on the concentration of the donor solvent present and also on the ability of the asphaltene molecules to accept hydrogen. This observation suggests that only a portion of asphaltene cores are capable of accepting hydrogen, and hydrogen transfer can continue only as long as this portion of cores can continue to accept hydrogen. Accordingly, asphaltene core, A^*, was subdivided into two types: cores that can accept hydrogen, A^{*A}, and cores that cannot accept hydrogen, A^{*NA}. At any time, $A^{*A} + A^{*NA} = A^*$. Reaction (7) was introduced in order to allow the asphaltene aromatic cores to abstract hydrogen from tetralin. This reaction is assumed to convert aromatic cores to heptane-soluble species.

$$A^+ \xrightarrow{\quad k_A \quad} (c-d)A^{*NA} + dA^{*A} + (1-c)(H^* + V) \tag{7}$$

$$A^{*A} \xrightarrow{\quad k'[TN] \quad} H^* \tag{8}$$
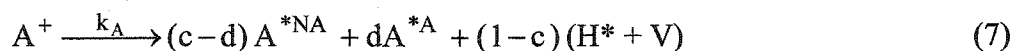
The solubility limit was restated as follows:

$$A^*_{ex} = A^{*NA} + A^{*A} - A^*_{max} \tag{9}$$

After exceeding the solubility limit, A^*_{ex} forms coke by equation (5a) as in the earlier modeling work. The resulting system of differential equations (see Appendix) was solved using with a variable order solver for differential equations (Matlab, Mathworks Inc, Natick, MA). The parameter d was estimated from the difference in heptane solubles plus volatiles (which were estimated indirectly from the mass balance) between two reactions: 25 wt% asphaltenes with 1-MN and 25 wt% asphaltene with TN. The increase

103

in heptane solubles plus volatiles gave the amount of aromatic cores that did not form

coke in the presence of tetralin and therefore contributed to the formation of H^* according

to equation (8). From this calculation the value of d was determined to be 0.16 g/g. The

data for coke and asphaltene yield as a function of time were then used to estimate the

rate constants k' and k_c.

Table 5-3 Comparison of the values for apparent rate constant for coke formation, k_C

Reactant	Rate constant, k_C, min^{-1}
Asphaltene + 75 wt% 1-MN	0.17 ± 0.025
Asphaltene + 10 wt% TN + 65 wt% 1-MN	0.04 ± 0.0057
Asphaltene + 25 wt% TN + 50 wt% 1-MN	0.028 ± 0.005
Asphaltene + 75 wt% TN	0.028 ± 0.0077

The data of Figure 5.6 show the fit of the model to the experimental data with

optimal values of $k' = 0.23 \pm 0.087$ (wt fraction)$^{-1}$ min^{-1} and k_c values as shown in Table

5-3. From the values of rate constant, k_C, it is evident that k_C was same for maltenes and

1-MN system, but the value changed dramatically when a hydrogen donor solvent was

added as liquid medium. Figure 5.7 shows the model values when infinite values of k_C

were used for the experiments at different concentrations of tetralin. The significant

104

mismatch between the model and the data validates the use of decreasing values of k_C with increasing TN concentration. This observation suggests that the solvent has a chemical influence on the formation of toluene-insoluble coke even in the new phase where asphaltene cores are deficient in solvent. The coke formed in these studies had H/C molar ratios of 0.64-0.73, very similar to values for bituminous coal (Stock, 1985). Donor solvents such as tetralin significantly enhance conversion of such material into liquid products; therefore, donor solvents are also likely to interact with coke precursors from asphaltenes and help to suppress coke formation.

105
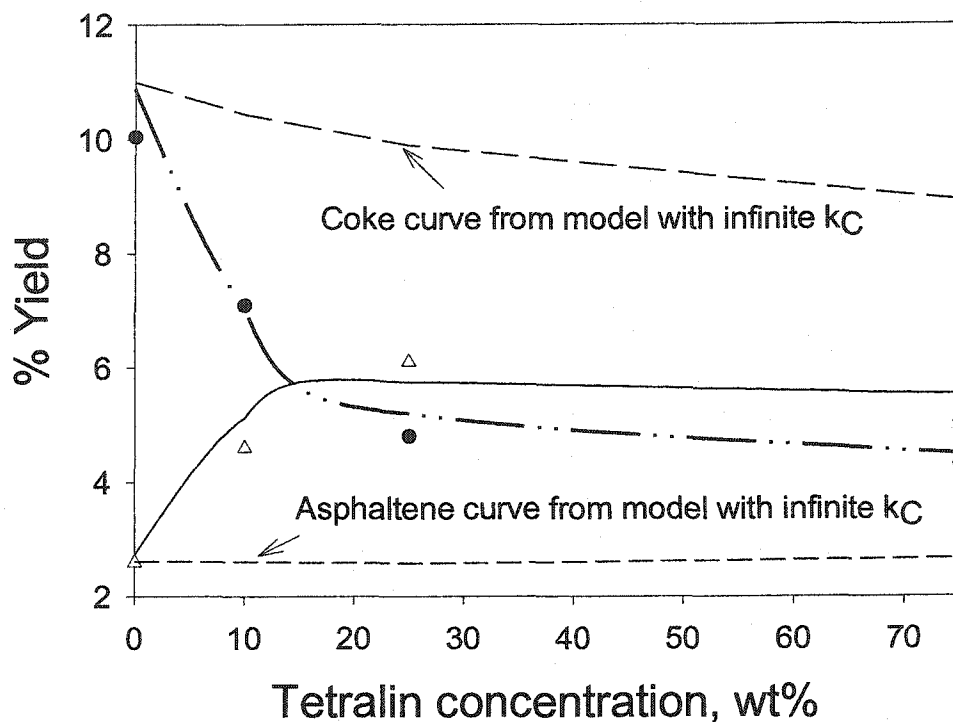
Figure 5.7 Variation of coke and asphaltene yield (●, coke; Δ, asphaltene) from the thermolysis of 25 wt% asphaltene in a mixture of TN and 1-MN. Yields are presented as a percentage of total feed. Reaction time = 40 min. Curves are drawn from the model (Equations 7-9 & 5a).

5.7. Conclusions

Coke formation was strongly influenced by chemical interactions between the asphaltenes and the solvent medium. The hydrogen donating ability of the solvent and the hydrogen accepting ability of the asphaltenes both played an important role in determining the ultimate yield of coke. Addition of DDS as an initiator increased the rate of cracking and coke formation, but not the yield of coke formation after 40 min. A modified kinetic model based on phase separation, following Wiehe (1993), was consistent with the data on coke formation from asphaltenes in different solvents with low hydrogen donation ability. Addition of a hydrogen transfer reaction to the model gave consistent results for tetralin mixtures with high hydrogen donating capacity.

5.8. References

Altgelt, K. H. and Boduszynski, M. M., '*Composition and Analysis of Heavy Petroleum Fractions*', Marcel Dekker Inc., New York, **1994**

Banarjee, D. K., Laidler, K. J., Nandi, B. N. and Patmore, D.J., "Kinetic Studies of Coke Formation in Hydrocatbon Fractions of Heavy Crudes", *Fuel*, **1986**, 65, 480-484

Barton, A. F. M., Handbook of Solubility Parameters and Other Cohesion Parameters, CRC Press, Inc., Boca Raton, Florida, **1983**

Blanchard, C. A. and Gray M. R., "Free Radical Chain Reactions in Thermal Hydrocracking of Residues", *Abstr. Pap. Am. Chem. Soc.*, APR 13 **1997**, *213*: 4-PETR Part 1

Freund, H. and Olmstead, W., "Thermal Conversion Kinetics of Petroleum Residua", AIChE Spring Meeting, New Orleans, LA, **1998**, paper 34b.

Himmelblau, D. M., *Process Analysis by Statistical Methods*, John Willey & Sons, New York, **1970**

Khorasheh F. and Gray, M. R., "High Pressure Thermal Cracking of *n*-Hexadecane in Aromatic Solvent", *Ind. Eng. Chem. Res.*, **1993**, *32*, 1864-1876

Magaril, R. Z. and Aksenova, E. I., "Study of the Mechanism of Coke Formation in The Cracking of Petroleum Resins", *Inter. Chem. Eng.*, **1968**, *8(4)*, 727-729

Moschopedis, S. E., Parkash, S., and Speight, J. G., "Thermal Decomposition of Asphaltenes", *Fuel*, **1978**, *57*, 431-443

Neurock, M., Nigam, C., Trauth, D. and Klein M. T., "Asphaltene Pyrolysis Pathways and Kinetics; Feedstock Dependence," *Preprints AIChE Meeting*, San Diego, CA, August **1990**

Shucker, R. C. and Kewshan, C. F., "The Reactivity of Cold Lake Asphaltenes", *ACS Preprints, Div. Of Fuel Chemistry*, **1980**, *25(3)*, 155-165

Savage, P. E., Klein, M. T. and Kukes, S. G., "Asphaltene Reaction Pathways. 1. Thermolysis", *Ind. Eng. Chem. Proc. Des. Dev.*, **1985**, *24*, 1169-1174

Savage, P. E., Klein, M. T. and Kukes, S. G., "Asphaltene Reaction Pathways. 1. Effect of Reaction Environment", *Energy & Fuels*, **1988**, *2*, 619-628.

Savage, P. E., "Are Aromatic Diluents Used in Pyrolysis Experiments Inert?", *Ind. Eng. Chem. Res.*, **1994**, *33*, 1086- 1089

Savastano, C. and Salvatore, M., "Polymer Solubility Theory Predicts Efficiency of Residual Oil Extraction by Polar Solvents", *Fuel Sci. Technol. Int.*, **1993** , 11(3-4), 445-461

Speight, J. G., *The Desulfurization of Heavy Oils and Residua*, Marcel Dekker Inc., New York, **1981**

Speight, J. G., *In Catalysis on the Energy Scene*, Kaliaguine S., and Mahay, A. (Editors), Elsevier, Amsterdam, **1984**

Stock, L. M., "Hydrogen Transfer Reactions", In *'Chemistry of Coal Conversion'*, Schlosberg, R. H., Ed., Plenum Press, New York, **1985,** Chapter 6

Storm, D. A., Barresi, R.J. and Sheu, E.Y., " Flocculation of Asphaltenes in Heavy Oil at Elevated Temperatures", *Fuel Sci. Technol. Int.,* **1996**, 14 (1&2) , 243-260

Wiehe, I. A., "A Solvent Ressid phase Diagram for Tracking Resid Conversion", *Ind. Eng. Chem. Res.,* **1992**, 31, 530-536

Wiehe, I. A., "A Phase Separation Kinetic Model for Coke Formation", *Ind. Eng. Chem. Res.,* **1993**, *44,* 2447-2457

6. COKING KINETICS AS A FUNCTION OF ASPHALTENE STRUCTURE

The objective of this part of work was to examine the behavior of several different feedstocks under coking conditions, and finally to predict the coke formation from feed properties. In order to obtain a universal relationship, it is necessary to use feedstocks with very different structures. For this purpose, several asphaltenes from around the world were chosen: Athabasca asphaltenes from Canada, Arabian Light and Arabian Heavy from Saudi Arabia, Maya from Mexico and Gudao from China. The aim of this selection was to get feed materials of different chemical composition, based on the available data from the literature (Zhao et al., 1994; Trauth et al., 1992; Ali et al., 1994). These asphaltenes span a range of sulfur and nitrogen content, and in the fraction of aromatic carbon. The range of chemical properties of the selected asphaltenes taken from literature data is presented in Table 6-1.

Table 6-1 The data range of chemical properties of asphaltenes (literature data)

Properties	Range of data
H/C atomic ratio	1.04~1.29
S, wt%	2.26~7.6
N, wt%	0.86~1.48
Fraction of aromatic H	0.052~0.235
Molecular weight	3930~8950

110

The literature provides some useful data on the properties of the asphaltenes; however, the properties of asphaltenes vary greatly depending on the method of separation, also on the solvent used for separation. Moreover, the complex nature of asphaltenes make the measurement of the properties difficult. To get a consistent result, the properties were measured again after separating the asphaltenes following the same procedure for each asphaltene. The following sections discuss the chemical composition and the structural parameters of the five samples chosen.

6.1. Feedstock properties

6.1.1. Molecular weight and Elemental analysis

Molecular weights of the feed asphaltenes are presented in Table 6-2. Molecular weights were measured by vapor pressure osmometry using o-dichlorobenzene as solvent. From the table Arab Light has the lowest molecular weight of the five on a relative basis. All other molecular weights are not significantly different from each other considering the error involved in the measured molecular weight, which is ± 10 % of the molecular weight.

Figure 6.1 shows the elemental analysis of the feed asphaltenes. Arab Light and Arab Heavy asphaltenes are low in nitrogen (0.83 and 0.91 wt%). All other asphaltenes have similar nitrogen content (1.17~1.27 wt%). The asphaltenes from Gudao vacuum residue is highest in H/C atomic ratio (1.41); Arab Light asphaltene is the lowest (1.07), and the others are similar (1.16~1.18). Athabasca and Arab Heavy asphaltenes have the highest sulfur content (7.47 and 7.15 wt%), whereas Gudao and Arab Light have the lowest sulfur content (4.44 and 5.67 wt%).

111
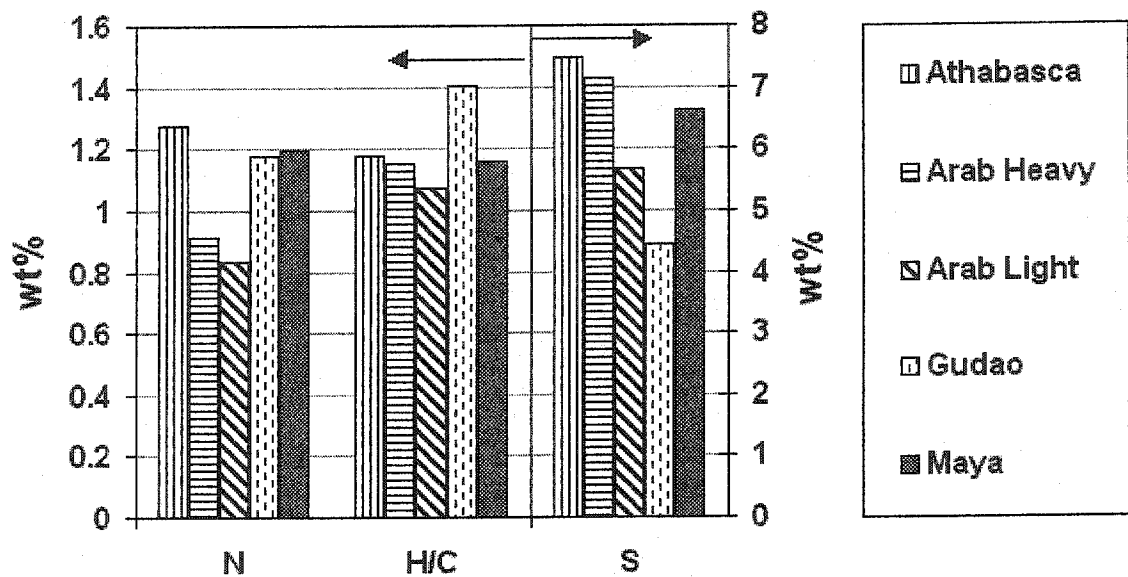
Figure 6.1 Elemental composition of the feed asphaltenes

112

Table 6-2 Molecular weights of the feed asphaltenes

Feed Asphaltene	Molecular weight
Athabasca	2861
Arab heavy	2563
Arab Light	1827
Gudao	2830
Maya	2495

6.1.2. Nuclear magnetic resonance (NMR)

The proton and carbon NMR spectra of a representative asphaltene are shown in Figure 6.2. Like any other complex mixture of bitumen molecules, they did not show any sharply defined peaks characteristic of pure compounds, but they consisted mainly of featureless envelopes resulting from a large range of chemical shifts from isomers and complicated spin-spin couplings in the ^{1}H NMR spectra. The basis of quantitative analysis of such spectra is dependent upon the resonances that are characteristic of different functional groups. Carbon functional groups were quantified based on the peak assignments and calculation procedure described in Chapter 3. Figure 6.3 shows the aromatic carbon functional group analysis for all the asphaltenes. It was observed that Arab Light had the highest percentage of quaternary aromatic carbon (Qar) and Gudao has the lowest. All other asphaltenes had comparable quantities of quaternary carbon (Qar). A similar trend was observed for protonated carbon. As a whole, among all the asphaltenes, Arab Light had the highest aromaticity and Gudao the lowest. NMR data were also used to calculate aromatic cluster size, i.e. the number of carbons in an

113

aromatic cluster. For example, naphthalene has an aromatic cluster size of 10. This parameter was calculated using the aromatic functional group contents and the method described by Solumn et al. (1989). Again, cluster size was highest in Arab Light asphaltenes and lowest in Gudao asphaltenes.

Paraffinic carbon functional group species are shown in Figure 6.4 and Figure 6.5. Paraffinic CH (CH), that indicates branched chains or substituted cycloparaffins, were highest in Arab Heavy and Gudao asphaltenes and lowest in Arab Light. Chain CH_2 groups (CHAIN) that are at least six carbons in length were highest in Gudao asphaltenes. All other asphaltenes had similar values. NMR data were also used to calculate another useful parameter, the average chain length. Chain length was calculated using the ratio of CHAIN and $C-CH_3$ functional groups, assuming one end of the paraffin chain is attached to an aromatic. Gudao had the highest chain length among the asphaltenes. Cycloparaffinic (naphthenic) CH_2 (NAPH) that are, at least, β to an aromatic ring, or not attached to an aromatic ring were highest in Gudao asphaltenes. Also, Athabasca asphaltene had a high NAPH content compared to the others. CH_2 groups that are α or β either to alkyl attachment sites in rings or chains, or to terminal methyls in chains (ab-CH_2) were lowest in Arab Light asphaltenes. The sum of NAPH and ab-CH_2 group that roughly represent the total naphthenic carbon was higher in Gudao and Athabasca compared to the other asphaltenes. Overall, the five samples obtained from around the world were very different in elemental compositions and structural parameters. This result suggests that the five samples used in this study were representative of the range of variations in chemical and structural compositions in petroleum asphaltenes.

114
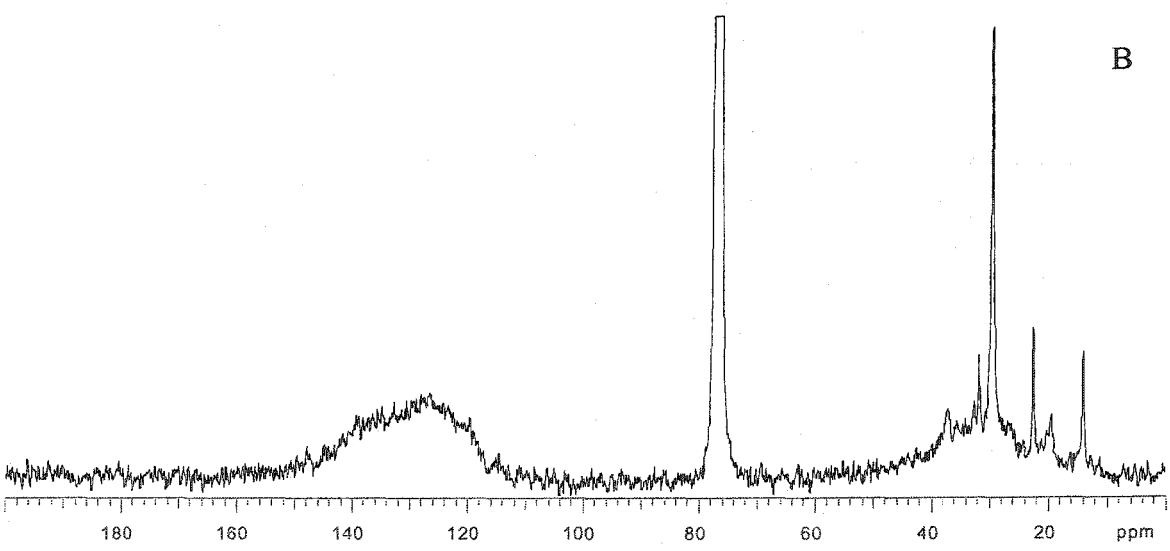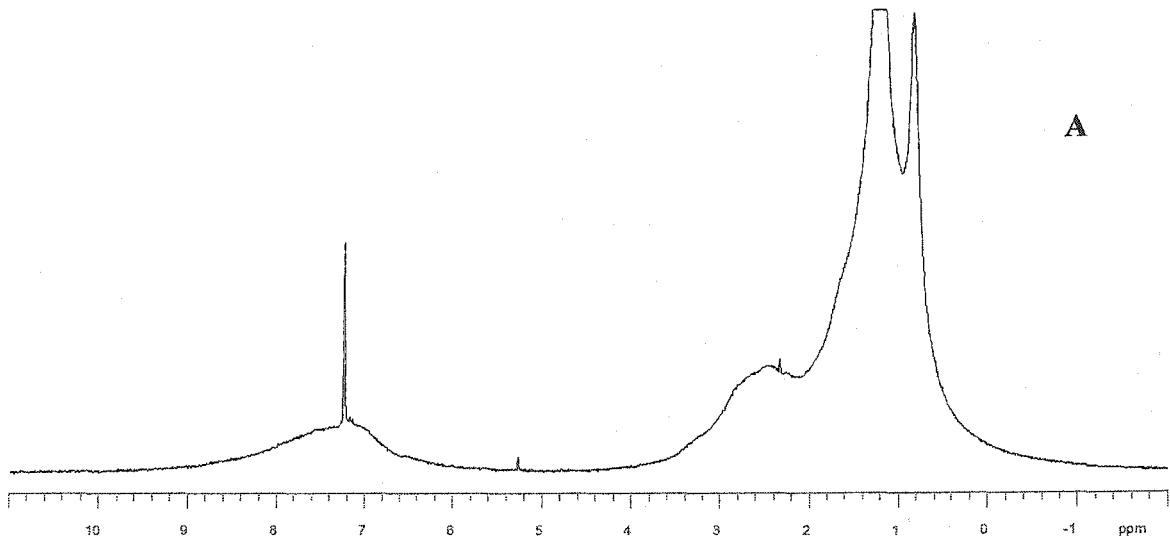
Figure 6.2 ^{1}H NMR (A) and ^{13}C NMR (B) spectra for Athabasca asphaltenes

115
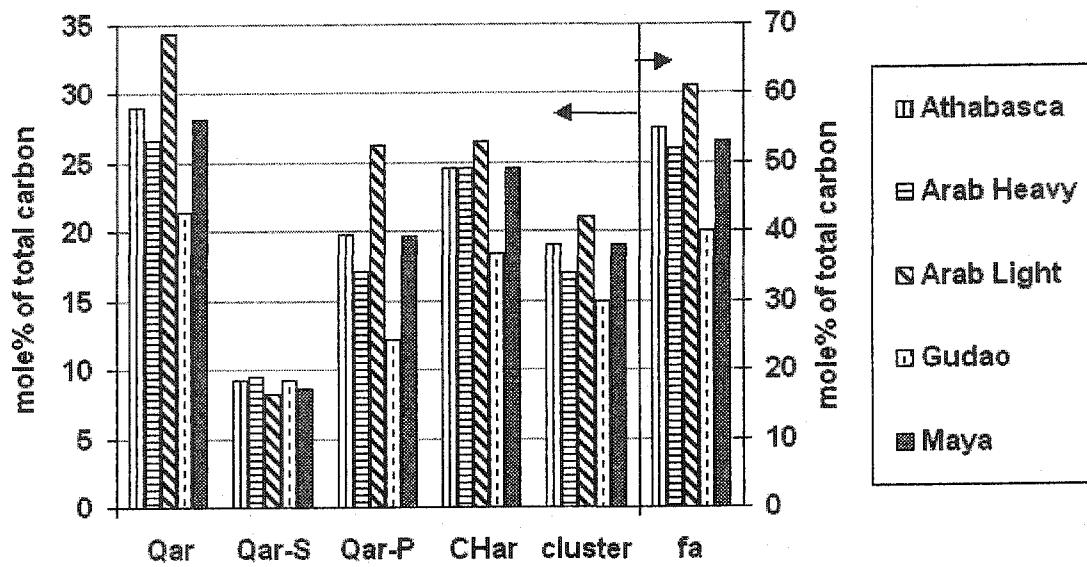
Figure 6.3 NMR analysis data for aromatic carbon functional groups

116
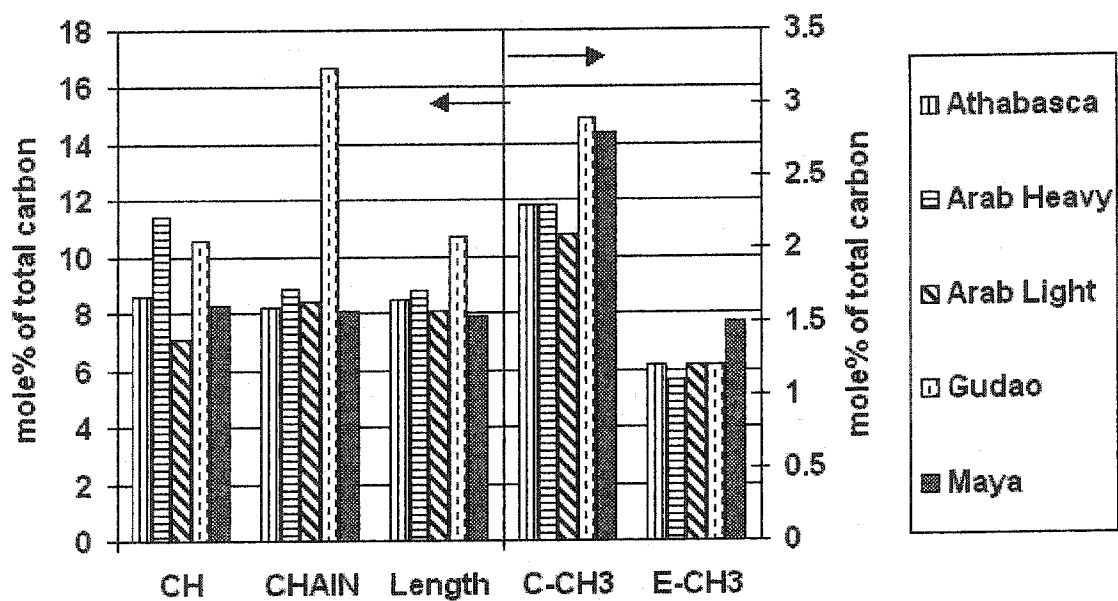
Figure 6.4 NMR analysis data for paraffinic carbon functional groups (A)

117
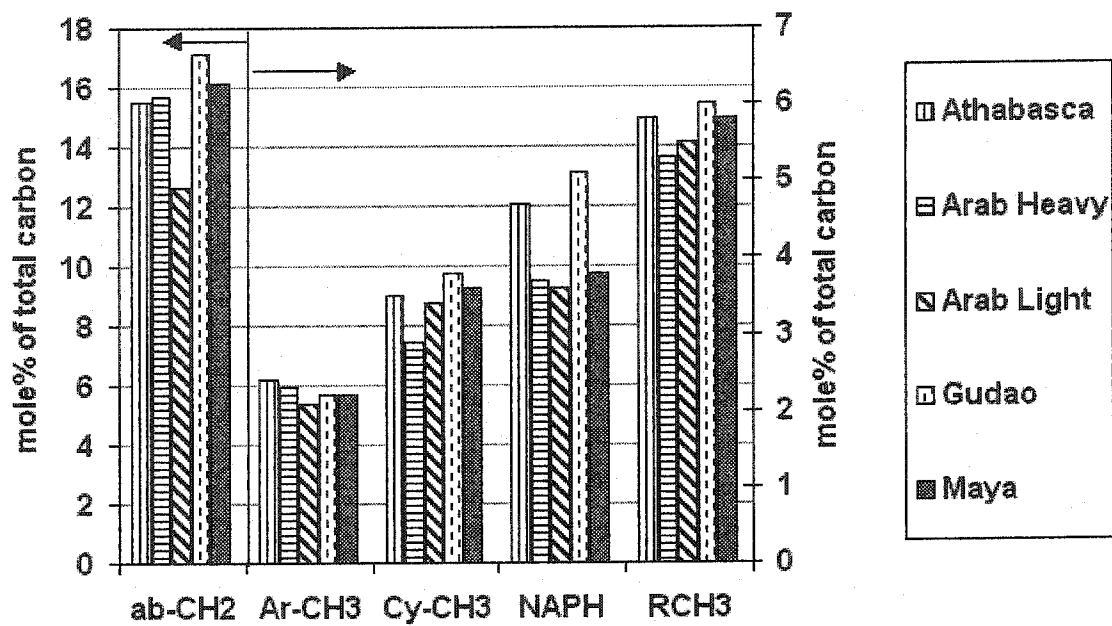
Figure 6.5 NMR analysis data for paraffinic carbon functional groups (B)

118

6.2. Thermal Cracking of Asphaltenes in 1-Methyl Naphthalene

All of the asphaltenes were reacted in 1- methyl naphalthalene (MN) for a series of reaction times. A concentration of 25 wt% initial asphaltene was used for all of the reactions. Coke and product asphaltene yields were measured for each experiment. Figure 6.6 shows the product asphaltene yield from the thermal cracking of five different asphaltenes in 1-methyl naphthalene. Gudao and Arab Light cracked slightly slower than the other three asphaltenes. These two asphaltenes had the lowest amount of sulfur among the five. Yields of residual asphaltenes after long reaction times were not significantly different between the samples.

After long reaction times, the unreactive asphaltene cores should remain in the solution and contribute to the product asphaltenes. Similar yields of residual asphaltenes from different feeds then suggest that their solubilities in 1-methyl naphthalene were similar, or in other words, structurally the asphaltene cores from different asphaltenes were not very different from each other. In order to test this hypothesis NMR analyses of residual asphaltenes from highly paraffinic Gudao and fairly aromatic Athabasca asphaltenes were done. The NMR spectroscopic data gave quantitative confirmation of the increase in aromatic carbon from the feed asphaltene to residual asphaltene for the both feeds (Table 6-3). The difference in aromaticity between the two asphaltenes decreased from 15 % in the feed to 4 % in the product. Aromaticity (without olefin) of the product asphaltenes became 72.6% for Athabasca and 68.7 % for Gudao. Paraffinic carbon disappeared considerably in both cases. Therefore, although the starting materials were very different in chemical structure, after they went through the thermal cracking

119

they became very similar in structure. This similarity helps to explain the yields of residual asphaltenes after 60 min in Figure 6.6.

Table 6-3 Comparison of aromaticity between feed and product asphaltenes

Asphaltene	Feed	Product
Athabasca	55	72.6
Gudao	40	68.7

Figure 6.7 shows the coke yield from the same sets of experiments. Gudao had the lowest coke yield among all asphaltenes. The other four samples clustered together. However, careful observation suggested that the Arab Light reacted slowly, but ultimately produced the highest amount of coke. Data from the reactions in 1-methyl naphthalene were used in the modified phase separation kinetic model (Chapter 5). The solubility limit, S_L, and first order rate constant, k_C were taken to be the same for all the asphaltenes as for Athabasca asphaltenes, assuming that the asphaltene cores were not significantly different from each other. Asphaltene cracking rate constant, k_A, and the stoichiometric coefficient, c, were estimated by minimizing the sum of squares of the error following the same procedure as described in Chapter 5. Figure 6.6 and Figure 6.7 shows the fit of the experimental data to the model. Estimated parameters, k_A and c, are presented in Table 6-4. The error estimates represent the 95% confidence interval in the parameter estimation and was calculated using the same procedure as described in Chapter 5. Arab Light had significantly lower cracking rate constant compared to Athabasca and Arab Heavy. On the other hand, the stoichiometric coefficient, c, of Gudao was significantly lower than all other asphaltenes.

120
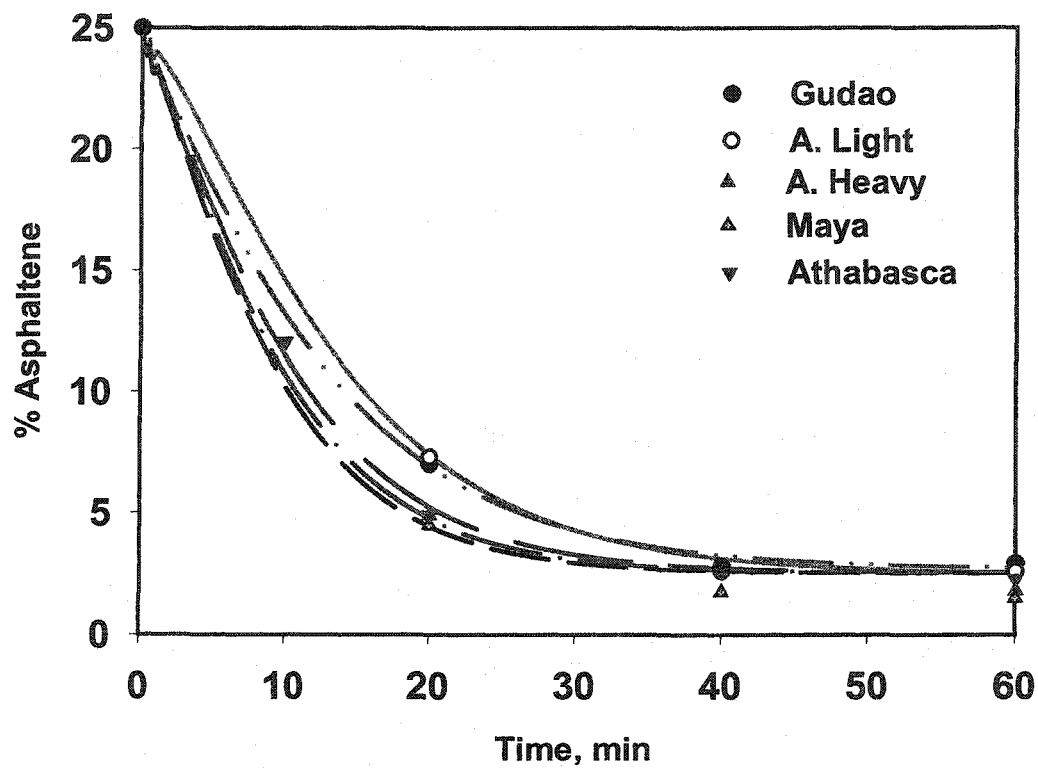
Figure 6.6 Residual asphaltene yields from the thermal cracking of asphaltenes from different sources in 1-methyl naphthalene. Curves are drawn from the model.

121
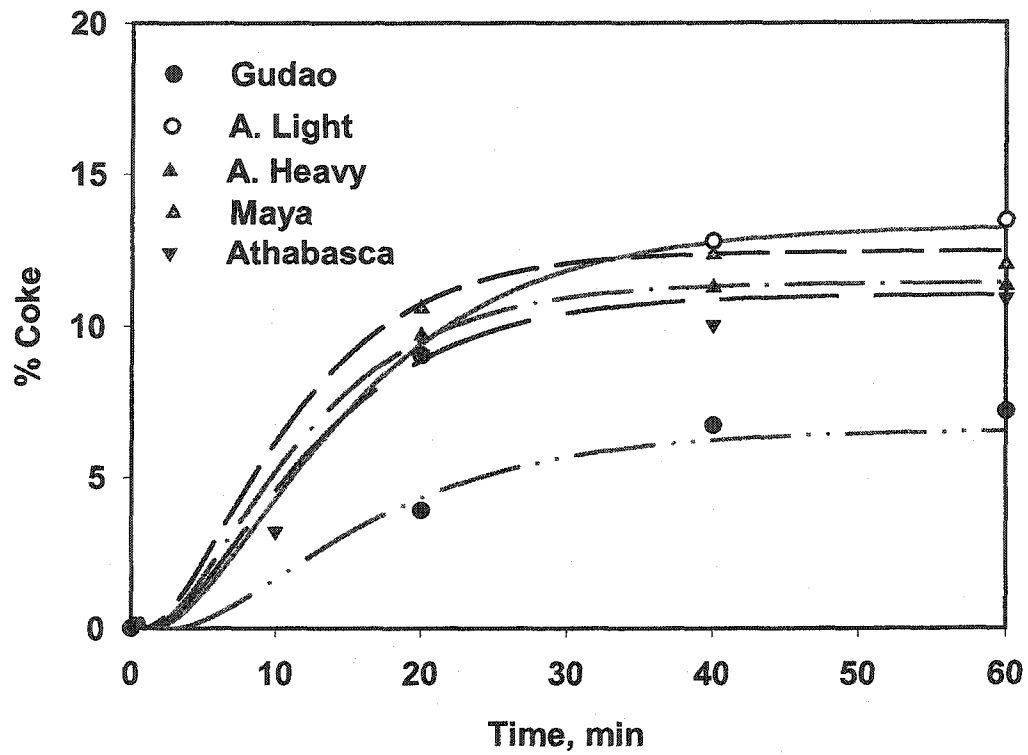
Figure 6.7 Coke yields from the thermal cracking of asphaltenes from different sources in 1-methyl naphthalene. Curves are drawn from the model.

122

Table 6-4Estimated parameters for different asphaltenes

Feed Asphaltenes	Rate constant, k_A (min^{-1})	Coefficient, c
Athabasca	0.15 ± 0.03	0.54 ± 0.03
Arab heavy	0.172 ± 0.04	0.52 ± 0.05
Arab Light	0.11 ± 0.01	0.63 ± 0.03
Gudao	0.10 ± 0.03	0.37 ± 0.02
Maya	0.19 ± 0.09	0.60 ± 0.05

6.3. Thermal Cracking of Asphaltenes in Tetralin

6.3.1. Product Yield

All the asphaltenes were reacted in the presence of tetralin for 40 minutes. From the study with Athabasca asphaltene (Chapter 5) it was found that the reactions were almost complete after 40 minutes, therefore, this reaction time was used to avoid the error involved due to heating time and overcracking of the products. A concentration of 25 wt% initial asphaltene was used for all of the reactions. Coke and product asphaltene yields were measured for each experiment. Figure 6.8 shows that the coke yield was suppressed by the addition of tetralin for all asphaltenes. Asphaltenes from Gudao vacuum residue produced the lowest amount of coke, whereas coke yields from all other asphaltenes were not significantly different from each other. On the other hand, the

123

residual asphaltenes yield varied significantly among the different feeds. In some cases more asphaltenes were converted into heptane-soluble products compared to others, which suggests that tetralin could suppress the coke yield but the hydrogen donation reactions did not occur at the same rate for all asphaltenes. The reactions involving a hydrogen donor solvent are likely much more complex than an inert solvent. Data from the reactions in tetralin can be explained by the modified phase separation kinetic model developed in Chapter 5. For asphaltenes, the same rate constant, k_A, and stoichiometric coefficient, c, were used as shown in Table 6-4. The stoichiometric coefficient, d, was estimated from the difference in heptane solubles plus volatiles formed when each each sample of asphaltenes was reacted in TN and 1-MN, following the same procedure as described in Chapter 5. The product yields were then represented in the kinetic model by adjusting the rate constant, k_C. Estimated rate constants, k_C are presented in Table 6-5. Data were too limited to estimate error bounds except for Athabasca. From the results presented in Table 6-5, the value of k_C for Athabasca was significantly higher than the other asphaltenes.

Table 6-5 Estimated rate constant, k_C, for different asphaltenes

Feed Asphaltenes	Rate constant, k_C (min^{-1})
Athabasca	0.028 ± 0.005
Arab heavy	0.0089
Arab Light	0.0125
Gudao	0.0108
Maya	0.0167
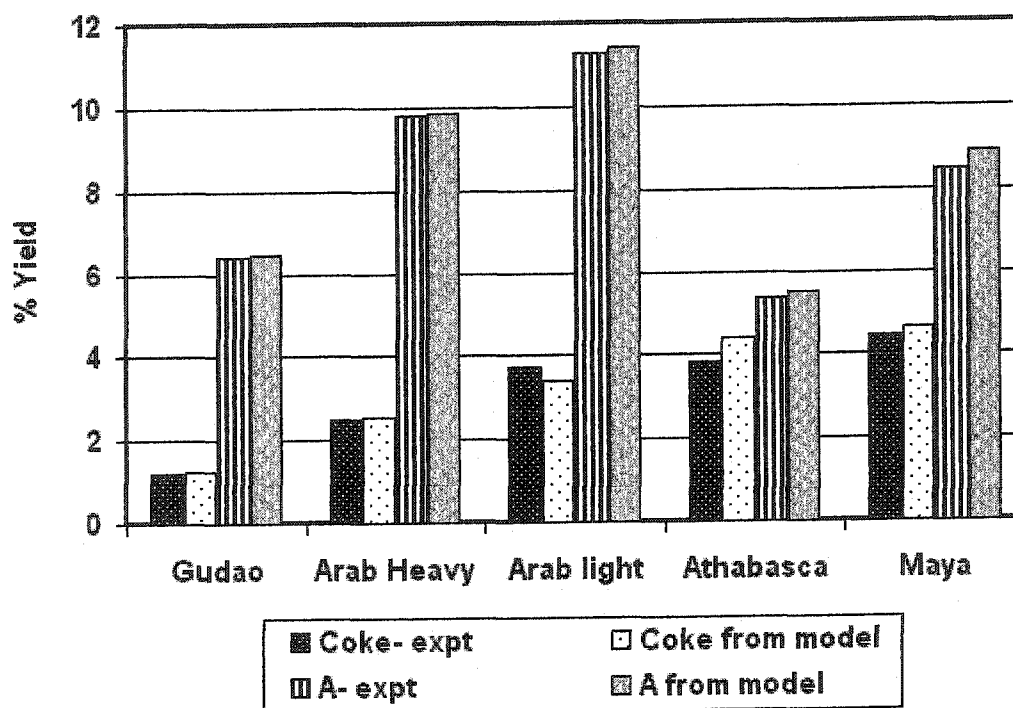
Figure 6.8 Coke and asphaltene yield from the thermolysis of different asphaltenes in Tetralin for 40 min. A=asphaltene

125

6.3.2. Analysis of the Heptane-soluble Product

The heptane-soluble portion of the products was analyzed by GC for each experiment. Naphthalene was identified as the major reaction product by comparing the retention time with pure naphthalene and by confirmation with GC-MS. A peak for 1-methyl indane was identified as the other major product by GC-MS. Trace quantities of butyl benzene, 1-methyl tetralin and 1- and 2- methylnaphthalene were also observed.

The major products of tetralin found in this study are the same as those found by other authors (Curran et al., 1967; Bockrath and Schroeder, 1981; Collin et al., 1985). In this study asphaltene was present at a sufficient quantity with tetralin. These asphaltenes could generate a large quantity of free radicals; therefore, in the presence of reacting asphaltenes there would be a larger quantity of α- tetralyl radical because of hydrogen removal at the α position by asphaltene radicals. Thus dehydrogenation to form naphthalene would dominate over ring contraction to form methyl indane at the conditions employed in this study.

Total recovery of tetralin, naphthalene and 1-methylindane was approximately 85 wt % of the original tetralin in the reactor. Hydrogen transfer to asphaltenes was calculated from the ratio of the remaining tetralin to naphthalene in the heptane solubles. This approach assumes that the missing tetralin underwent addition reactions without donating hydrogen, as observed by Khorasheh and Gray (1993). Table 6-6 gives the amount of hydrogen transfer to each asphaltene after 40 min reaction in tetralin. The numbers presented in the table are somewhat biased due to the assumptions made in the calculations, which do not account for hydrogen transfer from the missing tetralin.

126

However, from the table it is obvious that hydrogen transfer to Athabasca asphaltenes was higher than any of the other asphaltenes. This observation might seem to be somewhat contradictory to the fact that Athabasca asphaltene had the highest concentration of naphthenic groups. These naphthenic groups can transfer hydrogen and become aromatics, therefore, hydrogen acceptance from an outside donor should be lowered. However, the differences in naphthenic groups were small and the potential hydrogen transfer from naphthenes would also be small, i.e. in the range of 0.0144 to 0.0197 mg H/g asphaltene, compared to 13.27 mg H/g measured for Athabasca.. thus the hydrogen transfer was greatly influenced by the hydrogen acceptance capacity of the asphaltenes.

Table 6-6 Hydrogen transfer to asphaltenes

Feed Asphaltene	H Transfer, mg H/g A
Athabasca	13.3
Arab heavy	8.7
Arab Light	7.7
Gudao	7.7
Maya	8.73

6.4. Relationship Between Structure and the Estimated Parameters

The aim of this series of experiments was to predict the behavior of asphaltenes (coke formation and asphaltenes conversion) based on their properties. Coke formation in

127

two different solvents could be correlated by the kinetic model described in Chapter 5. Therefore, the model can be used for prediction of coke formation, if the parameters in the model can be estimated using some structural property of the asphaltenes. Although general predictions for different feeds are difficult, it might be possible to find correlations among the properties of asphaltenes and the estimated parameters in the model. The kinetic parameters obtained in this study together with the structural property data were analyzed statistically in order to predict coke formation.

6.4.1. Estimated rate constant, k_A

There are few structural properties in the feedstock that will have a strong influence on the cracking rate of asphaltenes. The most important is the sulfide component of the feed. The facile rupture of the sulfide bonds has been postulated as a major mechanism for cracking of the high molecular weight components of bitumen (Gray, 1994). The thermal reactions of sulfur compounds generate considerable amounts of free radicals. The presence of sulfide as a free radical initiator was found to increase the rate of reaction (Chapter 5). Similar observations are expected for the cracking rate of asphaltenes. In order to check this hypothesis, the amount of sulfide in each asphaltene was determined by selectively oxidizing the sulfide component in the asphaltenes and then measuring the sulfoxide concentration by infrared spectroscopy as described in Chapter 3. The amount of sulfide in the various asphaltenes was linearly correlated with the cracking rate constant of asphaltenes (Figure 6.9). The correlation was statistically significant (to 99% confidence). The weighted-least-squares method was used to do the regression and the slope was found to be significantly different from zero (to 95% confidence).

128
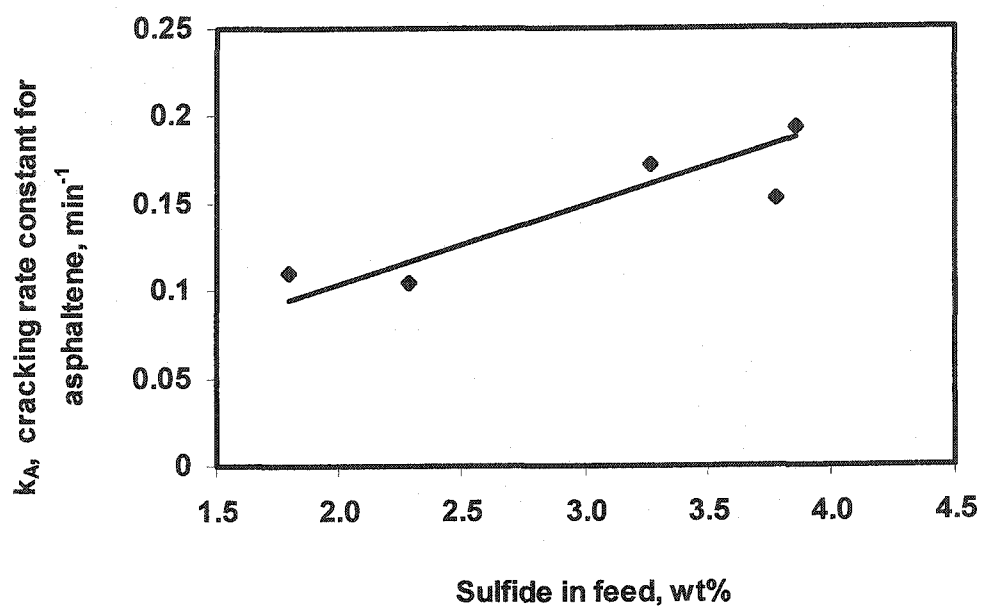
Figure 6.9 Correlation between asphaltene cracking rate constant, k_A, and sulfide concentration in feed

129

Incorporation of the influence of other structural properties of the feed will make the relationship more accurate. The rate of thermal cracking reactions is expected to increase with molar mass of asphaltenes (Asoka et al., 1983). Gray et al. (1991), however, found a monotonic decrease in the thermal cracking rate with increasing molar mass when they hydrocracked different Alberta residues to find out the relationship between chemical structure and reactivity. According to these authors, when the residue molecules decompose into large fragments, a heavier feed molecule would require more scission reactions in order to appear as distillate. If the decomposition were dominated by the loss of side chains and groups, leaving a more aromatic residual core, then the residue conversion should be independent of molar mass. In this study no relationship was found between the feed molecular weight and the reactivity of the asphaltenes, supporting the observation of Gray et al. (1991).

The C-N bonds present in asphaltene molecules are thermally stable, however, the nitrogen can activate the C-C bonds adjacent to nitrogen containing heterocyclic rings (Speight, 1987). Therefore, it seems possible that an increase in the nitrogen content will enhance the cracking conversion of asphaltenes. Long chain paraffins can also have an impact on the rate constant, since they are more reactive compared to the other constituents present in the oil (Gray, 1994). However, only the amount of sulfide had a strong correlation with the cracking rate constant. None of the other structural properties had a significant correlation with the value of k_A based on a 95% confidence limit. These observations suggest that though the cracking rate was likely due to the combined effect of several different structural properties of the feed, the sulfide content was clearly a dominating factor.

130

6.4.2. Stoichiometric coefficient, c

The stoichiometric ratio, c, determines what fraction of the asphaltene will form aromatic cores and then react to form coke if no other inhibition is present. Since the aromatic cores, defined in Chapter 5, are mostly aromatic, it is logical to assume that the ratio, c, will correlate with the fraction of aromatic carbon in the feed. Although not all the aromatic carbons in each feed are polynuclear aromatic clusters and likely to go to asphaltene cores, the correlation between stoichiometric coefficient, c, and the aromaticity of the feed, f_a, was statistically significant (to 99.5 % confidence), in the experimental data from the coking reactions with 1-methyl naphthalene (Figure 6.10). The coke yield from Arab Light started slowly since it has a low sulfide content, but finally reached the highest value among all the feeds because of its high aromatic content.

131
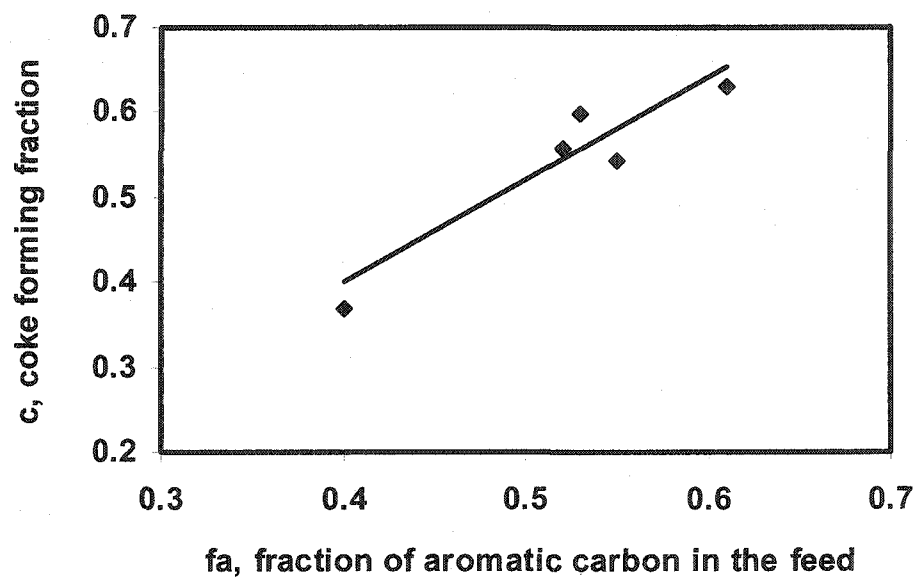
Figure 6.10 Correlation between stoichiometric coefficient, c, and aromaticity of the feed

132

6.4.3. Estimated Rate Constant, k_c

The study of the role of solvents suggested that the solvent has a chemical influence on the formation of toluene-insoluble coke, even in the new phase where asphaltene cores are deficient in solvent (Chapter 5). This mechanism was consistent with the kinetic model, where k_C was changed in different solvents. Analysis with different feedstocks suggested that k_C also depended on the structural properties of the asphaltenes, since the rate constant was different for different feeds (Table 6-5) when the feeds were reacted in the presence of TN. However, no simple correlation between any of the structural properties of the asphaltenes and the rate constant k_C was found. All the correlations were statistically insignificant, even at the 80% confidence level. This observation is not surprising considering the complex nature of the reactions involved. Cronauer et al. (1982) examined the exchange reactions of tetralin and hydrogen with several aromatic compounds. They used 1,2 diphenylethane to initiate the reaction. They found the deuterium incorporation into pyrene from tetralin-d_{12} in a N_2 atmosphere was 23.5% when expressed as percentage of deutorium in total hydrogen. Compared to pyrene, deuterium incorporation into chrysene was only 16%. Although, both chrysene and pyrene have same average structural properties, hydrogen transfer to these two isomers from tetralin was significantly different. Significant changes in behavior between simple model components that have similar chemical structures, suggest that it is not surprising that average properties in a much more complex structure like asphaltene would not correlate well with hydrogen transfer and k_C.

133

6.5. Prediction of coke formation in 1-methyl naphthalene

Two asphaltenes apart from the asphaltenes used in this study were used to validate the model. The kinetic constants for cracking of a range of asphaltenes, from different locations around the world, in 1-methylnapthalene were linearly correlated with the chemical structure of the asphaltenes (Section 5.4). The rate constant for cracking of asphaltenes was correlated as follows:

$$k_a = 0.0377 S_d + 0.0336 \tag{1}$$

where S_d is the weight % of sulfide sulfur in the asphaltenes, as determined by oxidation analysis. The yield coefficient for coke formation was correlated as follows:

$$c = 1.2434 f_a - 0.1091 \tag{2}$$

where f_a is the fraction of aromatic carbon in the asphaltenes as determined by ^{13}C NMR. These relationships would allow the prediction of cracking of asphaltenes on the basis of simple chemical analysis. Sulfide content of these asphaltenes was not determined experimentally. The average sulfide fraction of the sulfur in the five asphaltenes was found to be 0.47 ± 0.09. Assuming a constant fraction of sulfide sulfur in the two asphaltenes of 0.43, the kinetic parameters were estimated (Table 6-7). The modified phase separation model was then used to calculate the time course of coke formation and asphaltene conversion. Agreement between the predictions from the model and the experiments (Figure 6.11 and Figure 6.12) was excellent. The results from coking in 1-methylnaphthalene were very encouraging because they showed that simple models for asphaltene chemistry can give predictions of kinetics in some controlled conditions. The ability of a correlation based on sulfide concentration and aromaticity to predict reaction kinetics was very significant.

134
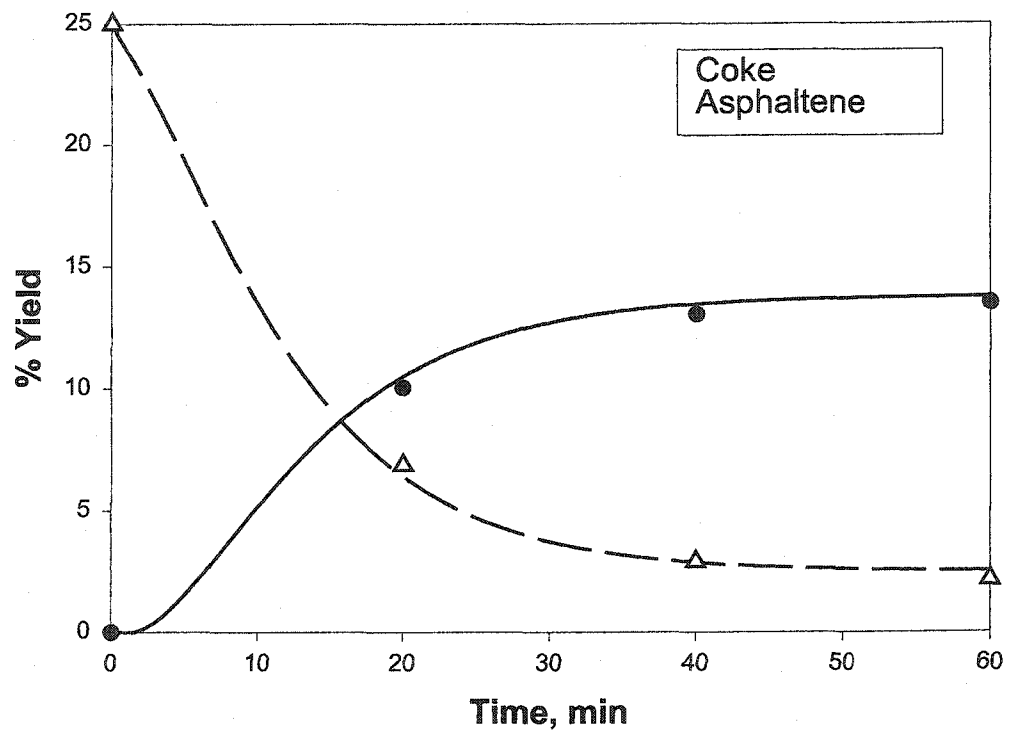
Figure 6.11 Coke and asphaltene yield from the thermal cracking of Iranian Light asphaltenes in 1-methyl naphthalene

135
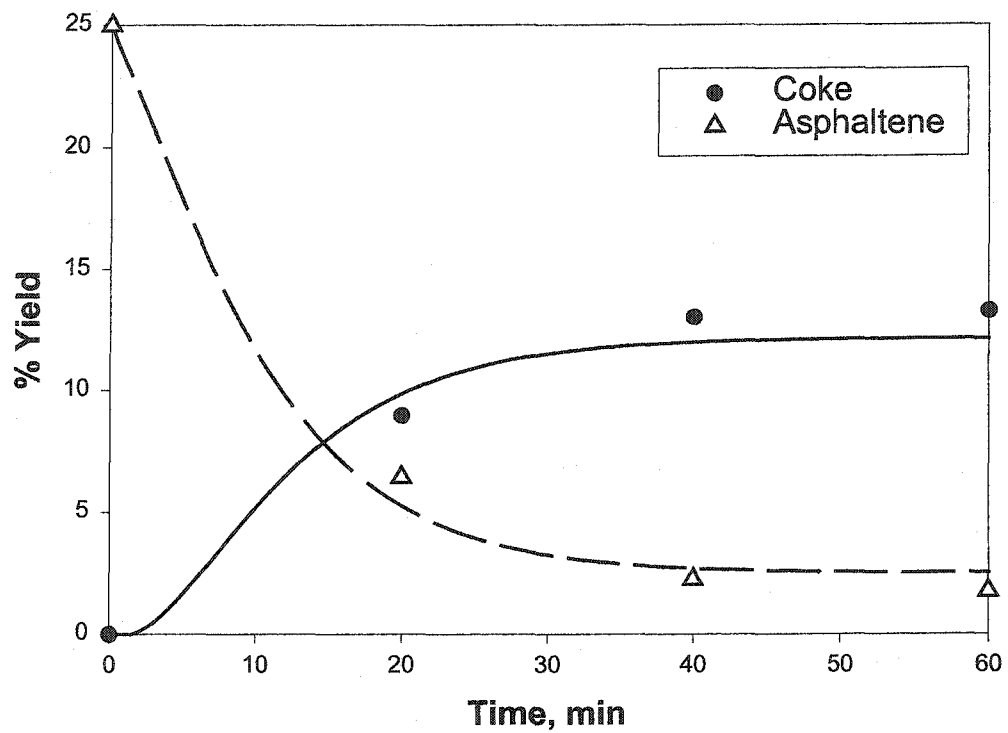
Figure 6.12 Coke and asphaltene yield from the thermal cracking of Khafji asphaltenes in

1-methyl naphthalene

136

Table 6-7 Prediction of the parameters

Feed	Experimental		Predicted	
	S, wt%	f_a	k_A	c
Iranian Light	5.9	0.61	0.129	0.649
Khafji	7.6	0.56	0.157	0.587

6.6. Conclusions

Modified phase separation kinetic model, following Wiehe (1993), was consistent with the data on coke formation from asphaltenes with different structural properties in solvent 1-MN and tetralin. The two fitting parameters, asphaltene cracking rate constant (k_A) and stoichiometric coefficient (c), were found to correlate with two experimental properties, sulfide content and aromaticity of the asphaltenes. Consequently, the model can be used for prediction of coke formation in solvent 1-MN at 430 °C from the structural properties of asphaltenes.

6.7. References:

Ali, M. F. and Saleem, M.,"Composition of Asphaltenes from Saudi Arabian Crude Oils", The Arabian Journal for Science and Engineering, 1994, 19(2B), 319-333

Asaoka, S., Nakata, S., Shiroto, Y., and Takeuchi, C., "Asphaltene Cracking in Catalytic Hydrotreating of Heavy Oils. 2.Study of Changes in Asphaltene Structure During Catalytic Hydroprocessing", Ind. Eng. Chem. Proc. Des. Dev., 1983, 22, 242-248

Bockrath, B. C., and Schroeder, K. T., "Coal Mineral Matter Catalysis in Liquefaction, New Approaches in Coal Chemistry", *ACS Symposium Ser. No. 196, chap. 11, American Chemical Society*, Washington D.C., **1981**

Collin, P. J., Gilbert, T. D., Rottendorf H. and Wilson, M. A., "Ring Contraction and Dehydrogenation in Polycyclic Hydroaromatics at Coal Liquefaction Temperatures", *Fuel*, **1985**, 64, 1280-1285

Cronauer, D. C., McNeil, R. I., Young, D. C. and Ruberto, R. G.,"Hydrogen/Deuterium Transfer in Coal Liquefaction", *Fuel*, **1982**, 610-619

Curran, G. P., Struck, R. T., and Gor, E.," Mechanism of the Hydrogen-Transfer Process to Coal and Coal Extract", *Ind. Eng. Chem. Proc. Des. Dev.* **1967**, 6(2), 166-173

Gray, M. R., "Upgrading Petroleum Residues and Heavy Oils", Marcel Dekker, Inc., New York, **1994**, Chapter 3

Gray, M. R., Jokuty, P., Yeniova, L., Nazarewycz, L., Wanke, S. E., Achia, U., Krzywicki, A., Sanford, E. C., Sy, O. K. Y., "The Realtionship Between Chemical Structure and Reactivity of Alberta Bitumens and Heavy Oils", *Can. J. Chem. Eng.*, **1991**, 69, 833-843

Khorasheh, F. and Gray, M. R., "High-Pressure Thermal Cracking of n-Hexadecane in Tetralin", *Energy & Fuels*, **1993**, 7, 960-967

Solum, M. S., Pugmire, R. J. and Grant, D. M., "^{13}C Solid- State NMR of Argonne Premium Coals", *Energy & Fuels*, **1989**, 3, 187-193

Speight, J. G., "Initial Reactions in the Coking of Residua", *Preprints. Div. Petrol. Chem. Am. Chem. Soc.*, **1987**, 32(2), 413-418

Trauth, D. M., Yasar, M., Neurock, M., Nigam, A., Klein, M. and Kukes, S. G.,

"Asphaltene and Resid Pyrolysis: Effect of Reaction Environment", *Sci. Technol. Int'l.*, **1992**, 10(7), 1161-1179

Zhao, J., Baoquan, M. and Guohe, Q.,"A Study on Hydrogen Transfer of Gudao Vacuum Residue in VRDS Process", *208th National Meeting, Div. Petrol. Chem. Am. Chem. Soc., Washington D. C.*, **1994**, 426-429

7. CONCLUSIONS AND RECOMMENDATIONS

7.1. Conclusions

Three objectives were set out in Chapter 1

1) Examine the kinetics of solvent interactions with asphaltene during coke formation,

2) Study coking kinetics as a function of asphaltene structure, and

3) Explore the phase behavior during coke formation

The conclusions arrived at for each objective is considered in the following section.

7.1.1. Kinetics of Solvent Interactions with Asphaltene

The formation of coke from asphaltenes during thermal cracking was significantly affected by both reactions with the liquid components and the solvent properties of the liquid medium. Reaction of Athabasca asphaltenes in maltenes at different concentrations and reactions in a series of aromatic solvents (1-methyl naphthalene (1-MN), tetralin (TN) and naphthalene (NP)) were used to investigate the role of liquid. Pure maltenes produced 6.99% coke and 13.9% product asphaltenes. When the contribution from the maltenes was subtracted from the total coke produced from a mixture of asphaltenes and maltenes, the coke formation from asphaltenes was almost constant at 0.455 ± 0.035 g/g of initial asphaltenes. This result was consistent with an apparent first-order kinetic conversion of asphaltenes to coke.

The aromatic solvents used in this study had similar solvent strength, thus the change in solubility could be neglected. Comparison of coke and asphaltene yield from the thermolysis of 25wt% asphaltene in these four solvents showed considerable

140

reduction in coke yield in tetralin, which is consistent with its hydrogen donating ability. 1-MN and NP behaved similar in terms of coke formation and product asphaltenes. Coke formation in these two solvents, however, was reduced compared to maltene. This reduction may arise from the different solvent strengths of these three solvents. However, maltenes are more complex and reactive than 1-MN and NP and produced a significant amount of asphaltenes.

The most important characteristics of the liquid phase were hydrogen donating ability and the ability to initiate cracking reactions. The later mechanism was studied by adding an alkyl sulfide, n-dodecylsulfide (DDS) to a mixture of asphaltene and 1-MN to match the approximate sulfide content of maltenes. DDS increased the rate of thermal cracking of asphaltene, increasing the rate of coke formation but not its ultimate yield after 40 min of reaction.

Hydrogen transfer was studied using three different concentrations of TN in 1-MN, which served as solvent of different hydrogen donating ability. It was found that the hydrogen donating ability of the solvent and the hydrogen accepting ability of the asphaltenes both played an important role in determining the ultimate yield of coke. A mixture of TN and 1-MN at 1:2 ratio should have approximately one third of the overall hydrogen donating ability of pure TN, but this reduction gave no significant change in yield of coke or asphaltenes relative to the pure solvent. This observation was verified by measuring the hydrogen transfer to asphaltenes.

A modified kinetic model based on phase separation, following Wiehe (1993), was consistent with the data on coke formation from asphaltenes in different solvents with low hydrogen donation ability. The phase separation model was further extended in

141

order to account for the significant reduction in coke yield due to hydrogen donation. Addition of a hydrogen transfer reaction to the model gave consistent results for tetralin mixtures with high hydrogen donating capacity.

7.1.2. Kinetics as a Function of Asphaltene Structure

Coking kinetics as a function of asphlatene structure was examined by reacting several different asphaltenes in 1-MN and TN. Asphaltenes were selected from around the world in order to represent feed materials of diverse chemical properties. The selected asphaltenes were Athabasca asphaltenes from Canada, Arabian Light and Arabian Heavy from Saudi Arabia, Maya from Mexico and Gudao from China. Among these asphaltenes Arabian Light was the most aromatic and Gudao was the most paraffinic asphaltenes. On the other hand, both of them had lower sulfur content compared to the other asphaltenes. Thermal cracking of these asphaltenes in 1-MN showed that Gudao and Arab Light crack slightly slower than the other three asphaltenes. These two asphaltenes had the lowest amount of sulfur among the five. Yields of residual asphaltenes after long reaction time were not significantly different from each other. Similar yields of residual asphaltenes from different feeds then suggest that their solubility in 1-methyl naphthalene was similar. NMR analyses of residual asphaltenes from highly paraffinic Gudao and fairly aromatic Athabasca asphaltenes showed that the difference in aromaticity between the two asphaltenes decreased from 15 % in the feed to 4 % in the product. Paraffinic carbon disappeared considerably in both cases. Therefore, although the starting materials were very different in chemical structure, after they went through the thermal cracking they became very similar in structure. This similarity helps to explain the yields of residual asphaltene after 60 min of reaction. Gudao had the lowest coke yield among all

142

asphaltenes. Arab Light reacted slowly, but ultimately produced the highest amount of coke.

Thermal cracking of these asphaltenes in tetralin showed that the coke yields from the asphaltenes were not significantly different from each other. However, the residual asphaltene yield varied significantly among the different feeds, which suggests that tetralin could suppress the coke yield but the hydrogen donation reactions did not occur at the same rate for all asphaltenes. Analysis of the heptane soluble product from reaction in tetralin suggested that dehydrogenation was dominated over ring contraction at the reaction conditions employed in this study.

All of these data from 1-MN and tetralin could be fitted to the modified phase separation model as described in Chapter 5. The two fitting parameters for the thermolysis in 1-MN, asphaltene cracking rate constant (k_A) and stoichiometric coefficient (c), were found to correlate with two experimental properties, sulfide content and aromaticity of the asphaltenes. Consequently, the model can be used for prediction of coke formation in solvent 1-MN from the structural properties of asphaltenes. However, rate constant of the hydrogen deficient phase, k_C, was not found to correlate with any of the structural properties of the feed. This observation was likely due to the fact that this work used average structural properties of the asphaltenes. The averrage structural property may not be sufficient to account for the significant changes in the hydrogen transfer behavior that may occur between compounds that have similar functional group characteristics, e. g. isomers.

143

7.1.3. Phase Behavior during Coke Formation

Phase behavior during coke formation was investigated by observing the coke produced from selected reactions under scanning electron microscopy (SEM). The influence of fine solids and diluent on the morphology of the coke phase and the possibility of phase inversion during coking was studied. Solid-free Athabasca asphaltenes mixed with 1-MN or maltene and a mixture of two supercritical fluid extraction (SFE) fractions of Athabasca vacuum residue were used as the feed materials for coking reactions.

The observed behavior of coke spheres was consistent with the fact that coke under coking conditions was in a well-defined second liquid phase. Coke spheres were better dispersed in coke samples from dilute feed. More coalescence was observed in coke produced from concentrated feed. The average particle size was found to be larger for coke from pure asphaltene compared to the coke from a dilute system, e.g. 30wt% asphaltene in 1-MN, likely due to the higher concentration of coalescing particles in pure asphaltene. The addition of fine solids decreased the coalescence and droplet size significantly. The solids might have initially acted as highly dispersed nucleation sites and let coke deposit on it. Therefore, the dispersion was better in presence of solids that resulted in less coalescence and smaller size of spheres.

In order to study the phase inversion during coke formation, coke from the reaction of only solid-free feeds was considered, since solid was found to influence the coke morphology considerably. Phase inversion was inferred from the observed micrographs of coke produced from pure asphaltene. Feasibility of phase inversion was confirmed from free energy point of view by calculating the entropy difference for a set

144

of representative conditions. Qualitatively, as the volume fraction of the coke increases, there is more chance of having a phase inversion. This result agrees with the phenomena observed in polymer blends and mesophase formation where phase inversion occurs at high concentration depending on the viscosity ratio.

7.2. Recommendations

1) The ultimate goal is to predict the coke formation of real feed to a coker, which consists of both asphaltenes and maltenes. A thorough study of the kinetics of maltenes of different structural properties would be useful for the model to give prediction of coke formation from various coker feeds. In order to study the behavior of maltenes, several experiments can be done. Coking of maltenes will give the rate constant, k_H, and stoichiometric coefficient, b, as described in Chapter 4. These rate constants and stoichiometric coefficients from several different maltenes could then be used to find any correlations between the structural properties and the parameters. Coking reactions of different maltenes mixed with one particular asphaltenes can serve as a check of the behavior of maltene in the resid environment. This experiment would also determine if the solubilizing role of the resins has any significance at coking conditions.

2) The temperature at which the reactions were done in this study was comparatively lower than the temperatures that are being used in industrial cokers. Repetition of these experiments at higher temperatures would give more practical data. Measurement of activation energies of the rate constants will make the model more useful for any reaction conditions.

3) The entropy calculations in Chapter 6 gave only qualitative estimation. In order to get quantitative estimation, all the properties of the coke and oil need to be calculated

145

or measured at reactor conditions. If experimental measurement of the properties at reactor condition becomes possible, the ability of the free energy calculation to measure the phase inversion point will be much stronger.

146

A1 Entropy Calculation

For state 1, average radius of the spheres was assumed to be R_1. Number of spheres of R_1 radius was calculated from equation (1). Surface area of the spheres was then calculated following equation (2).

$$V^\alpha = n_1 \frac{4}{3}\pi R_1^3 \tag{1}$$

$$A_1^\sigma = n_1 4\pi R_1^2 \tag{2}$$

Similarly, assuming R_2 as the average radius of the spheres for state 2, total number of spheres and surface area for state 2 were calculated using equations (3) and (4).

$$V^\beta = n_2 \frac{4}{3}\pi R_2^3 \tag{3}$$

$$A_2^\sigma = n_2 4\pi R_2^2 \tag{4}$$

Weight of the coke and oil for 1 ml of mixture was calculated from coke and oil density. Number of moles in the coke and oil phase was calculated from their average MW as follows:

$$N^\alpha + N^\beta = V^\alpha \times \rho^\alpha + V^\beta \times \rho^\beta \tag{5}$$

Then number of moles at the interface was calculated as follows:

$$N^\sigma = 0.01 \times (N^\alpha + N^\beta) \tag{6}$$

Total number of moles, N, was obtained by adding equations (5) and (6). Entropy difference, $(S_2-S_1) \times T/\gamma$, was then calculated using the following equation

$$(S_2 - S) \times \frac{T}{\gamma_1} = \left[\frac{2}{R_2}(V - Nv^\beta) - \left(A_2^\sigma - A_1^\sigma + \frac{2V^\alpha}{R_2} + \frac{2V^\alpha}{R_1} \right) \right] \tag{7}$$

147
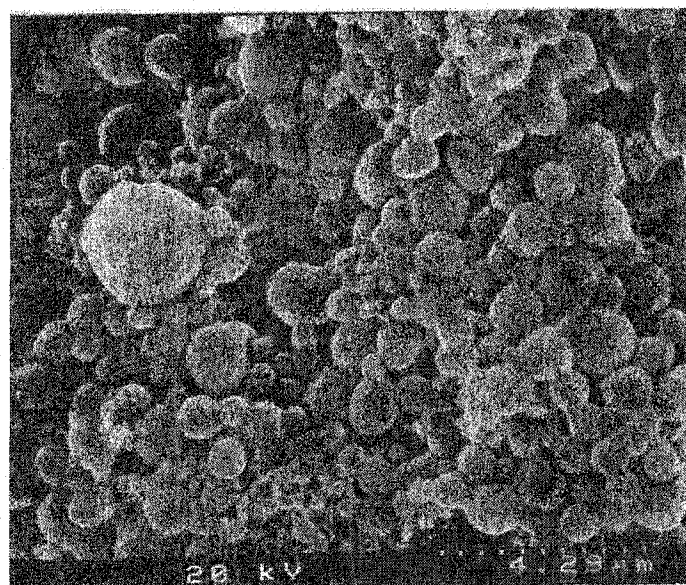
A
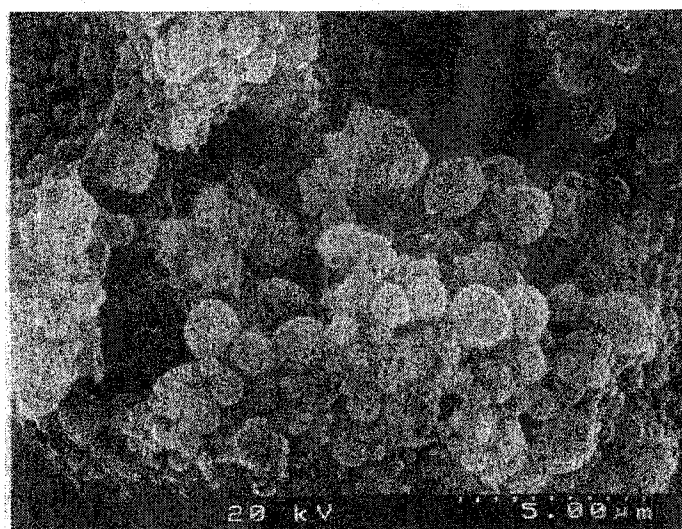
B

Figure A1. Micrograph of coke from the mixture of 10 wt% end cut with fraction-1 (A)

and 20 wt% end cut with fraction-1 (B) of SFE fraction at 430°C and 40 min

148
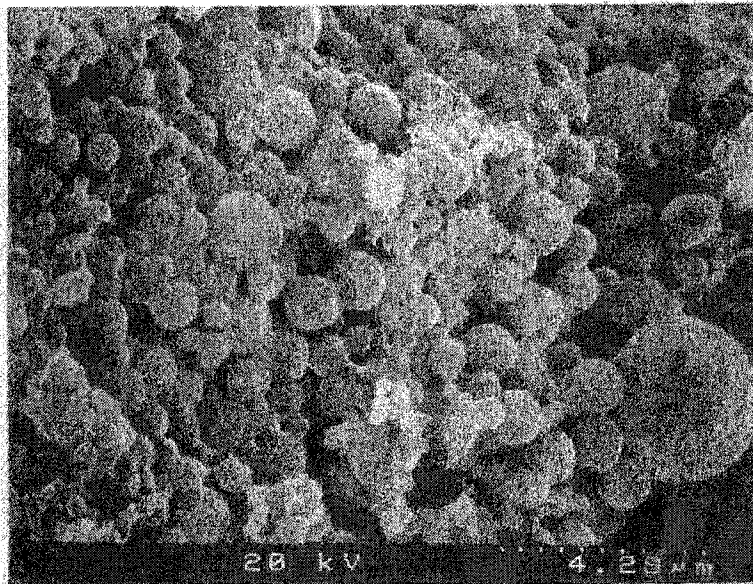
A
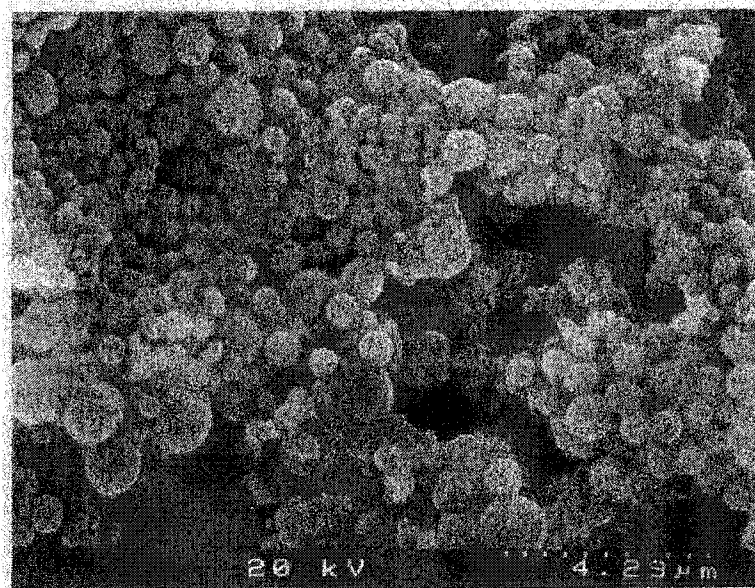
B

Figure A2. Micrograph of coke from the mixture of 10 wt% end cut with fraction-1 (A) and 20 wt% end cut with fraction-1 (B) of SFE fraction at 430°C and 40 min

149

A3 Kinetic Model

A3.1 Differential equations

The following differential equations were solved to obtain the curves shown for the model for hydrogen donor solvent. The same nomenclature as defined in the text is used here.

Cracking of initial asphaltenes:

$$\frac{d[A^+]}{dt} = -k_A[A^+] \tag{1}$$

Reaction of asphaltene cores capable of accepting hydrogen:

$$\frac{d[A^{*A}]}{dt} = d\,k_A[A^+] - k'[TN][A^{*A}] - k_C\left(\frac{[A^{*A}]}{[A^{*A}]+[A^{*NA}]}\right)[A^*_{ex}] \tag{2}$$

Reaction of asphaltene cores that cannot accept hydrogen:

$$\frac{d[A^{*NA}]}{dt} = (c-d)\,k_A[A^+] - k_C\left(\frac{[A^{*NA}]}{[A^{*A}]+[A^{*NA}]}\right)[A^*_{ex}] \tag{3}$$

Reaction of tetralin with aromatic cores:

150

$$\frac{d[TN]}{dt} = -k'\,[TN][A^{*A}]$$

(4)

Rate of formation of maltenes and liquid products:

$$\frac{d[H^* + V]}{dt} = (1-c)\,k_A\,[A^+] + k'\,[TN][A^{*A}]$$

(5)

Rate of formation of toluene-insolubles (coke):

$$\frac{d[TI]}{dt} = k_C\,[A^*_{ex}]$$

(6)

The differential equations were solved numerically. During the induction time, the asphaltene cores were below the critical concentration in the liquid phase ($A^{*ex} = 0$, [TI]=0) and equations (2) and (3) were written as follows:

$$\frac{d[A^{*A}]}{dt} = d\,k_A\,[A^+] - k'\,[TN][A^{*A}]$$

(7)

$$\frac{d[A^{*NA}]}{dt} = (c-d)\,k_A\,[A^+]$$

(8)

151

A3.2 Matlab program

Integration using the estimated parameters

```
clc
clear
global ka ktn kc Sl a  b S kca kcn

TN(1,1:4)=[0 10 25 75];TN(2,1:4)=[0 10 25 75];

ka=0.1532;
CA(1,1:4)=25;
CN_core(1,1:4)=0;
CA_core(1,1:4)=0;
H_core(1,1:4)=0;
TI(1,1:4)=0;
A(1,1:4)=25;
kcd=[0.172 0.04 0.028 0.028];
c=0.543;
ktnm=[0.0023];
b=0.16;
a=c-b;
S=75;
Sl=0.0295;
t=[0:0.1:60];

for i=1:2
CN_core(i,1:4)=a*CA(1,1:4)*(1-exp(-ka(1)*t(i)));
CA_core(i,1:4)=b*CA(1,1:4)*(1-exp(-ka(1)*t(i)));
H_core(i,1:4)=(1-a-b)*CA(1,1:4)*(1-exp(-ka(1)*t(i)));
CA(i,1:4)=CA(1,1:4)*exp(-ka(1)*t(i));
A(i,1:4)=CN_core(i,1:4)+CA_core(i,1:4)+CA(i,1:4);
TI(i,1:4)=0;
end

for j=1:4

 ktn=ktnm;
 kcn=0;
   kc=0;
   kca=0;
   for i=3:601
   [t1,y1]=ode15s('Aca',  [t(i-1)  t(i)],  [CA(i-1,j)  ;TN(i-
1,j); CN_core(i-1,j)  ; CA_core(i-1,j);H_core(i-1,j)  ; TI(i-
1,j)]);

        CA(i,j)=y1(max(size(y1)),1);
```

152

```
TN(i,j)=y1(max(size(y1)),2);
CA_core(i,j)=y1(max(size(y1)),4);
CN_core(i,j)=y1(max(size(y1)),3);
H_core(i,j)=y1(max(size(y1)),5);
TI(i,j)=y1(max(size(y1)),6);
CAmax(i,j)=Sl*(H_core(i,j)+S);
Aex(i,j)=CA_core(i,j)+CN_core(i,j)-CAmax(i,j);
A(i,j)=CA_core(i,j)+CN_core(i,j)+ CA(i,j);

if Aex(i,j)<=0
    kc=0;
    kca=0;
    kcn=0;
    else
        kc=kcd(j);
        kca=kcd(j);
        kcn=kcd(j);
    end

if CA_core(i,j) <= 0
    ktn=0;
   else
     ktn=ktnm(j);
end

if CA_core(i,j)<=0
    kca=0;
    end

end
end


Function file (Aca) for integration

function out2= Aca(t,y)
global ka ktn kc Sl a  b S m kca kcn

out2=[-ka*y(1);             -ktn*y(2)*y(4);          a*ka*y(1)-
kcn*(y(3)/(y(3)+y(4)))*(y(3)+y(4)-Sl*(y(5)+S));...
      b*ka*y(1)-ktn*y(4)*y(2)-
kca*(y(4)/(y(3)+y(4)))*(y(3)+y(4)-Sl*(y(5)+S));...
      (1-a-b)*ka*y(1)+ktn*y(2)*y(4);           kcn*(y(3)+y(4)-
Sl*(y(5)+S))];
```

Residual sum square of error for 0% TN

153

```
time1=[0 10 20 40 60];
coke_0=[0 3.2  9.09 10.05 10.896 ];
Asphaltene_0=[25 12.08 4.9 2.6 2.26 ];
Y=(                          TI(101,1)-coke_0(2))^2+TI(201,1)-
coke_0(3))^2+(TI(401,1)-coke_0(4))^2+(TI(601,1)-
coke_0(5))^2;
Z=(                          A(101,1)-Asphaltene_0(2))^2+A(201,1)-
Asphaltene_0(3))^2+(A(401,1)-Asphaltene_0(4))^2+(A(601,1)-
Asphaltene_0(5))^2;
df=Y+Z;
```

A4   Error Estimation

The parameter errors were estimated by a 95% confidence limit. Each standard deviation parameter was calculated using the principal diagonal terms in the variance-covariance matrix. This matrix was obtained by the following equation:

$$V=(J^T J)^{-1} S_o^2$$

Where J is the Jacobian matric (N × M) and S_o^2 is the experimental error variance. The jacobian matric and the experimental error variance were calculated as follows:

Let, $f_i = f(x_i, p)$,

where x is the continuous variable array in the ith run and p is the parameter array in the model. The Jacobian matrix can then be expressed according to the following equation:

$$J=\begin{vmatrix} \left(\dfrac{\partial f}{\partial p_1}\right)_1 & \left(\dfrac{\partial f}{\partial p_2}\right)_1 & \cdots & \left(\dfrac{\partial f}{\partial p_j}\right)_1 & \cdots & \left(\dfrac{\partial f}{\partial p_m}\right)_1 \\ \left(\dfrac{\partial f}{\partial p_1}\right)_i & \left(\dfrac{\partial f}{\partial p_2}\right)_i & \cdots & \left(\dfrac{\partial f}{\partial p_j}\right)_i & \cdots & \left(\dfrac{\partial f}{\partial p_m}\right)_i \\ \left(\dfrac{\partial f}{\partial p_1}\right)_n & \left(\dfrac{\partial f}{\partial p_2}\right)_n & \cdots & \left(\dfrac{\partial f}{\partial p_j}\right)_n & \cdots & \left(\dfrac{\partial f}{\partial p_m}\right)_n \end{vmatrix}$$

154

where, i is the experimental run index and j is the parameter index. Each term in the Jacobian matrix was calculated numerically around the estimated parameter following two- point finite difference (forward) method.

The experimental error variance was computed from the matrix of residual as follows:

$$S_0^2 = \frac{E^T E}{n - m}$$

Where, E is the matrix of residual between the experimental values and calculated values from the estimated parameters.

For 95% confidence interval and (n-m) degrees of freedom, individual parameter confidence intervals were calculated as $\pm t_{0.975} \sqrt{V_{jj}}$.

155

A5 NMR Spectra of the Feed Asphaltenes

A5.1 Proton Spectra

Athabasca

Gudao

156

Arab Heavy

Arab Light

157

Maya

A5.2 Carbon Spectra

Athabasca

158

Arab Heavy

159

Arab Light

Maya

160
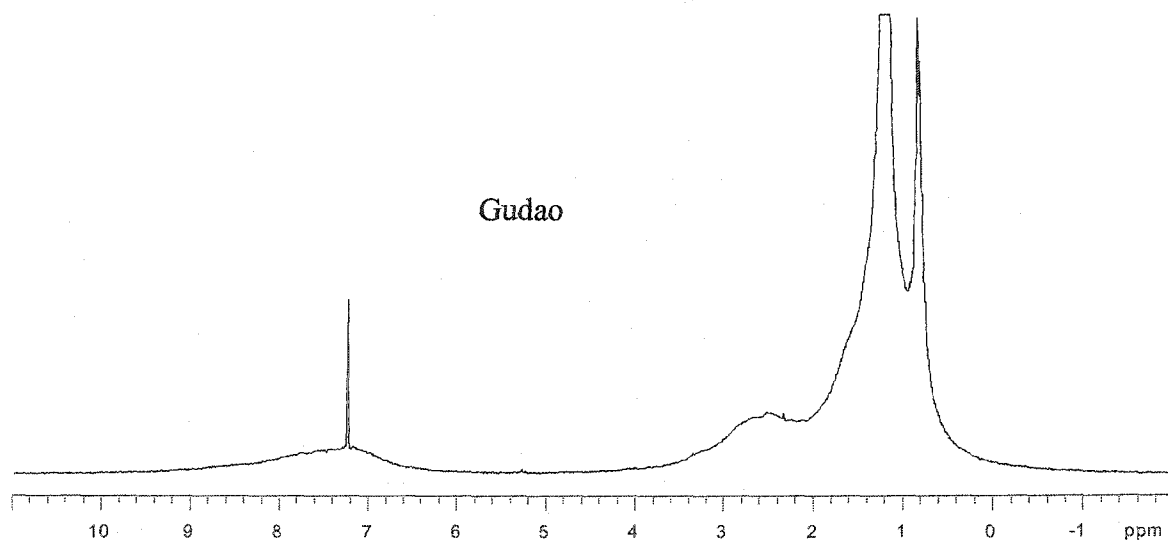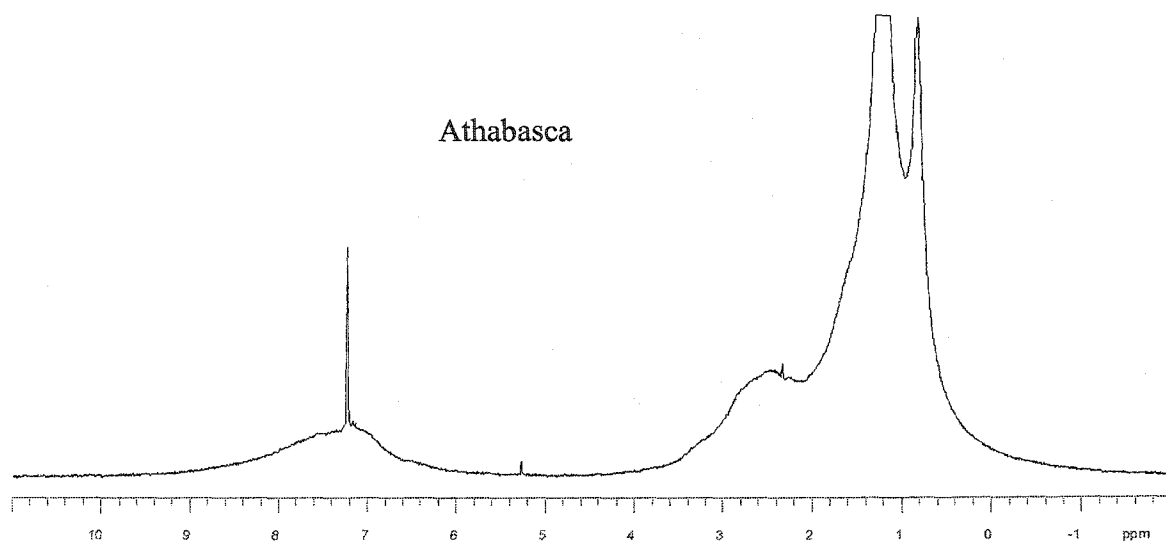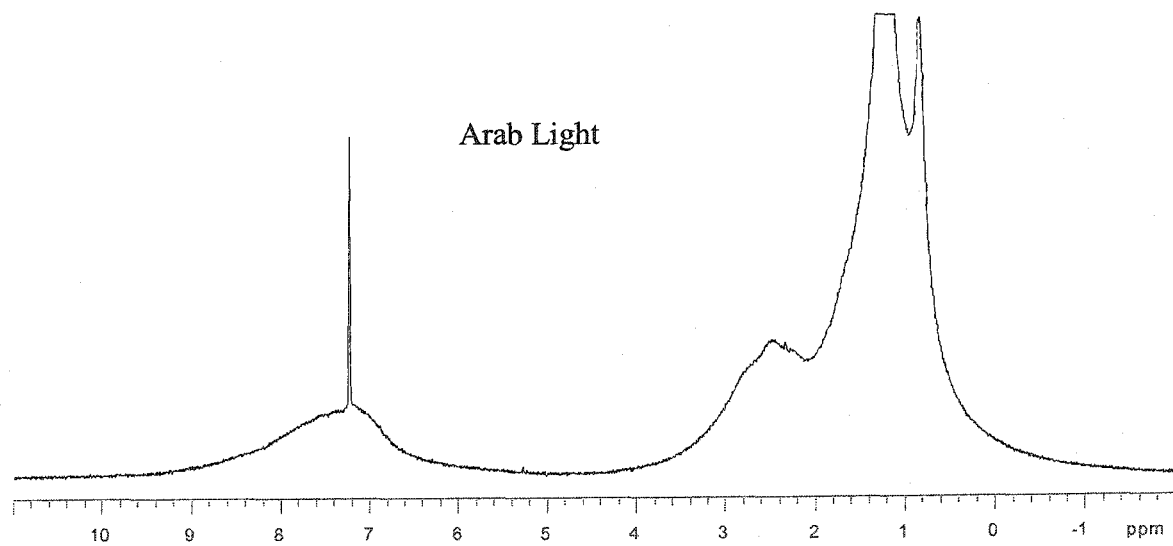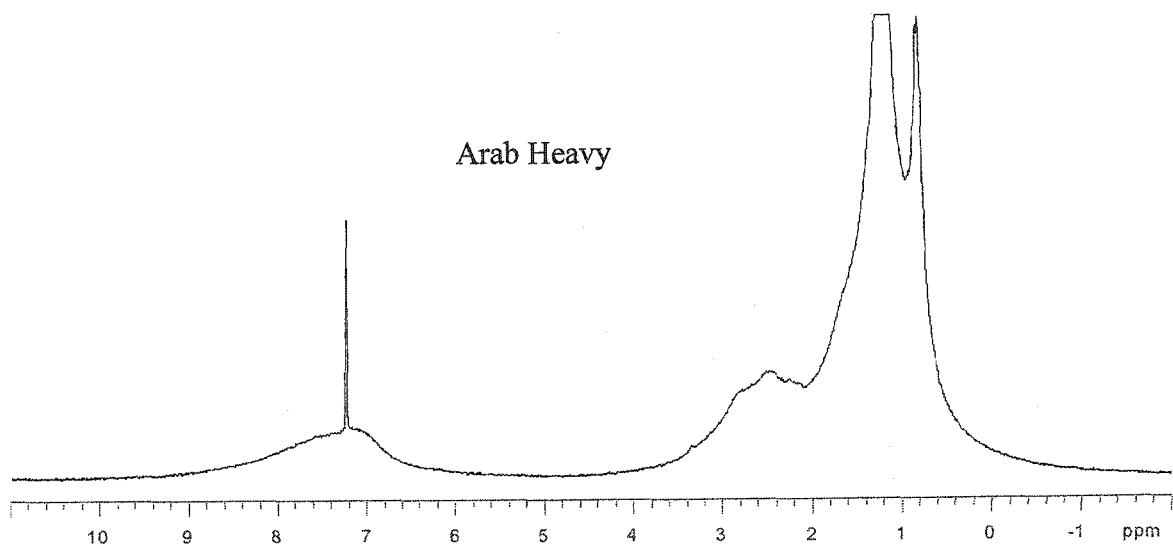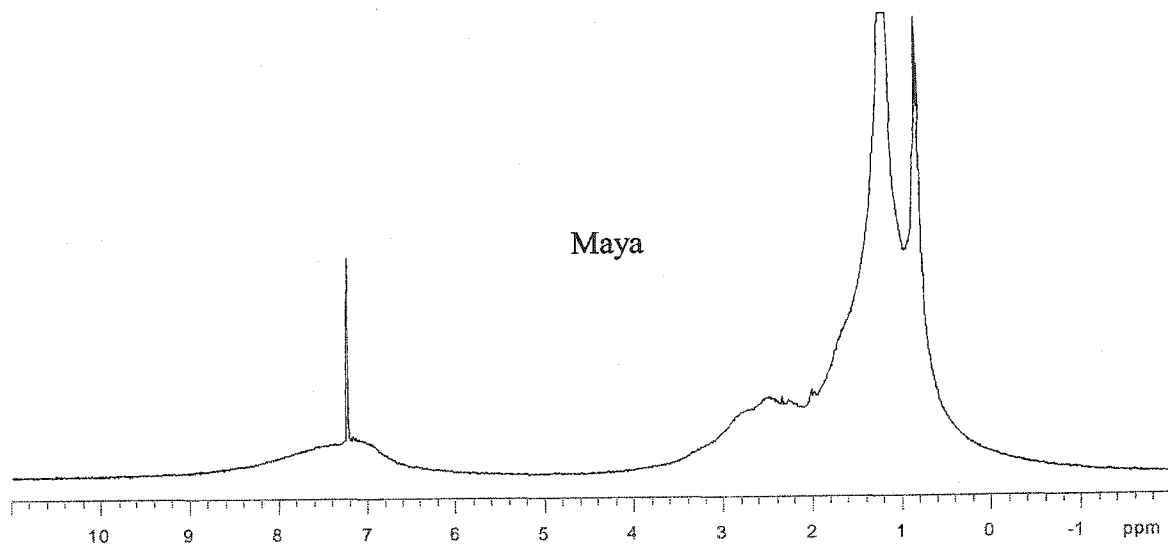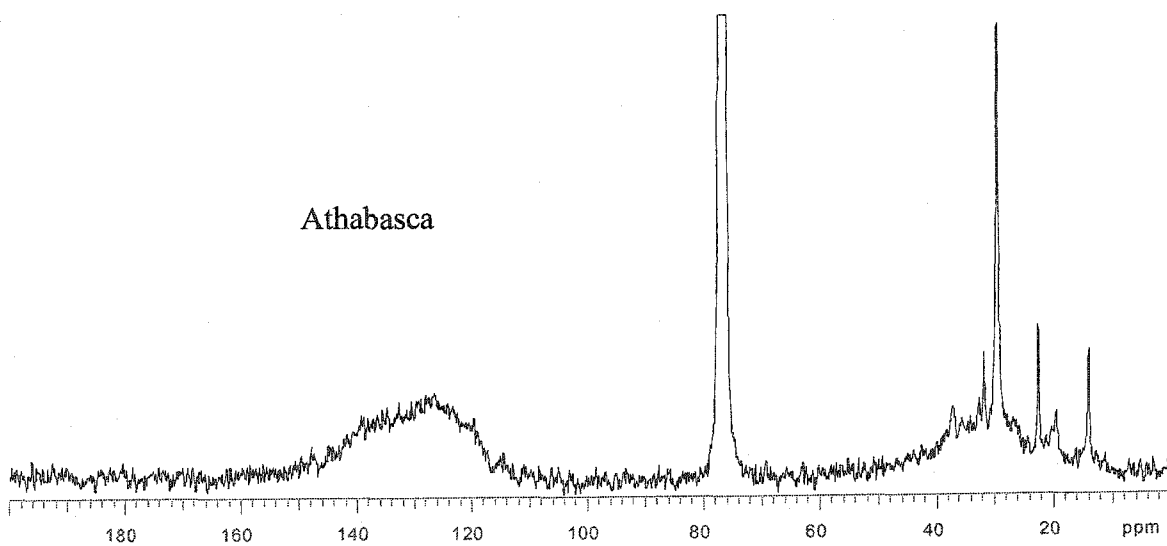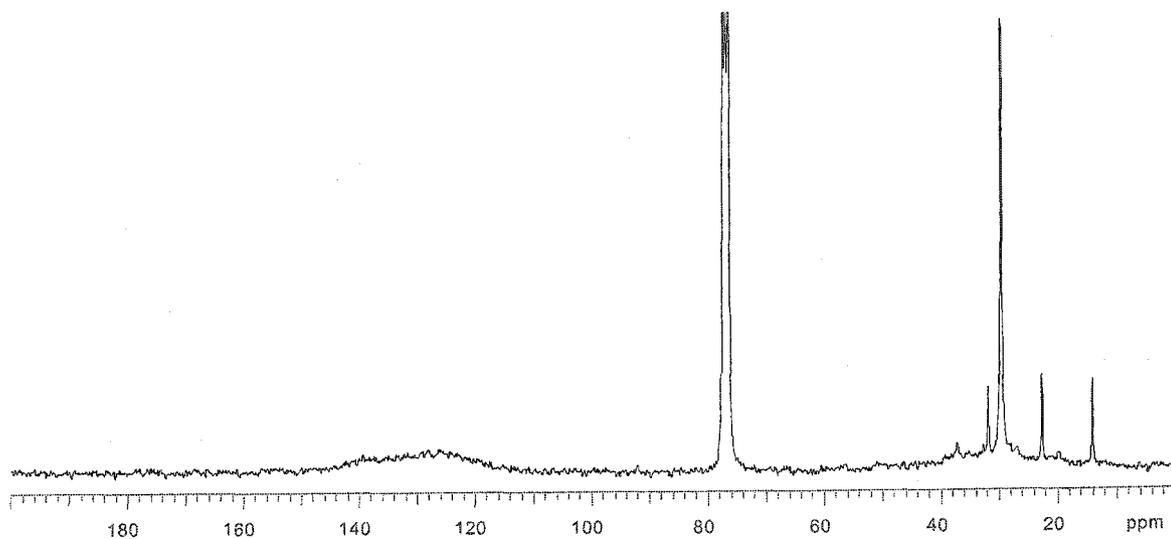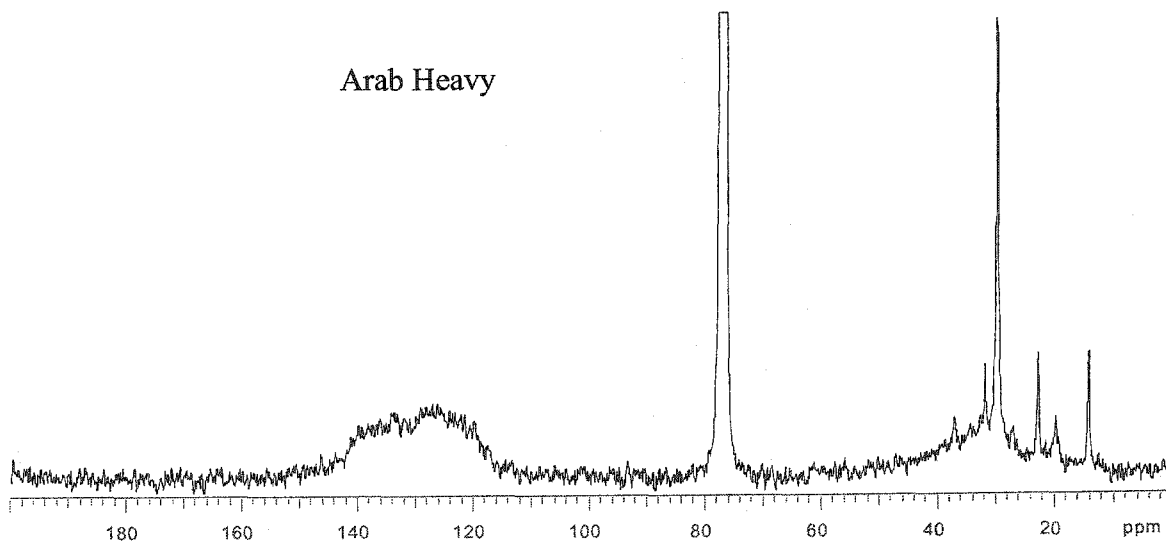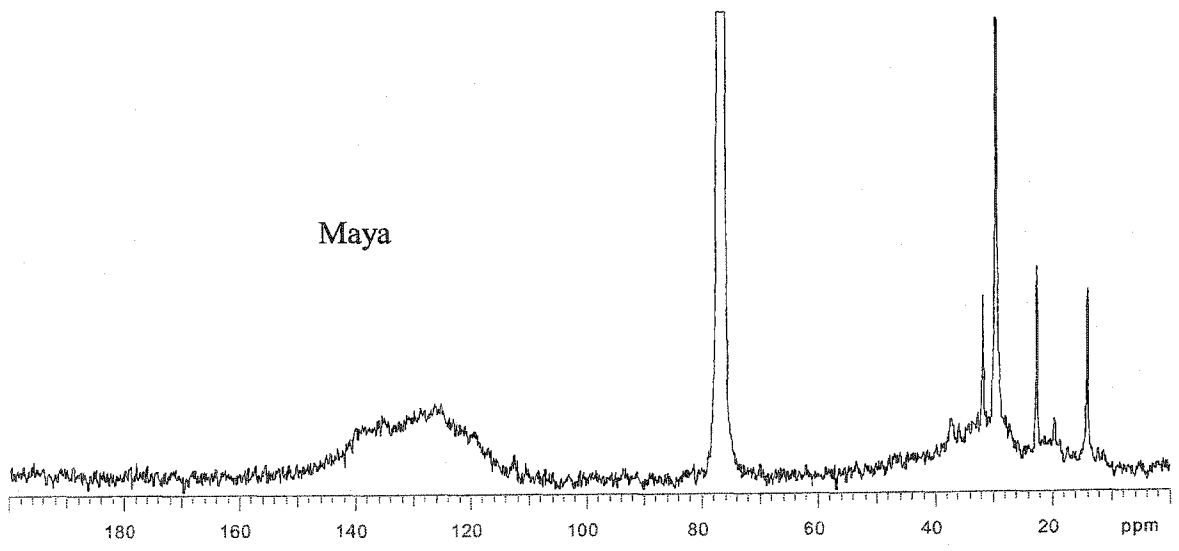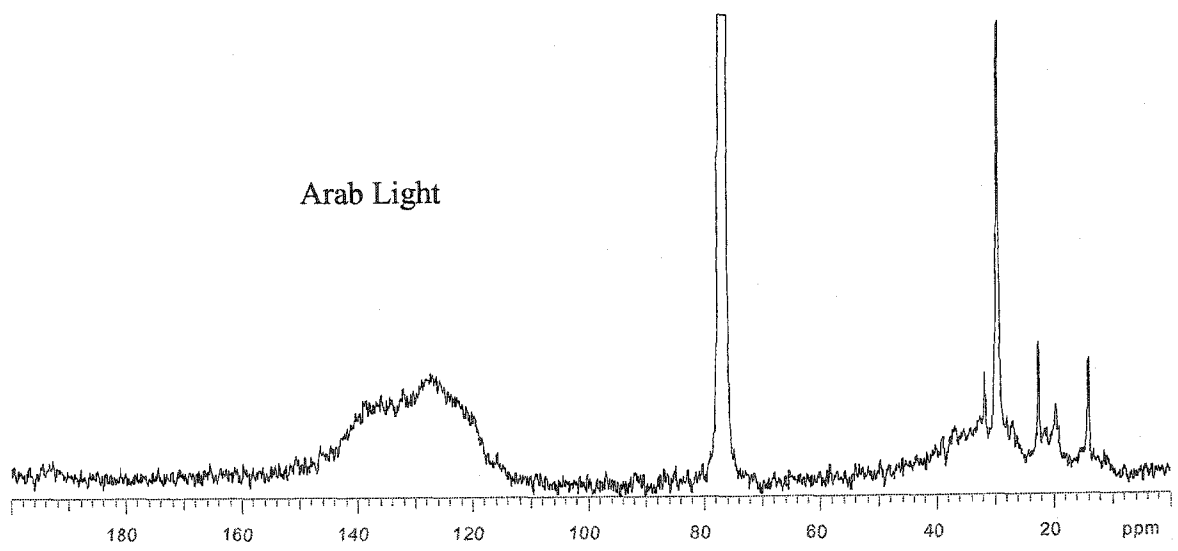
A6 Experimental Data

A6.1 Cracking of Asphaltene in Maltene

A6.1.1 Checking the Mixing Method

In order to check the mixing method used in Chapter 4, two experiments were done. Asphaltenes were first separated from vacuum residue (VR) following the asphaltene separation method. Dried asphaltenes were then added back to maltene following the procedure described in Chapter 3. Yields of coke and asphaltenes from the thermal cracking of this mixture (VR mix) and VR are presented in the following table.

Table A 1 Checking the mixing method

Feed	% Coke	% Asphaltene
VR mix	16.2	11.7
VR	16.9	13.3

161

A6.1.2 Experimental Yields

Following reactions were done at 430°C for a length of 40 min under nitrogen atmosphere (P_{cold}= 1 atm).

Table A 2 Coke and asphaltene yield from the thermal cracking of asphaltenes in maltene

Wt fraction of A	% Coke	% Asphaltene
0.00	7.0	13.9
0.13	12.1	11.6
0.25	15.5	13.3
0.50	23.8	11.3
0.62	31.1	10.6
0.76	37.8	10.0
0.80	42.1	6.5
1.00	47.5	7.1

Coke yield was calculated as follows:

$$\% \text{ Coke} = \frac{Toluene\ insoluble - solid\ in\ feed}{Feed - solid\ in\ feed}$$

Table A 3 Solid free reactions of asphaltenes in maltene

wt fraction of A	%Coke	%Asphaltene
0.00	7.0	13.9
0.25	19.1	11.2
0.50	28.1	9.7
1.00	47.5	7.1

162

A6.2 Cracking of Athabasca Asphaltene in Aromatic Solvents

Following reactions were done at 430°C for 40 minute under nitrogen atmosphere under 3.5-4 MPa cold pressure. TN= tetralin, NP= naphthalene, 1-MN=1-methyl naphthalene.

Table A 4 Comparison of coke and asphaltene yield in different solvents

Reactant	% Coke	Stdev of coke	% Asphaltene	Stdev of asphaltene
A+ TN	3.6	0.6	6.2	0.5
A+ NP	11.0	0.6	2.3	0.7
A+ 1-MN	10.2	0.5	2.7	0.3
A+maltene*	13.8	0.5	1.6	0.8

*Coke and asphaltene contribution from maltene was deducted in the table.

Following reactions were done at 430°C for 60 minute under nitrogen atmosphere under 3.5 MPa cold pressure.

Table A 5 Coke and asphaltene yield from the thermal cracking of asphaltenes in 1-MN

Wt fraction of A	% Coke	% Asphaltene
0.20	9.0	1.5
0.20	8.7	1.4
0.20	8.8	1.5
0.25	10.9	2.3
0.30	12.9	2.2
0.40	19.5	2.1
0.70	34.1	3.0

163

Following reactions were done at 430°C for 25 wt% initial asphaltene content under nitrogen atmosphere under 3.5 –4 MPa cold pressure.

Table A 6 Temporal variation of coke and asphaltene yield from the thermal cracking of asphaltenes in 1-MN

Time	% Coke	% Asphaltene	%H*+V
0	0.0	25.0	0.0
10	3.2	12.1	9.7
20	9.1	4.9	11.0
40	10.1	2.6	12.4
60	10.9	2.3	11.8

Table A 7Temporal variation of coke and asphaltene yield from the thermal cracking of asphaltenes in mixture of 1-MN and TN

TNo=75, 1-MN=0			
time	% coke	% A	%(H* +V)
0	0	25	0
20	2.7	9	13.3
40	4.3	5.1	15.6
60	3.8	5.2	16
TNo=25, 1-MN=50			
time	% coke	% A	%(H* +V)
0	0	25	0
20	2.8	9.3	12.9
40	4.8	6.1	14.1
60	6	3.8	15.2
TNo=10, 1-MN=65			
time	% coke	% A	%(H* +V)
0	0	25	0
20	3.5	9.4	12.1
40	7.1	4.6	13.3
60	8.6	3.6	12.9

164

Table A 8Thermolysis of asphaltene in 1-MN with or without added n-dodecyl sulfide (DDS)

Time, min	Reactant	% Coke	% Asphaltene
10	A+1-MN	3.2	12.1
10	A+1-MN+DDS	7.8	6.8
40	A+1-MN	10.1	2.6
40	A+1-MN+DDS	9.8	2.8

A6.3 Properties of the Feed Asphaltenes

Table A 9 Elemental composition of the feed asphaltenes

Feed	% C	% H	% N	% S	H/C
Athabasca	80.84	7.99	1.28	7.47	1.18
Arab Heavy	83.11	8.04	0.92	7.15	1.15
Arab Light	83.65	7.53	0.83	5.67	1.07
Gudao	83.41	9.83	1.18	4.44	1.40
Maya	83.60	8.16	1.19	6.61	1.16

Table A 10 NMR analysis data for aromatic carbon functional group

Feed	Qar	Qar-S	Qar-P	CHar	cluster	fa
Athabasca	29	9.2	19.8	24.6	19	55
Arab Heavy	26.6	9.5	17.1	24.6	17	52
Arab Light	34.4	8.2	26.2	26.5	21	61
Gudao	21.4	9.2	12.2	18.4	15	40
Maya	28.2	8.6	19.6	24.6	19	53

165

Table A 11 NMR analysis data for paraffinic carbon functional groups

Feed	CH	CHAIN	Length	C-CH3	E-CH3
Athabasca	8.6	8.2	8.5	2.3	1.2
Arab Heavy	11.4	8.9	8.8	2.3	1.1
Arab Light	7.1	8.4	8.1	2.1	1.2
Gudao	10.6	16.7	10.7	2.9	1.2
Maya	8.3	8.1	7.9	2.8	1.5

Table A 12 NMR analysis data for paraffinic carbon functional groups (*contd.*)

Feed	ab-CH2	Ar-CH3	Cy-CH3	NAPH	R-CH3
Athabasca	15.5	2.4	3.5	4.7	5.8
Arab Heavy	15.7	2.3	2.9	3.7	5.3
Arab Light	12.6	2.1	3.4	3.6	5.5
Gudao	17.1	2.2	3.8	5.1	6
Maya	16.1	2.2	3.6	3.8	5.8

A6.4 Coking reactions with different asphaltenes

A6.4.1 Cracking in 1-methyl naphthalene

Following reactions were done for with 25 wt% initial asphaltene content.

Table A 13 Coke yields from the thermal cracking of asphaltenes in 1-methyl naphthalene

Time	Maya	Arab Light	Arab Heavy	Gudao
0	0	0	0	0
20	10.6	9.1	9.7	3.9
40	12.9	11.3	11.3	6.7
60	12	13.5	11.3	7.2

Table A 14 Asphaltene yields from the thermal cracking of asphaltenes in 1-methyl naphthalene

Time	Maya	Arab Light	Arab Heavy	Gudao
0	25	25	25	25
20	4.5	7.3	4.9	7.0
40	1.5	2.6	2.6	2.8
60	1.5	2.6	1.8	2.9

A6.4.2 Cracking in tetralin

Table A 15 Coke and asphaltene yields from the thermal cracking of asphaltenes in tetralin for 40 minutes

Feed	% Coke	% Asphaltene	Coke + Aspheltene
Athabasca	4.3	5.1	9.4
Arab Heavy	2.5	9.8	12.3
Arab light	3.7	11.3	15.0
Gudao	1.2	6.4	7.6
Maya	4.4	8.5	12.9

A6.5 Change of Molecular Weight with Coke Formation

sample from Athabasca	MW	Coke/100 g of A
Feed asphaltene	2861	0
Product asphaltene from 24.7%A in 1-MN, 40 min	947	44
Product asphaltene from 24.7%A in 1-MN, 40 min	821	44
product asphaltene from 40.59%A in 1-MN, 40 min	624	48
product asphaltene from 69.5%A in 1-MN, 40 min	822	49
Product asphaltene from maltene, 40 min	984	
product asphaltene from SFVR, 40 min	817	55
Product asphaltene from asphaltene, 40 min	690	47
Product asphaltene from 25%A in TN reacted for 20 min	1676	11
Product asphaltene from 25%A in TN reacted for 20 min	1636	11
Product asphaltene from 25%A in TN reacted for 40 min	1247	17
Product asphaltene from 25%A in TN reacted for 60 min	1134	15
Sample from different feeds	MW	Coke/100 g of A
Product asphaltene from Gudao 25%A +TN, 40 min	1625	5
Product asphaltene from AHVR 25%A +TN, 40 min	2124	10
Product asphaltene from Maya 25%A +TN, 40 min	1748	18
Product asphaltene from ALVR 25%A +MN, 40 min	1333	15
Product asphaltene from Maya 25%A +MN, 40 min	950	52
Product asphaltene from AHVR 25%A +MN, 40 min	1068	45

168